การตรวจวัดทางเคมีไฟฟ้าของสารอินทรีย์และสารชีวภาพด้วยขั้วไฟฟ้าดัดแปร

นางสาวศิริวรรณ นันทพล

วิทยานิพนธ์นี้เป็นส่วนหนึ่งของการศึกษาตามหลักสูตรปริญญาวิทยาศาสตรดุษฎีบัณฑิต
สาขาวิชาเคมี ภาควิชาเคมี
คณะวิทยาศาสตร์ จุฬาลงกรณ์มหาวิทยาลัย
ปีการศึกษา 2559

ELECTROCHEMICAL DETECTION OF ORGANIC AND BIOLOGICAL COMPOUNDS WITH MODIFIED ELECTRODE

Miss Siriwan Nantaphol

A Dissertation Submitted in Partial Fulfillment of the Requirements
for the Degree of Doctor of Philosophy Program in Chemistry
Department of Chemistry
Faculty of Science
Chulalongkorn University
Academic Year 2016

Thesis Title	ELECTROCHEMICAL DETECTION OF ORGANIC AND BIOLOGICAL COMPOUNDS WITH MODIFIED ELECTRODE
By	Miss Siriwan Nantaphol
Field of Study	Chemistry
Thesis Advisor	Professor Dr.Orawon Chailapakul, Ph.D.
Thesis Co-Advisor	Associate Professor Dr.Weena Siangproh, Ph.D.

Accepted by the Faculty of Science, Chulalongkorn University in Partial Fulfillment of the Requirements for the Doctoral Degree

.....Dean of the Faculty of Science
(Associate Professor Dr.Polkit Sangvanich, Ph.D.)

THESIS COMMITTEE

.....Chairman
(Associate Professor Dr.Vudhichai Parasuk, Ph.D.)

.....Thesis Advisor
(Professor Dr.Orawon Chailapakul, Ph.D.)

.....Thesis Co-Advisor
(Associate Professor Dr.Weena Siangproh, Ph.D.)

.....Examiner
(Associate Professor Dr.Narong Praphairaksit, Ph.D.)

.....Examiner
(Associate Professor Dr.Nattaya Ngamrojanavanich, Ph.D.)

.....External Examiner
(Dr.Amara Apilux, Ph.D.)

ศิริวรรณ นันทพล : การตรวจวัดทางเคมีไฟฟ้าของสารอินทรีย์และสารชีวภาพด้วยขั้วไฟฟ้าดัดแปร (ELECTROCHEMICAL DETECTION OF ORGANIC AND BIOLOGICAL COMPOUNDS WITH MODIFIED ELECTRODE) อ.ที่ปรึกษาวิทยานิพนธ์หลัก: ศ. ดร.อรวรรณ ชัยลภากุล, อ.ที่ปรึกษาวิทยานิพนธ์ร่วม: รศ. ดร. วีณา เสียงเพราะ, 156 หน้า.

วิทยานิพนธ์ฉบับนี้พัฒนาวิธีและอุปกรณ์สำหรับวิเคราะห์สารประกอบและสารบ่งชี้ทางชีวภาพที่สำคัญสำหรับการนำไปใช้งานทางด้านเภสัชกรรมและการวินิจฉัยทางการแพทย์ ซึ่งสามารถแบ่งออกเป็นห้าส่วน โดยส่วนแรก เป็นการพัฒนาวิธีตรวจวัดสารเอ็น-อะเซทิล-แอล-ซีสเตอีนในตัวอย่างยาโดยใช้ขั้วไฟฟ้าฟิล์มบางเพชรเจือโบรอนร่วมกับระบบโฟลว์อินเจ็กชัน วิธีที่พัฒนาขึ้นให้ความเป็นเส้นตรงอยู่ในช่วง 0.5 – 5 ไมโครโมลาร์ ค่าขีดจำกัดต่ำสุดของการตรวจวัดเท่ากับ 10 นาโนโมลาร์ ให้ผลการวิเคราะห์ที่แม่นยำและมีเสถียรภาพสูง ในส่วนที่สอง เป็นการพัฒนาอุปกรณ์รับรู้ทางเคมีไฟฟ้าสำหรับตรวจวัดคลอเรสเตอรอลโดยใช้อนุภาคเงินขนาดนาโนเมตรดัดแปรผิวหน้าของขั้วไฟฟ้ากลาสสิคาร์บอน โดยตรวจวัดหาปริมาณคลอเรสเตอรอลจากการติดตามปริมาณของไฮโดรเจนเปอร์ออกไซด์ที่เกิดจากปฏิกิริยาของเอนไซม์ โดยอนุภาคเงินขนาดนาโนเมตรจะแสดงสมบัติเป็นตัวเร่งการเกิดปฏิกิริยารีดักชันของไฮโดรเจนเปอร์ออกไซด์ ซึ่งสามารถกำจัดปัญหาการรบกวนจากสารอื่นๆที่เกิดปฏิกิริยาออกซิเดชันได้ง่าย วิธีที่พัฒนานี้ให้ความเป็นเส้นตรงอยู่ในช่วง 3.87 - 773.40 มิลลิกรัมต่อเดซิลิตร และค่าขีดจำกัดต่ำสุดของการตรวจวัดอยู่ที่ 0.99 มิลลิกรัมต่อเดซิลิตร ส่วนที่สาม เป็นการพัฒนาอุปกรณ์รับรู้สำหรับตรวจวัดกลูโคสแบบไม่ใช้เอนไซม์โดยใช้โลหะผสมแพททินัมและทองดัดแปรขั้วไฟฟ้าฟิล์มบางเพชรเจือโบรอน โดยโลหะผสมแพททินัมแสดงสมบัติในการเร่งการเกิดปฏิกิริยาออกซิเดชันของกลูโคสในสภาวะปกติ ได้ความเป็นเส้นตรงสำหรับตรวจวัดอยู่ในช่วง 0.01 – 7.5 มิลลิโมลาร์ และค่าขีดจำกัดต่ำสุดของการตรวจวัดอยู่ที่ 0.01 มิลลิโมลาร์ ส่วนที่สี่ เป็นการพัฒนาอุปกรณ์วิเคราะห์บนฐานกระดาษร่วมกับขั้วไฟฟ้าฟิล์มบางเพชรเจือโบรอนดัดแปรด้วยอนุภาคเงินขนาดนาโนเมตรสำหรับนำไปใช้ในการตรวจวัดคลอเรสเตอรอล วิธีการตรวจวัดทำได้โดยการหยดเอนไซม์คลอเรสเตอรอลออกซิเดสและสารตัวอย่างคลอเรสเตอรอลลงบนกระดาษที่สร้างขึ้นและตรวดวัดไฮโดรเจนเปอร์ออกไซด์ที่เกิดขึ้นด้วยเทคนิคโครโนแอมเพอโรเมตตรี โดยได้เป็นเส้นตรงค่าขีดจำกัดต่ำสุดของตรวจวัดเท่ากับ 0.01 - 7 มิลลิโมลาร์ และ 6.5 มิลลิโมลาร์ ตามลำดับ ส่วนสุดท้าย เป็นการพัฒนาขั้วไฟฟ้าฟิล์มบางเพชรเจือโบรอนเพลทร่วมกับอุปกรณ์วิเคราะห์ของไหลจุลภาคบนฐานกระดาษสำหรับการวิเคราะห์หาปริมาณนอร์เอพิเนฟรินและเซโรโทนิน และการวิคราะห์หาปริมาณโลหะหนักด้วยเทคนิคสแควร์เวฟแอโนดิกสตริปปิงโวลแทมเมตรี โดยอุปกรณ์ตรวจวัดที่นำเสนอขึ้นนี้สามารถวิเคราะห์นอร์เอพิเนฟรินและเซโรโทนินแบบพร้อมกันได้ความเป็นเส้นตรงสำหรับตรวจวัดอยู่ในช่วง 2.5 – 100 ไมโครโมลาร์ และ 0.5 – 7.5 ไมโครโมลาร์ ตามลำดับ สำหรับการวิเคราะห์โลหะหนักเป็นการออกแบบอุปกรณ์วิเคราะห์ของไหลจุลภาคบนฐานกระดาษแบบไหลผ่านร่วมกับการตร วจวัดด้วยด้วยเทคนิคสแควร์เวฟแอโนดิกสตริปปิงโวลแทมเมตรีเพื่อเพิ่มประสิทธิภาพในการสะสมของโลหะบนขั้วไฟฟ้ามากขึ้น ซึ่งเป็นผลทำให้ความไวของการตรวจวัดเพิ่มขึ้นเมื่อเปรียบเทียบกับอุปกรณ์วิเคราะห์บนฐานกระดาษแบบไม่มีการไหลของสารละลาย ซึ่งผลการศึกษานี้แสดงให้เห็นว่าวิธีและอุปกรณ์วิเคราะห์ที่พัฒนาขึ้นมา ให้ความไวในการวิเคราะห์สูง มีความจำเพาะเจาะจง ราคาถูก และสามารถพกพาได้

ภาควิชา เคมี ลายมือชื่อนิสิต .....

สาขาวิชา เคมี ลายมือชื่อ อ.ที่ปรึกษาหลัก .....

ปีการศึกษา 2559 ลายมือชื่อ อ.ที่ปรึกษาร่วม .....

5572838323 : MAJOR CHEMISTRY
KEYWORDS: ELECTROCHEMICAL DETECTION / BORON-DOPED DIAMOND ELECTRODE / MODIFIED ELECTRODE / PAPER-BASED ANALYTICAL DEVICE

SIRIWAN NANTAPHOL: ELECTROCHEMICAL DETECTION OF ORGANIC AND BIOLOGICAL COMPOUNDS WITH MODIFIED ELECTRODE. ADVISOR: PROF. DR.ORAWON CHAILAPAKUL, Ph.D., CO-ADVISOR: ASSOC. PROF. DR.WEENA SIANGPROH, Ph.D., 156 pp.

In this dissertation, analytical method/devices based on electrochemical detection are described for determining the important compounds/biomarkers in pharmaceutical and medical diagnostic applications, which can be separated into five parts. In the first part, electrochemical method for N-acetyl-L-cysteine (NAC) detection in drug formulations was developed using boron doped diamond (BDD) sensor coupled with flow injection analysis (FIA) system. The proposed method offers a linear range of 0.5 – 50 µmol/L, a limit of detection (LOD) of 10 nM, excellent response precision, and high stability. In the second part, an electrochemical cholesterol sensor was developed using silver nanoparticles modified glassy carbon electrode (AgNPs/GCE). Hydrogen peroxide (H_2O_2) produced from the enzymatic reaction was monitored for indirect cholesterol quantification. AgNPs showed the catalytic activity of H_2O_2 reduction, with no observed interference from easily oxidizable species. The proposed method displayed wide linear range of 3.87 - 773.40 mg/dL with LOD of 0.99 mg/dL. In the third part, a selective non-enzymatic glucose sensor was successfully developed using bimetallic Pt/Au modified BDD electrode. Pt/Au nanocatalyts possess high electrocatalytic activity for glucose oxidation in physiological conditions. A linear range of 0.01 -7.5 mM and a LOD of 0.01 mM were obtained. In the fourth part, a silver nanoparticle-modified boron-doped diamond (AgNP/BDD) electrode coupled with paper-based analytical devices (PADs) was developed for cholesterol detection. Cholesterol and cholesterol oxidase (ChOx) were directly drop-casted onto the hydrophilic area of PAD followed by monitoring of H_2O_2 from the enzymatic reaction using chronoamperometry. A linear range and a LOD were obtained at 0.01 - 7 mM and 6.5 uM, respectively. In the final part, the disposable boron doped diamond paste electrodes (BDDPEs) for microfluidic paper-based analytical devices (µPADs) were developed and employed for two applications; the quantitative detection of norepinephrine (NE) and serotonin (5-hydroxytryptamine, 5-HT), and the anodic stripping voltammetry of heavy metals. In case of biological species, the electrochemical paper-based analytical device (ePAD) was capable of simultaneously detecting NE and 5-HT in concentration ranges of 2.5–100 µM and 0.5–7.5 µM, respectively. For heavy metal quantitation, a flow-through µPAD design using square-wave anodic stripping voltammetry (SWASV) to enhance the efficiency of metal deposition was presented, thereby improving the detection sensitivity compared to a static ePAD system. The results demonstrated that all proposed method/sensors provide high sensitivity, selectivity, low cost, and portability.

Department:	Chemistry	Student's Signature	.....
Field of Study:	Chemistry	Advisor's Signature	.....
Academic Year:	2016	Co-Advisor's Signature	.....

ACKNOWLEDGEMENTS

First of all, I would like to extend my sincere gratitude to my advisor Professor Dr. Orawon Chailapakul. This work would not have been possible without her guidance, support, motivation, enthusiasm, encouragement, and immense knowledge. Under her guidance I successfully overcame many difficulties and learned a lot. She also demonstrated what a brilliant and hard-working scientist could accomplish. It has been an honor to be her Ph.D. student.

My deepest acknowledgement goes to Associate Professor Dr. Weena Siangproh, who has generally offered her time, expertise, wisdom, and continuous encouragement in guiding me and mentoring me step by step through the whole research process. I am also thankful to her for encouraging the use of correct grammar in my writings and for reading and suggesting on countless revisions of my manuscripts. Without her advice, this thesis would not have come into being.

I take this opportunity to sincerely acknowledge Professor Dr. Charles S. Henry from Colorado State University, and Professor Dr. Yasuaki Einaga from Keio University, Japan, for giving me the internship opportunities in their groups and leading me working on diverse exciting projects. I appreciate all excellent guidance, support and valuable suggestions throughout 11 months in USA and 3 months in Japan.

I am also truly grateful to my thesis committees: Associate Professor Dr. Vudhichai Parasuk, Associate Professor Dr. Narong Praphairaksit, Associate Professor Dr. Nattaya Ngamrojanavanich, and Dr. Amara Apilux, for their time, insightful comments and questions.

I gratefully acknowledge the funding sources that made my Ph.D. work possible. I was funded by the Thailand Research Fund (TRF) via Royal Golden Jubilee Ph.D. Program (Grant No. PHD/0123/ 2554).

Also, I would like to thank all members of Electrochemistry and Optical Spectroscopy Research Unit (EOSRU) at Chulalongkorn University, Henry group at Colorado State University, and Einaga group at Keio University. They were always beside me during the happy and hard moments to push me and motivate me. Memories of hard work we shared helped me endure the frequent frustration.

Lastly, I would like to pay high regards to my parents and brother for their unconditional trust, timely encouragement, and endless patience. It was their love that raised me up again when I got weary, and helped me get through this agonizing period in the most positive way. I would not have been accomplished anything without them.

CONTENTS

Page

Page

Page

Page

Page

Page

Page

LIST OF TABLES

LIST OF FIGURES

LIST OF ABBREVIATIONS

O	Oxidized form of redox coupled
R	Reduced form of redox coupled
E^0	Standard potential for the redox reaction
$C_o(0,t)$	Concentration of oxidized form
$C_R(0,t)$	Concentration of oxidized form
R	Universal gas constant (8.314 J K^{-1} mol^{-1})
T	Kelvin temperature
n	Number of electrons transferred in the reaction
F	Faraday constant (96,487 coulombs)
°C	Degree celsius
A	Electrode area
C	Concentration
D	Diffusion coefficient
v	Scan rate
E_p	Peak potential
$E_{p,a}$	Anodic peak potential
$E_{p,c}$	Cathodic peak potential
ΔE_p	Peak separation potential
t	Time
Δi	Current difference
Q	Coulombs
N	Number of moles
µL	Microliter
RSD	The relative standard deviation
mol/L	Mole per liter
cm^2	Square centimeter
mm	Millimeter
V	Volt

I_p	Peak current
J_p	Peak current density
A	Ampere
V	Scan rate
µA	Microampere
µg/mL	Microgram per milliliter
mg/dL	Milligram per deciliter
mM	Millimolar
µM	Micromolar
M	Molar
s	Second
mV/s	Milli volt per second
U/mL	Unit per milliliter
K_m	The apparent Michaelis-Menten constant
I_{ss}	Steady-state current
I_{max}	Maximum current
LOD	Limit of detection
cm^3	Cubic centimeter
C_{dl}	Double layer capacitance
$i_{average}$	Current average from the forward and reverse sweep
$A_{geometric}$	Geometric electrode area
AgNP	Silver nanoparticles
PADs	Paper-based analytical devices
ePADs	Electrochemical paper-based analytical device
µPADs	Microfluidic paper-based analytical devices
SPCE	Screen-printed carbon paste electrodes
BDD	Boron-doped diamond
BDDPE	Boron-doped diamond paste electrode
CPE	Carbon paste electrode
ISE	Ion-Selective Electrode

CV	Cyclic voltammetry
DPV	Differential-pulse voltammetry
SWV	Square-wave voltammetry
SWASV	Square-wave anodic stripping voltammetry
FIA	Flow injection analysis
WE	Working electrode
CE	Counter electrode
RE	Reference electrode
GO	Graphene oxide

CHAPTER I

INTRODUCTION

1.1 Introduction

The increasing demand of analytical methods for various applications has encouraged the development of accurate, fast, and simple analytical techniques, especially for pharmaceutical management and medical diagnosis. Quality control is an essential function for the pharmaceutical productions because of their critical role in the treatment of disease and the maintenance of good health. Effective quality control procedures help to ensure the quality and consistency of pharmaceutical products. Numerous analytical methods have been developed, especially liquid chromatography-mass spectrometry (LC/MS), and gas chromatography-mass spectrometry (GC-MS). These techniques offer high accuracy, selectivity, and sensitivity. However, they still have the limitations in terms of requirement of derivatization step, time consumption, high instrumental and/or running costs as well as intricate instrumental setup. Therefore, the method development for applying in drug analysis is a challenge to search for the new methods that not only give the reliability and precision but also provide the simplicity, high throughput, low cost, and portability of the instruments [1-3]. Electrochemical method has proven to be very effective because of its inherent miniaturization, fast analysis time, simple instrumentation, low cost, and compatibility with microfabrication technologies. In addition, this technique is suitable to combine with automated analysis system [4, 5]. As mentioned above, a simple, high-throughput, and sensitive method for drug formulation analysis based on electrochemical detection coupled with automated flow injection analysis (FIA) system was developed in this work. *N*-acetyl-*L*-cysteine (NAC), commonly used as a mucolytic agent to reduce sputum viscosity in chronic asthma and bronchitis [6, 7], was used as the model to evaluate the developed

method. The motivation and details of developed method are described in Chapter III.

Besides using electrochemical technique for the development of analytical method for quality management in drug analysis, this technique was also used for the development of highly sensitive sensors for medical diagnostics. Cholesterol is one of the most important biomarkers for cardiovascular disease and high blood pressure [8], The enzymatic method has received great attention for cholesterol analysis because it provides greater sensitivity and selectivity than the nonenzymatic method. The well-known principle of an enzyme-based cholesterol sensor is typically based on the reaction between cholesterol and the cholesterol oxidase (ChOx) enzyme. Free cholesterol is oxidized by cholesterol oxidase to produce 4-cholestene-3-one and hydrogen peroxide (H_2O_2), and the H_2O_2 generated can be used for indirect quantification of cholesterol [9, 10]. Amperometric measurement of anodic current of H_2O_2 is the most frequently monitored. However, the interference from some species such as ascorbic acid and uric acid that are easily oxidized at high voltage will occur during H_2O_2 measurement resulting in the poor accuracy of method. To overcome the weak point, the possible interference from easily oxidizable species in biological samples can be minimized using the monitoring of reduction current of H_2O_2 at low applied potential instead of oxidation current of H_2O_2. However, poor electrochemical reduction of H_2O_2 on bare carbon-based electrode is challenged during the monitoring of H_2O_2 reduction [11]. Therefore, the method to improve the measurement was explored. Recently, the modification of electrode has been increasingly interested to improve sensitivity of analyte detection and/or achieve more specific recognition. Nanomaterials, refered to materials between 1 and 100 nanometers in size, are one of the most exciting forefront fields in electroanalytical chemistry due to their many desirable properties. The application of nanomaterials for the development of electrochemical sensors has attracted growing interest and offered attractive new features including enhancing electron transfer kinetics due to their extremely high conductivity along particular directions and increasing signal current from the high surface area of nanostructured electrode

modifiers [12-14]. In addition, nanostructured materials can function as highly selective and tunable catalysts, due to their unique electronic or plasmonic structure, which is especially useful within detection systems utilizing electrocatalysis. In this work, silver nanoparticles (AgNP) have been considered as the modifier for modification of the electrode surface because they have a large specific surface area, excellent conductivity and an extraordinary electrocatalytic activity. In addition, AgNP also shows an excellent electrocatalytic activity for H_2O_2 reduction [11, 15-17]. Therefore, the novel cholesterol sensor with high sensitivity and selectivity was developed based on AgNPs modified electrode as described in Chapter IV part A.

Despite the fact that enzyme-based sensors show good selectivity and are highly sensitive, they are limited by their inadequate long-term stability, which originates from the nature of the enzymes [18, 19]. As a result, there have been enormous efforts made to alleviate these problems. One of the more appealing approaches is the use of nonenzymatic electrochemical sensors based on the direct electrocatalysis of analyte at the electrode. Sensors of this type have some outstanding properties that set them apart; they are simple, reproducible and highly stable [20, 21]. For nonenzymatic sensors, the electrochemical performance much depends on the catalytic activity of the catalysts toward analyte reaction [22]. In many cases, bimetallic catalysts have been shown to be superior to single metal catalysts. The synergistic effect on the performance of heterometallic nanocatalysts is subject to the surface electronic states, which are greatly affected by changing in the geometric parameters of the catalysts, and are related in particular to the local strain and the effective atomic coordination number on the surface [23, 24]. Therefore, the development of the non-enzymatic sensor based on bimetallic nanocatalysts was demonstrated in this work. Glucose, an important biomarker for diabetes, was used as the model to evaluate the developed sensor. The details of this study were described in Chapter IV part B.

Besides improvement of sensitivity and selectivity, low-cost and disposable platforms are also important aspects for the development of analytical sensors. Paper-based analytical devices (PADs) are new platform designed to address the growing need for simple, quantitative, and point-of-need assay platforms. PADs provide the advantages of low cost, low sample consumption, ease of use, portability, and disposability, making them to be ideal sensors for resource-limited settings [25, 26]. The most common analytical detection technique for PADs is colorimetry because analysis is relatively simple, and the technology is compatible with smartphone-based reporting systems. However, the important challenge of colorimetric detection is achieving the low detection limits with high sensitivity and selectivity [27, 28]. Therefore, electrochemical detection has become the particularly attractive partner for PADs, due to its instrumental simplicity, fast analysis times, high sensitivity, high accuracy, simple instrumentation, and low power requirements. In addition, it provides more stable and quantifiable signals. Typically, carbon electrodes, especially screen-printed carbon paste electrodes (SPCEs), have been extensively employed in PADs due to their easy fabrication, low cost, and potential for large-scale production. Despite these advantages, SPCEs are prone to surface fouling, which negatively impacts on analyte adsorption, electron-transfer kinetics, and electrocatalysis, resulting in poor limits of detection and reduction of device lifetime [29, 30]. Boron-doped diamond (BDD) is an alternative electrode for electroanalytical chemistry due to its superior properties over more traditional carbon and metal electrodes. BDD is a carbon-based p-type semiconductor, which exhibits quasi-metallic conductivity at boron doping concentrations of around 1 boron atom per 1700 carbon atoms [31]. The attractive features of BDD electrodes include remarkably low background currents, high mechanical robustness, stability in strong alkaline and acidic media, very wide potential window, and high resistance to surface fouling [32, 33]. On this basis, we developed a novel analytical platform using PAD coupled with boron doped diamond (BDD) thin film electrode. The design and fabrication procedure of devices were described in Chapter V part A.

Although, BDD thin film electrode is successfully applied as a working electrode for PADs, the BDD thin film electrode still has the limitations for applying in PADs platform in terms of limited geometry, high cost and need of cleaning step. Conductive BDD powder was first demonstrated by Fischer and Swain in 2005 [34]. The BDD powder is easily prepared from an insulating diamond powder substrate through microwave plasma-assisted chemical vapor deposition (MPCVD). Combination of the BDD powder with a conducting ink, followed by screen printing, yields a BDD paste electrode (BDDPE), which can potentially overcome the aforementioned limitations of BDD thin film electrode. Specifically, these BDDPE are an attractive alternative to conventional BDD electrode in terms of lower cost, simpler and faster electrode fabrication, and are ideal as a disposable and portable platform.[35] Therefore, the last part of this study is to demonstrate the use of BDD powder for the fabrication of disposable BDD paste electrode (BDDPE) in a PADs platform. To demonstrate the scope of developed device, the BDDPE coupled with PADs are employed for two applications; 1) for the quantitative detection of norepinephrine (NE) and serotonin (5-hydroxytryptamine, 5-HT) and 2) for the heavy metal analysis. The details for the fabrication of devices and applications were described in Chapter V part B.

1.2 Objectives of the research

This research consists of three goals for development and improvement:

1. To develop analytical method for the determination of NAC in drug formulations based on electrochemical detection using boron doped diamond electrode coupled with FIA.

2. To improve the sensitivity and selectivity of electrochemical sensors using the modification of electrode with nanomaterials and apply the proposed sensors for the determination of cholesterol and glucose.

3. To develop the electrochemical device platforms with high sensitivity, low cost, portability and disposability using PADs coupled with boron doped diamond based electrodes.

1.3 Scope of the research

To achieve the research objectives, the scope of the research was set as following:

1. The method for the determination of NAC was developed using boron-doped diamond electrode coupled to FIA. The effects of experimental parameters for NAC detection including pH, applied potential and scan rate on the response were investigated. Under the optimal conditions, the analytical performance of the proposed method was studied, including range of linearity, limits of detection and quantification, repeatability and reproducibility. The developed method was also applied for NAC determination in commercial drug samples.

2. The cholesterol sensor based on the coupling of enzymatic assay and electrochemical detection was developed. Silver nanoparticles modified glassy carbon electrode was fabricated by electrodeposition technique and used as the working electrode. The developed sensor was applied to determine cholesterol in bovine serum.

3. The non-enzymatic glucose sensor was developed using bimetallic Pt/Au nanocatalyst modified BDD electrode. Pt/Au nanocatalyst was synthesized by electrodeposition technique by sequentially depositing Au and Pt on the surface of BDD electrode. The analytical performances including linearity and selectivity for glucose detection of Pt/Au/BDD electrode were studied and compared to Pt/BDD, Au/BDD, and commercial flat Pt electrodes.

4. A PADs coupled with silver nanoparticles modified boron doped diamond (AgNP/BDD) electrode was designed and fabricated. Wax printing was used to create the hydrophilic and hydrophobic areas on filter paper. The counter and reference

electrodes were fabricated on the hydrophilic area of wax-printed paper by screen-printing in house. The AgNP/BDD electrode was used as working electrode. The proposed device was applied as an enzymatic cholesterol sensor.

5. A BDD paste electrode (BDDPE) was prepared and used as a working electrode for microfluidic paper-based analytical device (μPAD). The electrochemical performance of BDDPE including capacitive current and solvent window was studied and found in contrast with carbon paste electrode (CPE) and traditional BDD electrodes. The developed devices were applied for the measurements of biological species (norepinephrine and serotonin) and heavy metals (Pb and Cd).

There are six chapters in this dissertation. Chapter I is the introduction. Chapter II is the theory of electrochemical technique, flow injection analysis, and paper-based analytical device. Chapter III reports on the development of electrochemical method for NAC determination in drug formulations. Chapter IV presents the improvement of sensitivity and selectivity for electrochemical sensors based on the modification of electrode with metal nanoparticles. Chapter V reports on the development of electrochemical sensing platform using PAD coupled with boron doped diamond based electrodes. Lastly, chapter VI is the conclusions and future perspectives.

CHAPTER II

THEORY

2.1 Electrochemical technique

Electroanalytical chemistry is a class of analytical chemistry techniques that studies an analyte by measuring the electrical quantities, such as current, potential, and charge, and their relationship to chemical parameters. Generally, electroanalytical measurements can be divided into two principal types including potentiometric and potentiostatic techniques.

Potentiometry is static or zero current technique in which the information about the sample composition is obtained from the measurement of the potential established across a membrane. Different types of membrane materials have been developed to impart high selectivity. The most commonly used potentiometric sensor is an Ion-Selective Electrode (ISE). ISE is a membrane electrode that converts the activity of a specific ion dissolved in a solution into an electrical potential. This potential is measured under condition of zero current, and it varies logarithmically with the activity (concentration) of the species generated according to the Nernst equation.

Potentiostatic or controlled-potential technique is based on the study of charge-transfer processes at the electrode-solution interface. The electrode potential is being used to derive an electron-transfer reaction and the resultant current is measured. Such a controllable parameter can be viewed as “electron pressure” which forces the chemical species to gain or lose an electron called reduction or oxidation, respectively. In this technique, the potential is applied from an external

source to drive the transfer of electrons in the electric circuit. The redox reaction occurs at the surface of an electrode. The current or electrode reaction rate is governed by the rates of processes such as mass transfer, electron transfer at the electrode surface, chemical reactions preceding, and other surface reactions, for example adsorption, desorption, or crystallization as shown in Figure 2.1. The advantages of controlled-potential techniques include high sensitivity, high selectivity, wide linear range, portable and low-cost instrumentation, and the capability for speciation analysis.

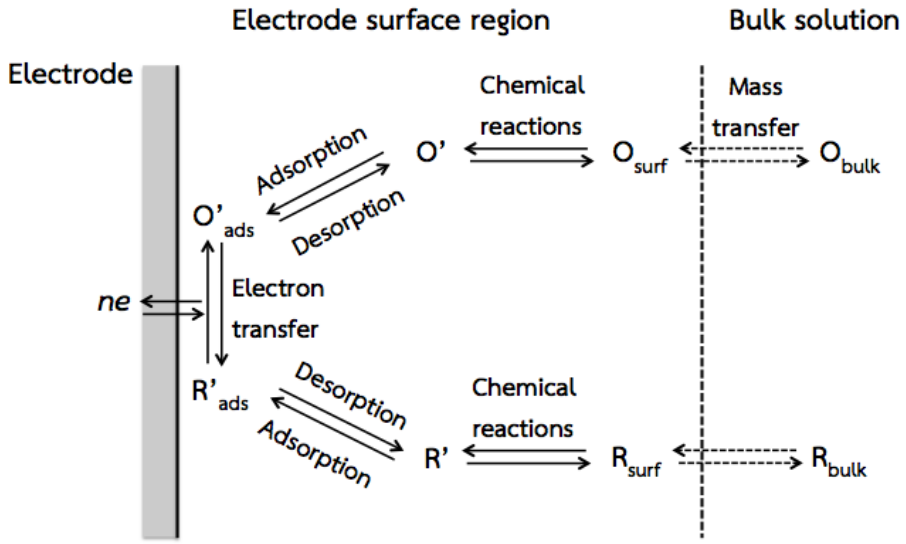

Figure 2.1 Pathway of electrode reaction [36]

The objective of controlled-potential electroanalytical experiments is to obtain a current response that is related to the concentration of the target analyte. This objective is accomplished by monitoring the transfer of electron(s) during the redox process of the analyte:

$$O + ne \longrightarrow R \quad \text{.....eq. 2.1}$$

where O and R are the oxidized and reduced forms of redox coupled, respectively. The reaction will occur in a potential region that makes the electron transfer thermodynamically or kinetically favorable. For a system controlled by the laws of

thermodynamic, the potential of the electrode can be used to determine the concentration of the electroactive species according to the Nernst equation:

$$E = E^{O} + \frac{2.3RT}{nF} \log \frac{C_o(0,t)}{C_R(0,t)} \quad \text{.....eq. 2.2}$$

where E^0 is the standard potential for the redox reaction, $C_o(0,t)$ and $C_R(0,t)$ are the concentration of oxidized and reduced form, *R* is the universal gas constant (8.314 J K^{-1} mol^{-1}), *T* is the Kelvin temperature, *n* is the number of electrons transferred in the reaction, and *F* is the Faraday constant (96,487 coulombs).

In this dissertation, the electrochemical measurements based on controlled-potential techniques are in focus.

2.1.1 Faradaic and nonfaradaic processes

There are two types of processes that occur at electrodes including faradaic and nonfaradaic processes. Faradaic current is the charge transferred across the metal-solution interface which resulted from a change in oxidation state of the electroactive species obeying Faraday's law. The faradaic process can be simply illustrated as follows: when the applied potential is higher than the potential of the electroactive species, the reduction reaction occurs at the working electrode. As a result electroactive species diffuses from the bulk solution to the electrode surface, and the reduction product simultaneously diffuses from the bulk solution to the electrode surface. The magnitude of this current depends on the rate of the electrochemical reaction.

For nonfaradaic, this process does not involve charge transfer. Nonfaradaic current is the result from the occurring of adsorption and desorption processes. In voltammetric measurements, nonfaradaic current is termed as the background current.[36]

2.1.2 Mass transfer

Mass transfer is the movement of material from one location in solution to another, arises either from differences in electrical or chemical potential at the two locations or from movement of a volume element of solution. The mass transfer occurs by three different modes as illustrated in Figure 2.2:

1. Diffusion is the movement of a species under the influence of a gradient of chemical potential. Ions will move from a region of high concentration to region of low concentration.

2. Migration is the movement of a charged body under the influence of an electric field. The positive ion species will move to the negative charged electrode, and the negative ion species will move to the opposite way. The increase or decrease velocity of ions depends on the potential at electrode surface. To eliminate the migration of interesting ions, the addition of a large concentration of electrolyte is usually applied.

3. Convection is the transport to the electrode by a gross physical movement. The flow of fluid occurs because of natural convection (convection caused by density gradients), and forced convection.

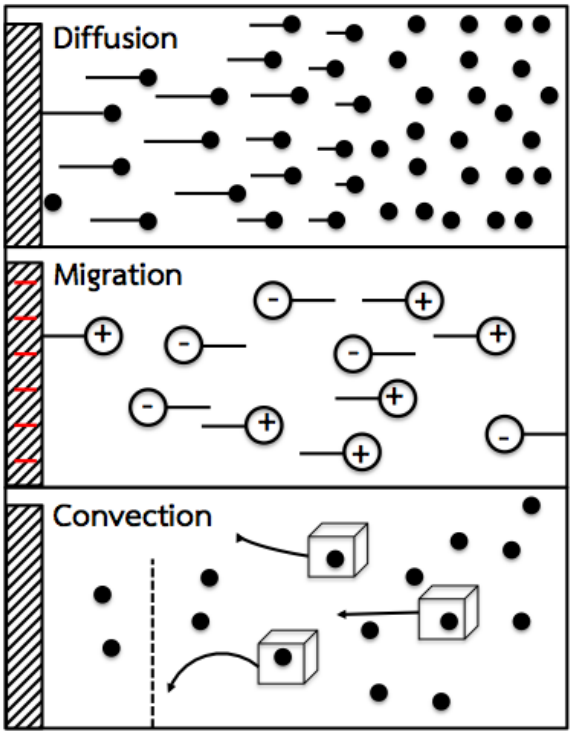

Figure 2.2 The three modes of mass transport [37]

2.1.3 Voltammetry

Voltammetry is a category of electroanalytical methods which the current at an electrode is measured as a function of potential or voltage applied to electrode. The resulting current-potential plot is called a voltammogram. Voltammetry can be used to analyze the electrochemical property of electroactive species that can be oxidized or reduced at the working electrode. The potential of electrode is the controlled parameter which causes the electroactive specied to be oxidized or reduced. When the potential of electrode is applied to more negative direction, it becomes more strongly reducing, and the reduction reaction occurs. In contrast, when the potential of electrode is applied to more positive direction, it becomes more strongly oxidizing, and the oxidation reaction occurs. Voltammetry can be classified as many types such as linear sweep voltammetry, polarography, cyclic voltammetry, staircase voltammetry, normal pulse voltammetry, differential pulse voltammetry, square wave voltammetry, anodic stripping voltammetry, cathodic stripping voltammetry, and adsorptive stripping voltammetry.

The voltammetric techniques used in this dissertation including cyclic voltammetry, differential pulse voltammetry, square wave voltammetry, anodic stripping voltammetry, amperometry, and chronoamperometry, are described.

2.1.3.1 Cyclic voltammetry

Cyclic voltammetry (CV) is a very popular technique for initial electrochemical studies of developed electrochemical system. This technique has proven very useful in obtaining qualitative information about electrochemical processes such as location of redox potentials of the electroactive species, a number of intermediates, a number of reaction steps, and the stability of the product from the electrochemical reaction. However, CV is rarely used for quantitative application [38-40].

In a cyclic voltammetry experiment, the working electrode potential (in an unstirred solution) is scanned linearly versus time as a triangular potential waveform as shown in Figure 2.3a. The potential is scanned linearly from an initial value to a set value (known as the switching potential), after the set potential is reached, the working electrode potential is scanned in the opposite direction to return to the initial potential. While the potential is being scanned, the resulting current is measured by potentiostat. The resulting plot of current versus potential is called a cyclic voltammogram.

The expected cyclic voltammogram of a reversible redox couple during a single potential cycle is illustrated in Figure 2.3b. It is assumed that there is only the oxidized form O in the initial solution. Thus, the potential is scanned in a negative direction for the first half-cycle, starting from a potential where no reduction occurs. When the applied potential reaches to the formal potential (E^0) for the redox process, a cathodic current begins to increase and it is then reached as a peak. During the potential is scanned to negative region in which the reduction process takes place, R molecules are generated and accumulated near the surface. After the applied potential traverse at least $90/n$ mV beyond the observed cathodic peak, the

potential sweep is reversed to the positive direction. R molecules are reoxidized back to O, and the anodic peak is observed [38, 39].

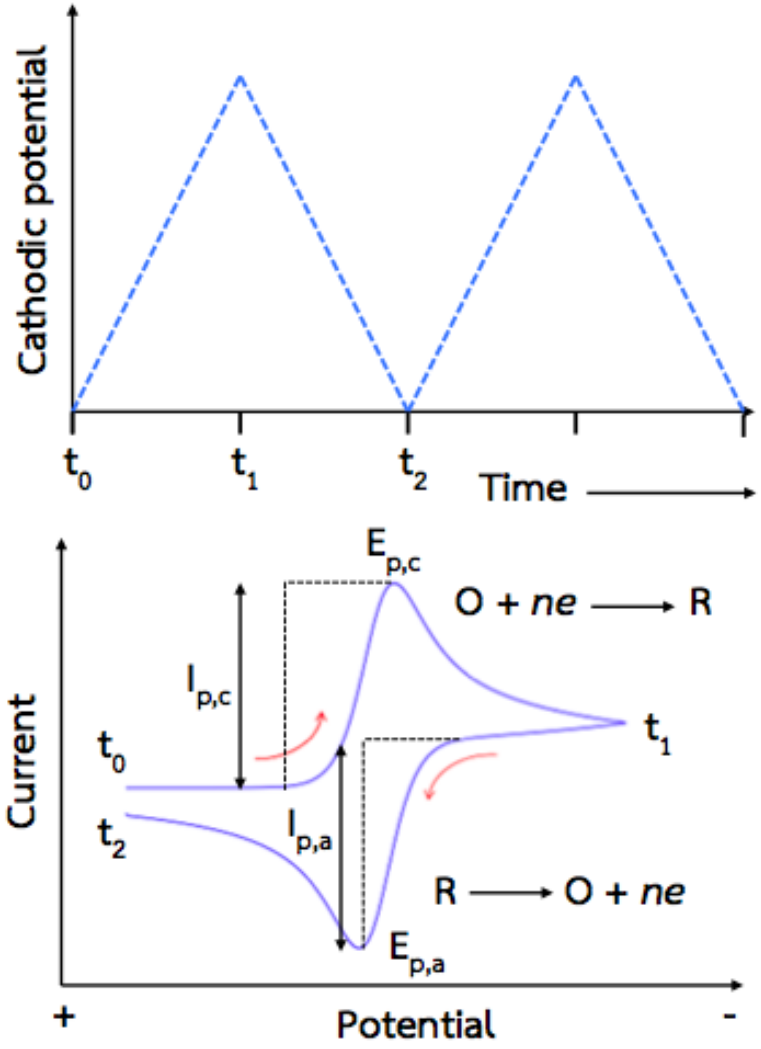

Figure 2.3 (a) Potential-time excitation signal in cyclic voltammetric experiment (b) typical cyclic voltammogram for a reversible process [39]

For reversible system, at 25 °C, the concentration is related to peak current by the Randles-Sevcik equation[37]:

$$i_p = (2.69\times10^5)n^{3/2}ACD^{1/2}v^{1/2} \text{.....eq. 2.3}$$

where n is the number of electrons, A is the electrode area (in cm^2), C is the concentration (in mol cm^{-3}), D is the diffusion coefficient (in $cm^2\ s^{-1}$), and v is the scan

rate (in V s^{-1}). The peaks position on the potential axis (E_p) is related to the formal potential of the redox process. For a reversible system, the formal potential is centered between $E_{p,a}$ and $E_{p,c}$:

$$E^O = \frac{E_{p,a} + E_{p,c}}{2} \quad \text{.....eq. 2.4}$$

The separation between the peak potentials is given by:

$$\Delta E_p = E_{p,a} - E_{p,c} = \frac{0.059}{n} V \quad \text{.....eq. 2.5}$$

Therefore, the number of electrons transferred in the redox reaction can be determined using the separation of cathodic and anodic peak potentials. For example, a redox reaction that has one electron transferred exhibits ΔE_p of about 59 mV. For a reversible wave, E_p is independent of scan rate. In addition, the current is proportional to the square root of the scan rate, which indicates the electrochemical process is controlled by diffusion [41, 42].

2.1.3.2 Differential-Pulse Voltammetry

Differential-pulse voltammetry (DPV) is an extremely useful technique for measuring trace levels of organic and inorganic species. The waveform of DPV is showed in Figure 2.4a. The fixed-magnitude pulses which superimposed on a linear potential ramp, are applied to the working electrode. For each pulse, current is measured at two points. The first point is before the application of the pulse (t_1), and the second point is at the end of the pulse when the charging current has decayed (t_2). The first current (i_1) is instrumentally subtracted from the second current (i_2), and this current difference ($\Delta i = i_1 - i_2$) at these points for each pulse is determined and plotted against the base potential. Figure 2.4b shows the resulting differential pulse voltammogram. The peak height is directly proportional to the concentration of the corresponding analytes.

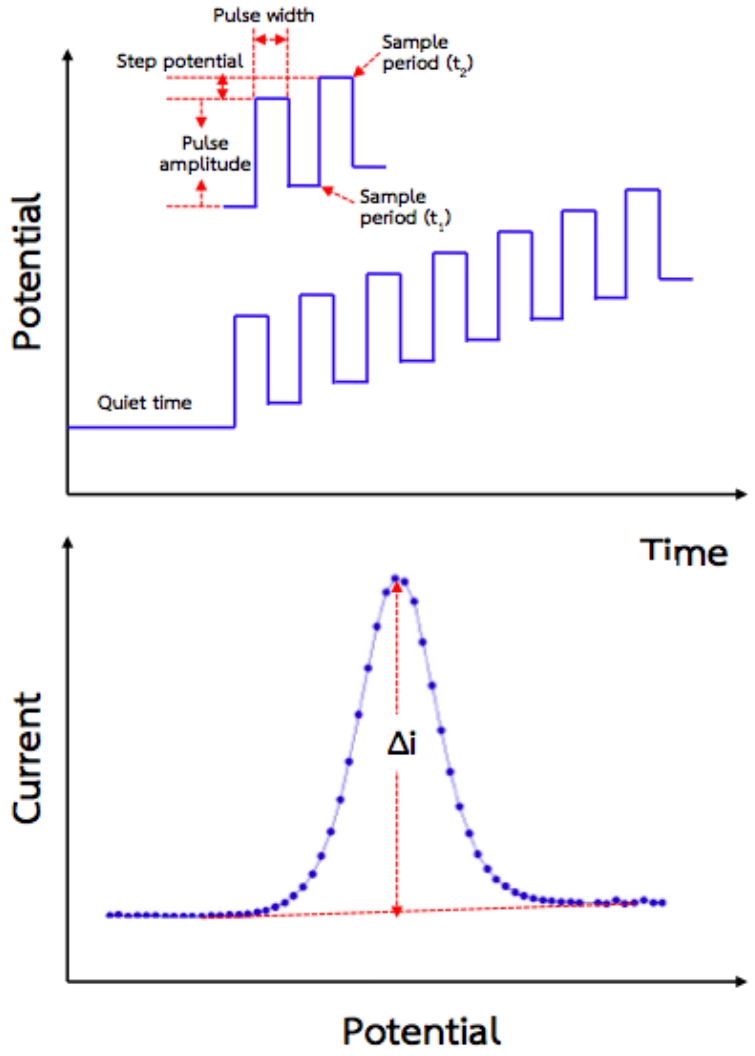

Figure 2.4 (a) Excitation signal for differential-pulse voltammetry (b) Differential-pulse voltammogram

2.1.3.3 Square-wave anodic stripping voltammetry

Square-wave anodic stripping voltammetry (SWASV) is a particularly attractive electrochemical technique for measuring trace heavy metals. This technique combines the advantages of square-wave voltammetry and anodic stripping voltammetry. Square-wave voltammetry (SWV) is a potential electrochemical technique among the various pulse techniques for analytical applications. The waveform of SWV composed of a symmetrical square wave, superimposed on a base staircase potential as shown in Figure 2.5a. Current samples are taken twice per cycle, once at the end of the forward pulse (t_f) and once at the end of the reverse

pulse (t_r). The forward current arises (i_f) from the first pulse per cycle, which is in the direction of the staircase scan. The reverse current (i_r) is taken at the end of the second pulse, which is in the opposite direction. A difference current (Δi) is calculated as $i_f - (-i_r)$. Since the opposite signs of forward and reverse current, the net current is larger than either the forward or reverse components, resulting in an excellent sensitivity of this technique. When the difference in current is plotted, the shape of the square wave volrammogram is obtained as shown in Figure 2.5b.

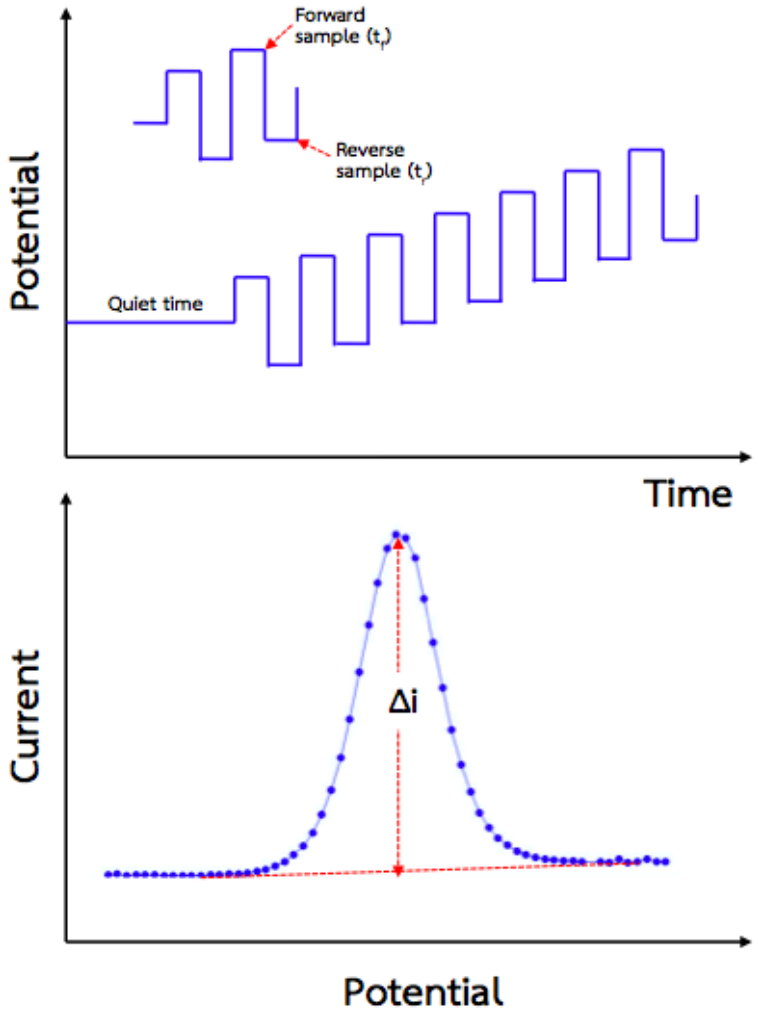

Figure 2.5 (a) Excitation waveform for square-wave voltammetry (b) square-wave voltammogram

For anodic stripping votammetry, there are two steps of deposition (accumulation) and stripping (measurement). Potential waveform is shown in Figure 2.6. In the first step of deposition, target metal ions are electrochemically deposited onto the electrode surface by applying an appropriately cathodic potential. This step is typically performed under controlled stirring conditions. Then, the deposition is ceased and the deposited metal is oxidized or stripped from the electrode, back into the solution, by scanning the square-wave potential sweep from negative to positive direction. The resulting anodic diffusion current is then used to determine the concentration of the metals.

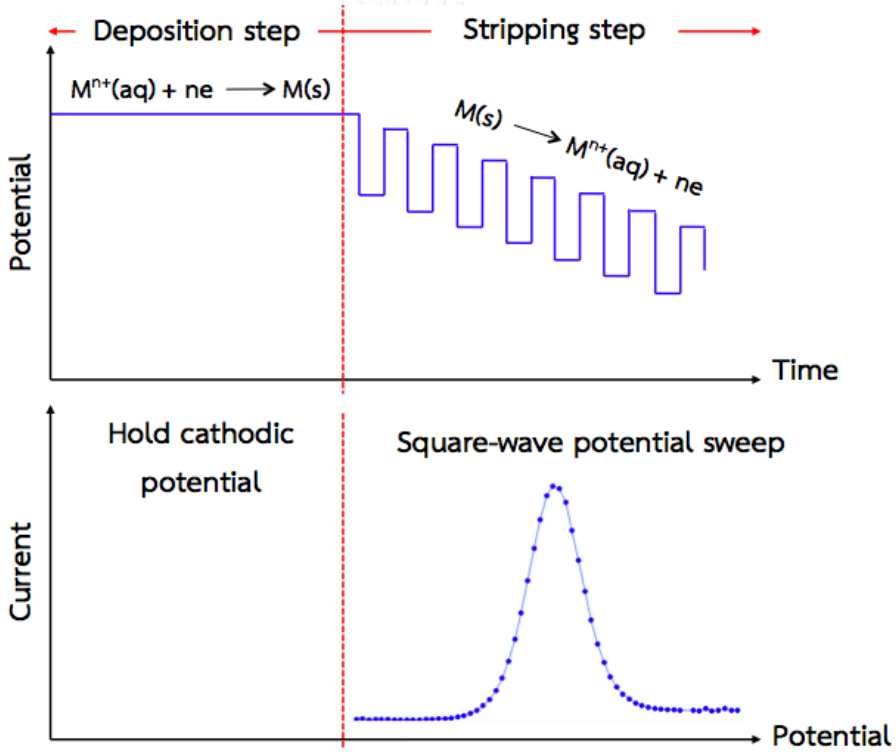

Figure 2.6 (a) Potential waveform for square-wave anodic stripping voltammetry (b) the resulting voltammogram

2.1.4 Amperometry

Amperometry is one of the most widely used detection method for electrochemical sensors. Amperometric detection involves the use of a potentiostat

for applying a constant potential to the working electrode, relative to a reference electrode. The current, produced from redox reactions that occur at the working electrode surface, is measured. With a conventional three-electrode setup, an auxiliary electrode is also used to ensure that no current passes through the reference electrode and to minimize ohmic potential drops. The resulting current is directly proportional to the number of moles of analyte oxidized or reduced at the electrode surface. This can be described by Faraday's law [36]:

$$Q = nFN \quad \text{.....eq. 2.6}$$

where Coulombs (*Q*) is obtained from the peak area for a particular analyte, and directly proportional to the number of moles (*N*) of product converted at the electrode surface, the number of electrons (*n*) transferred in the redox reaction, and Faraday's constant (96485 C/mol)

2.1.5 Chronoamperometry

Chronoamperometry is another powerful method for quantitative analysis. With the chronoamperometry, the current is measured versus time as a response to a sequence of potential pulse. As in the potential waveform (Figure 2.7a), the potential of the working electrode is held at E_1 at the beginning of the transient experiment. At t=0, the potential is instantaneously changed to a new value E_1, and corresponding current time response is recorded as shown in Figure 2.7b.

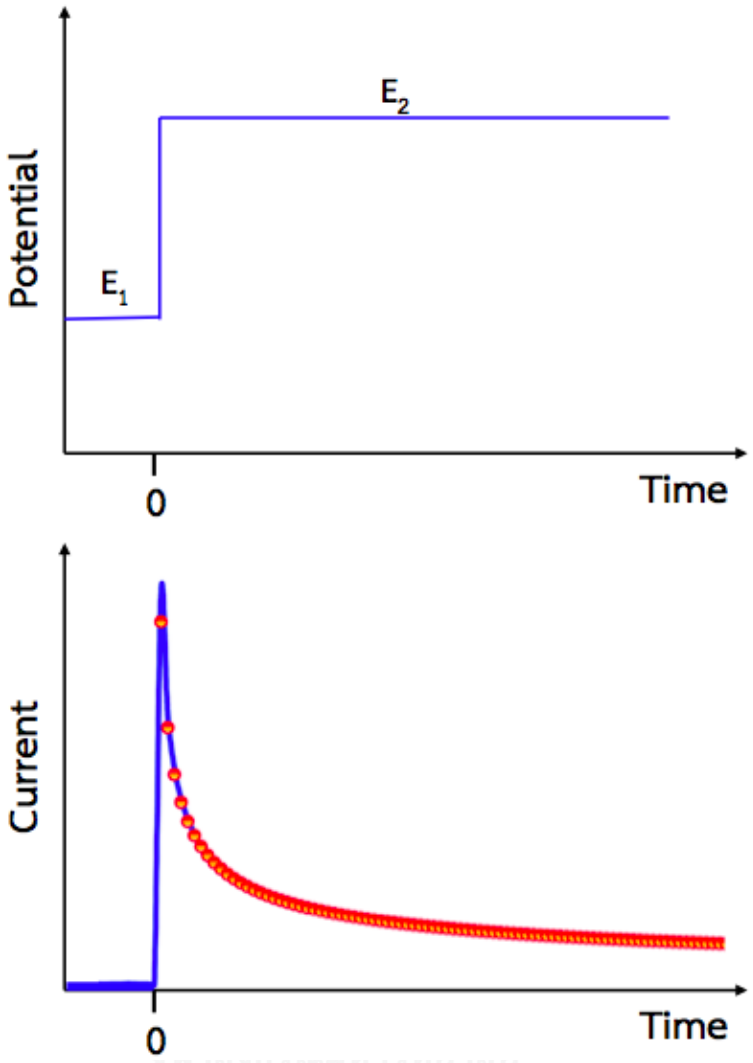

Figure 2.7 (a) potential-time waveform for chronoamperometry (b) the resulting current-time response [37]

2.1.6 Electrochemical cell/instrumentation

Typically, voltammetric measurements are performed in a three electrode system to maintain a stable reference potential. The three electrodes contain working electrode (WE), reference electrode (RE), and auxiliary/counter electrode (CE). These electrodes are immersed in an electrolyte solution. The most frequently used electrolytes are liquid solutions containing ionic species in either water or a non-aqueous solvent. Additionally, the solvent/electrolyte system must be of sufficiently low resistance [43].

2.1.6.1 Potentiostat

A potentiostat is a device used to keep a WE at desired potential with respect to a RE. This is done by a current which is passed from the working electrode to a CE. The arrengement of the potentiostat and the electrodes is sketched in Figure 2.8.

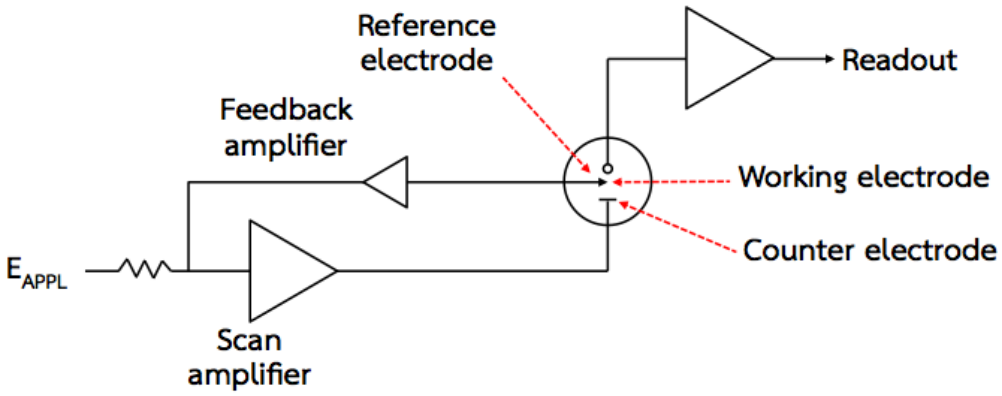

Figure 2.8 Schematic diagram of a three-electrode potentiostat [38]

2.1.6.2 Working electrode

Working electrode (WE) is an electrode in electrochemical cell that responds to the target analytes. WE should have large potential range suitable for both anodic and cathodic reactions. In addition, it should possess long term stability and an easily reproducible surface. WE is usually made from inert metals or carbon such as glassy carbon, boron doped diamond or screen-printed carbon. Although metal-based electrodes exhibit higher electron transfer rate than carbon-based electrode, carbon electrodes are still popular because of their broad potential window, low background current, rich surface chemistry, low cost, chemical inertness, and suitability for various sensing and detection applications. The properties of different types of carbon electrodes used in this dissertation are discussed below.

2.1.6.2.1 Glassy carbon electrode

Glassy carbon electrode (GCE) has become an interesting and widely applied electrode material which possesses the properties of both glassy and ceramic materials combined with graphite. The structure of glassy carbon involves thin, tangled ribbons of cross-linked graphite-like sheets. This electrode needs the surface pretreatment step to create active, and reproducible glassy-carbon electrodes and to enhance their analytical performance. The surface pretreatment is usually performed by polishing with successively smaller alumina particles (down to 0.05 mm). The electrode should then be rinsed with deionized water before use. GCE is suitable to use as an electrochemical sensor due to its excellent mechanical and electrical properties, wide potential window, chemical inertness (solvent resistance), and relatively reproducible performance [38].

2.1.6.2.2 Boron doped diamond electrode

Boron doped diamond (BDD) is a carbon-based p-type semiconductor, which exhibits quasi-metallic conductivity at boron doping concentrations of around 1 boron atom per 1700 carbon atoms [44]. Diamond is a cubic lattice structurally, the complete sp^3 hybridisation of carbon results in extensive tetrahedral bonding throughout the lattice, leading to many extreme properties such as hardness, very high thermal conductivity and extremely high electrical resistivity. Naturally, diamond is a good insulator with a large band gap of 5.4 eV. The semiconductor behavior can be generated after doping diamond crystals with impurities. Boron is the preferred dopant because boron atoms can effectively take up the same position as displaced carbon atoms, with relatively small activation energy (0.37 eV). Some of the valence band electrons are thermally promoted to the boron acceptors, leaving free electrons in the dopant band and holes in the valence band to support the flow of current. The electrical conductivity of the BDD is influenced by the boron-doping level. If the doping level is increased, the BDD becomes more metallic. As shown Figure 2.9a, the conventional BDD electrodes are typically grown on Si (111) wafer or TiO_2 substrates by chemical vapour deposition (CVD). Carbon source (methane or

acetone) and boron source (B_2H_6 or $B(OCH_3)_3$), are fed into the CVD reactor chamber in the presence of hydrogen (H_2) [45, 46]. The attractive features of BDD electrodes include remarkably low background currents, high mechanical robustness, stability in strong alkaline and acidic media, very wide potential window, and high resistance to fouling.[47, 48]

2.1.6.2.3 Boron doped diamond paste electrode

Boron doped diamond paste electrode (BDDPE) is demonstrated to overcome the conventional BDD electrodes which are incompatible with point-of-care sensors, in terms of limited geometry, manufacturing time, and cost. In 2005, conductive BDD powder was first fabricated by Swain group [34]. The BDD powder is easily prepared from an insulating diamond powder substrate (8–12 μm diameter) through microwave plasma-assisted chemical vapor deposition (MPCVD). The BDDPE can be easily fabricated by mixing the BDD powder with a conducting ink, following by screen printing (Figure 2.9b) [49]. The BDDPE is an attractive alternative compared to conventional BDD electrodes in terms of low cost, simple and fast electrode fabrication, and is ideal as a disposable and portable platform.

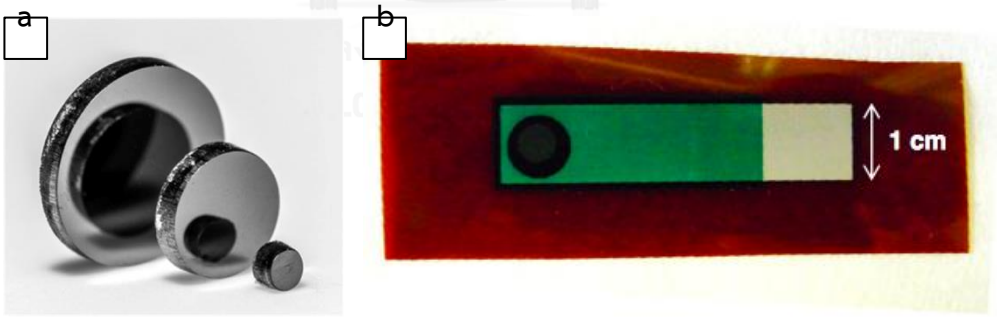

Figure 2.9 (a) Freestanding BDD electrode[45] (b) BDDP-printed electrode [49]

2.1.6.2.4 Nanomaterial modified electrode

The modification of conventional electrodes for enhancing current response and/or detection selectivity is very important in the development of electrochemical sensors. Nanomaterial modified electrode is known to have a number of attributes

that make them highly appealing to electrochemists, especially for use in electroanalysis. The properties of materials with nanometer dimensions are significantly different from those of atoms and bulks materials. These include high surface area, high catalytic activity, and allowing for the use of much less material [12, 13].

Metal nanoparticles such as Au, Ag and Pt, have been attracting great attention for modifying electrodes due to their unique electronic and catalytic properties [31, 41, 50]. The modification of electrodes with nanoparticulate metal species not only increases active surface area and enhances diffusion, but also makes the electrode sensitive to analytes that would not be ordinarily observed at the bare electrode. Metal nanoparticles exhibit high catalytic activity and facilitate electron transfer for many electrochemical reactions. Electrodeposition is a highly convenient and attractive technique for modifying electrode materials. Electrodeposition process uses electric current to reduce dissolved metal cations, so the reduced metals form a thin coherent metal coating on an electrode [41, 51]. This technique is outstanding in terms of simple, quick, reproducible, and can adapt to a wide range of substrates. In addition, it requires little or no advanced equipment with expensive technology.

2.1.6.3 Reference electrode

Reference electrode (RE) is of constant potential. RE should have a well-defined, stable equilibrium electrode potential unaffected by the electrolyte species. Most common primary reference electrode is Ag/AgCl electrode which is composed of an Ag wire immersed in a solution saturated with AgCl and KCl [36].

2.1.6.4 Counter electrode

Counter electrode (CE) permits the passage of current in an electrochemical reaction through it without disturbing the potential of the reference electrode. Pt electrode is often the best choice in this regard due to its inertness and speed which most electrode reactions occur at its surface [36].

2.2 Flow injection analysis

Flow injection analysis (FIA) is an automated analytical processing technique based on the injection of a definite liquid sample solution volume into an unsegmented continuously flowing stream, followed by the detection of the interested analyte. Schematic diagram of the basic FIA system is shown in Figure 2.10. which consists of a pump, injection valve, a reaction coil tubing, and a detector with flow-through cell connected to a recorder for recording the signal. FIA is compatible with a variety of chemical processes and detection systems. Additionally, it offers several advantages in terms of considerable decrease in sample (normally using 10 to 50 µL) and reagent consumption, high sample throughput (50 to 300 samples per hour), high reproducibility, reliability, and ease of automation [52, 53].

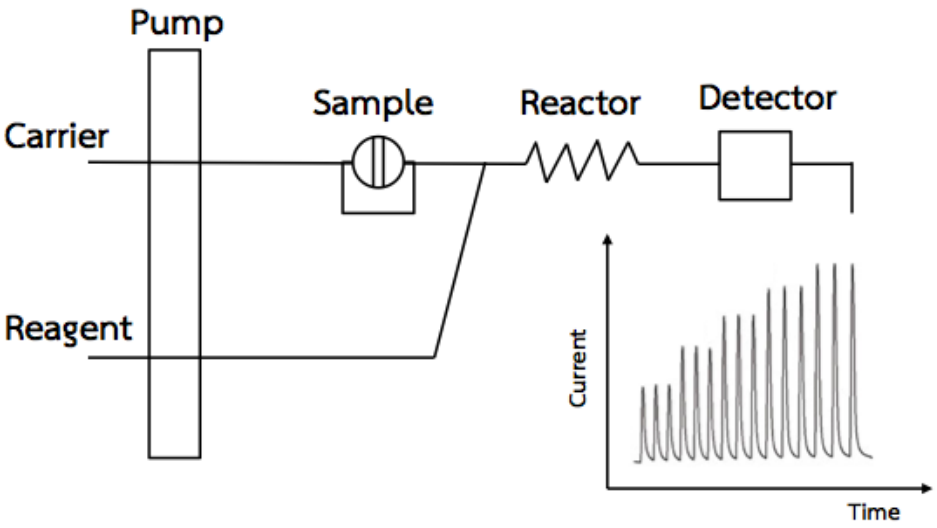

Figure 2.10 Schematic diagram of flow injection analysis system[53]

2.3 Paper-based analytical device

Paper-based analytical devices (PADs) are analytical devices that use a paper as the substrate. The hydrophobic material is deposited on the paper substrate and acting as the barrier for confining the aqueous or sample solution. PADs have

emerged as a promising technology to address the growing need for simple, quantitative, and point-of-need assay platforms. These devices provide the advantages of low cost, low sample consumption, ease of use, portability, and ease of disposability, making them ideal sensors for resource-limited settings. Moreover, flow can be generated via capillary forces, precluding the need for mechanical or electrical pumps [25, 54].

2.3.1 Fabrication

The hydrophobic barriers which constrain the flow can be easily fabricated by a variety of methods, such as wax printing[55], photolithography[56], or printing of hydrophobic polymers[57, 58]. In this dissertation, wax printing was chosen to create the paper pattern. The wax pattern can be easily designed by computer. The hydrophobic walls of wax can be patterned in the paper using a commercially available printer and hot plate. As shown in Figure 2.11, the fabrication process involves two core operations: (i) printing patterns of wax on the surface of paper and (ii) melting the wax into the paper to form complete hydrophobic barriers. Wax printing is outstanding in terms of low cost, fast, simple, and no mask required. Additionally, it is particularly well-suited for large scale production.

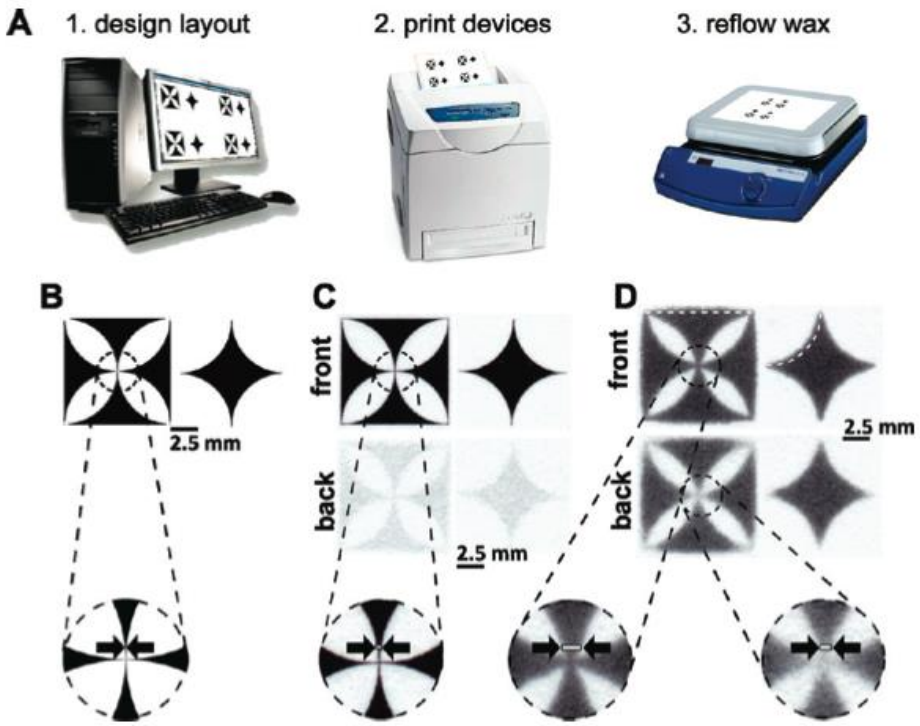

Figure 2.11 Wax printing process [55]

2.3.2 Detectors

One critical step for PADs is the ability to quantify the analyte. Various classical detection motifs such as colorimetry [59], electrochemistry [44], electrochemiluminescence [60], chemiluminescence [61], and fluorescence [62], have been applied for PADs. Colorimetry is the most common analytical detection technique for PADs because analysis is relatively simple. The colorimetric device configurations work on the principle that visible colors result from the reaction between analyte and chromogenic reagents (Figure 2.12). The chromogenic reagents are chosen to selectively react with the analyte with minimal interference from other substances. The color intensity is proportional to analyte concentration. In addition, colorimetric detection is compatible with smartphone-based reporting systems. However, the important challenge for colorimetric PADs is achieving low detection limits with high sensitivity and selectivity.

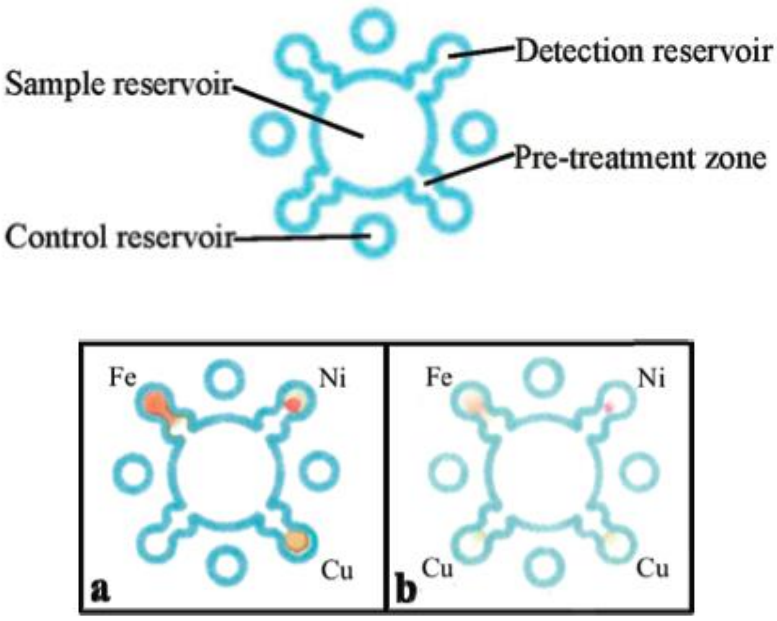

Figure 2.12 Colorimetric paper-based analytical device [63]

Electrochemistry is an attractive alternative because detection limits are lower and sensitivity is higher. Electrochemical paper-based analytical device (ePAD) was first demonstrated by Dungchai et al. in 2009 [56]. This detection motif is a particularly attractive partner for PADs, due to its instrumental simplicity, fast analysis times, high sensitivity, high accuracy, simple instrumentation, and low power requirements. For the fabrication of ePAD, three electrodes including working, reference, and counter electrodes, are typically prepared on the paper substrate as shown in Figure 2.13. The electrode materials that have been demonstrated for ePAD, include carbon, metals, and nanoparticle. These materials were fabricated by a variety of techniques including screen/stencil-printing, pencil/pen drawing, inkjet-printing and wire placement.

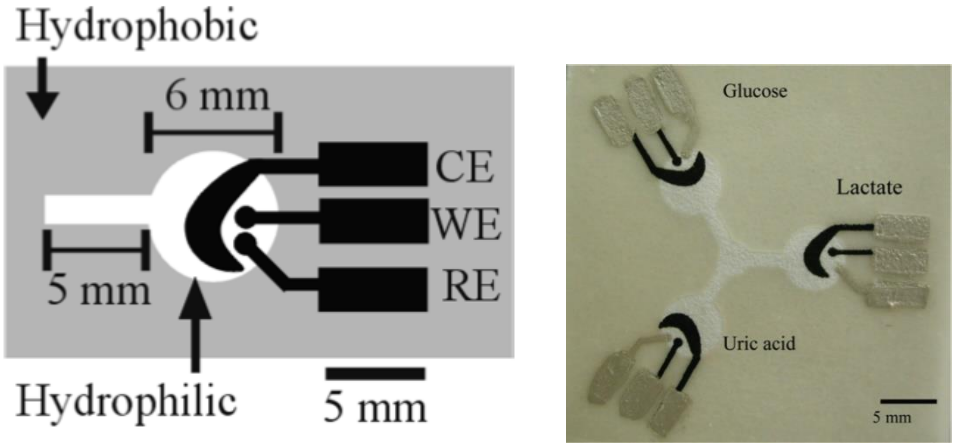

Figure 2.13 Basic design of electrochemical paper-based analytical device [56]

CHAPTER III

DEVELOPMENT OF ELECTROCHEMICAL METHOD FOR PHAMACUTICAL APPLICATIONS

Ultrasensitive and simple method for determination of N-Acetyl-L-Cysteine in drug formulations using diamond sensor

Siriwan Nantaphol,[a] Orawon Chailapakul,[a,] Weena Siangproh(s)[b]*

[a] Electrochemistry and Optical Spectroscopy Research Unit, Department of Chemistry, Faculty of Science, Chulalongkorn University, 254 Phayathai Road, Pathumwan, Bangkok 10330, Thailand

[b] Department of Chemistry, Faculty of Science, Srinakharinwirot University, Sukhumvit 23, Wattanna, Bangkok 10110, Thailand

* Corresponding author

Electroanalysis 26 (2014): 1024 – 1030

Abstract

A boron doped diamond (BDD) electrode coupled to flow injection analysis (FIA) was firstly developed for determination of *N*-acetyl-*L*-cysteine (NAC) in drug formulations. The effects of experimental parameters including pH, applied potential and scan rate on the response were investigated. FIA amperometry was applied as an automatic method for the quantitative detection of trace amounts of NAC. A wide linear range of 0.5 – 50 µmol/L and a low detection limit of 10 nmol/L were obtained. The results of amperometric determinations show a very good reproducibility, and the RSD for the measurement based on 10 measurements was <3.7% and <4.1% for intra- and inter-day, respectively. The benefits of the proposed method are fast, simple, sensitive and no requirement of complicated operational steps.

3.1 Introduction

N-acetyl-*L*-cysteine (NAC) is a small molecular weight thiol compound. It is an acetylated form of the amino acid *L*-cysteine. NAC is employed as a mucolytic agent that is commonly used to reduce sputum viscosity in chronic asthma and bronchitis and to reduce the viscosity of ophthalmic secretions[1, 6]. In addition, NAC has proven to be a very important antioxidant in a wide variety of situations: it decreases membrane damage by superoxide-generating systems in porcine aortic endothelial cells, decreases the toxicity of diquat to hepatocytes, protects animals against paracetamol toxicity, protects against UV-B-induced, against cardiovascular and respiratory diseases. It is also very beneficial in treatment of human immunodeficiency virus infection [64-66]. Presently with it was used in cancer treatment, NAC is one of the most promising chemopreventive agents [67].

As mentioned, NAC has received considerable attention, due to its pharmaceutical and clinical importance. Therefore, there is a pressing need to develop fast and sensitive method for the determination of NAC, particular in quality management in drug analysis.

Numerous laboratories based analytical methods have been developed to detect and quantitate levels of NAC in aqueous solutions as well as in biological fluids. Most of the methods involve reversed-phase high-performance liquid chromatography (RP-HPLC) using various detectors such as UV [68-73]. Liquid chromatography-UV-mass spectrometry (LC-UV-MS) or liquid chromatography-tandem mass spectrometry (LC-MS-MS), these are a relatively new method of quantitative analysis, which is usually used in the detection of impurities present along with NAC, in pharmaceutical formulations [1, 74, 75].

In a number of all mentioned application, the time delay in the derivatization steps are unacceptable. Moreover, the analyzing cost is high and analyzing instrument generally requires an experience operators. In order to improve on these weak points, electrochemical detection was taken to be a candidate for a novel analysis system. In literature, NAC was electrochemically detected using

voltammetric method. Generally, the oxidation of NAC at a glassy carbon electrode (GCE) has a very poor electrochemical response, while it is very complicated at Hg, Au, and Pt electrodes [76, 77]. Thus, different chemically modified electrodes were continuously developed to solve the analytical problem [78-85]. Anyhow, there still remains an important problem of reproducibility in electrode preparations.

Boron doped diamond thin film (BDD) electrode is an alternatative electrode that possesses many of the same attributes as conventional electrodes and, therefore, appears to be a viable material for the electroanalytical measurement. The unique properties of BDD electrode in term of (i) large overpotentials for hydrogen evolution and oxygen reduction, (ii) a large overpotential for oxygen evolution (large positive window), (iii) low background current, (iv) resistance to electrode fouling, (v) slightly adsorption onto electrode surface; which make it ideally suited for various applications [86]. For examples, BDD electrodes have successfully been applied as electrochemical sensor for direct determination of albendazole[87], simultaneous determination of hydrochlorothiazide and losartan [88], and this electrode was also applied for fast and simultaneous determination of nimesulide and paracetamol with batch injection analysis [89].

As a continuation of our previous works on the use of BDD electrode in applications, in the next section, BDD electrode was utilized to investigate the electrochemical property of NAC using cyclic voltammetry. For the following part, the BDD electrode will be applied as a detector in flow injection analysis system for the determination of NAC. The promising properties of BDD electrode coupled to on-line FIA showed potential to detect very low concentration of NAC. As mentioned, this is our first report on the use of BDD electrode for NAC analysis in drug samples. Good analytical detection performances were observed with limits of detection in the nano molar range, good sensitivity, and excellent response precision, and stability. Data for the detection of this analyte in five different samples are presented. The ultimate goals of this research were to (i) investigate the feasibility of detecting low amount of NAC in real samples using BDD electrodes, (ii) obtain a complete set of detection figures of merit for NAC present in the different drug

samples, and (iii) validate the method through comparison measurements using HPLC-UV. The originated sensitivity in this approach making the BDD electrode is very suitable for the detection of minor amounts of NAC in pharmaceutical and clinical preparations.

3.2 Experimental

3.2.1 Chemicals and Reagents

All chemicals were of analytical grade or better and were used without further purification. All solutions and subsequent dilutions were prepared in deionized water. Phosphate buffers (pH 5–8), 0.1 mol/L, were prepared from 0.1 mol/L potassium dihydrogen phosphate (Merck) and 0.1 M disodium hydrogen phosphate (Fluka). Phosphate buffer (pH 2.5) was prepared from 0.1 mol/L potassium dihydrogen phosphate and the pH was adjusted with orthophosphoric acid (85%, Carlo Erba). Phosphate buffer (pH 9), 0.1 mol/L, was prepared from 0.1 M potassium dihydrogen phosphate and the pH was adjusted with 0.1 mol/L sodium hydroxide. The standard *N*-acetyl-*L*-cysteine (Sigma) solutions were freshly prepared with the same buffer prior to use.

3.2.2 Electrode

The experimental conditions and the apparatus used for the diamond film growth have been described in detail elsewhere [87]. The films were prepared by deposition of the BDD thin films on highly conductive n-Si (111) substrates by microwave plasma-assisted chemical vapor deposition. Deposition was usually carried out for 10 hr to achieve a film thickness of approximately 30 mm. The nominal B/C atomic ratio in the gas phase was 1 : 100, and the typical boron-doping level in the film was ca. 10^{21} cm^{-3}. The BDD electrodes were rinsed with ultrapure water prior to use. The GC electrode was purchased from Bioanalytical System, Inc. (area 0.07 cm^2). Pretreatment involved sequential polishing with 1 and 0.05 micron of alumina/water slurries on felt pads, followed by rinsing with ultra-pure water prior to use.

3.2.3 Voltammetric Study

Electrochemical measurements were recorded using an Autolab Potentiostat 100 (PG100) (Metrohm, Switzerland) with a standard three-electrode configuration. The planar working BDD electrode was pressed against a smooth ground joint at the bottom of the cell, isolated by an O-ring. The geometric area of the working electrode is 0.07 cm^2. A platinum wire served as the auxiliary electrode and Ag/AgCl was used as the reference. Placing the backside of the Si substrate on a brass plate made ohmic contact. A GC electrode (0.07 cm^2, Bioanalytical System, Inc.) was also used as a working electrode in the comparison study with the BDD electrode. Cyclic voltammetry was used to probe the electrochemical reaction. The electrochemical measurements were housed in a Faradaic cage to reduce electronic noise. All experiments were done at room temperature.

3.2.4 Flow Injection Analysis with Amperometric Detection

The FIA system consisted of a thin layer flow cell (Bioanalytical System, Inc.), an injection port (Rheodyne7725) with a 20-µL injection loop, a peristaltic pump (Ismatec), and an electrochemical detector (PG100). The carrier stream, 0.1 M phosphate buffer (pH 9), was regulated by a reagent delivery module at a flow rate of 1 mL/min. A pulse dampener was used in series to reduce the pulsation introducing by the alternation of the roller of the peristaltic pump. The thin layer flow cell consisted of a silicone gasket as a spacer, Ag/AgCl as the reference electrode, stainless steel tube as an auxiliary electrode and outlet. The experiments were performed in a copper Faradaic cage to reduce electrical noise. A hydrodynamic voltammogram was obtained before the amperometric determination was carried out. The peak current after each injection was recorded, together with the corresponding background current. These data were plotted as a function of applied potential to obtain hydrodynamic voltammograms. The amperometric measurements were carried out at the potential giving a maximum signal to-background (S/B) ratio in the hydrodynamic voltammograms.

3.2.5 Sample Preparations

Tablets, powder containing NAC obtained from local drugstores were analyzed. The drug tablet was homogenized in an agar mortar. The amount of the powdered mass analyte was dissolved in 100 mL of 0.1 mol/L phosphate buffer (pH 9). This solution was diluted in such a way that the concentration of NAC in the final test solution was within the linear dynamic range (0.5–50 μmol/L).

3.3 Results and Discussion

3.3.1 Voltammetric Study

Cyclic voltammetry was initially used as means of examining and comparing the electrochemical signal of two electrodes (BDD electrode and GC electrode) to NAC. Figure 3.1a details the voltammetric response obtained at BDD electrode when it was placed in a 0.1 mol/L phosphate buffer (pH 9) solution, containing 1 mmol/L NAC whilst Figure 3.1b details the response of the GC electrode under analogous conditions. Analysis of the cyclic voltammograms recorded prior to the addition of NAC reveals that the response at each electrode produces no appreciable oxidative signals over the potential range studied (0.0–1.2 V). Furthermore, a comparison of the background currents observed at each electrode reveals that the BDD electrode exhibits a lower capacitance consistent than GC electrodes. Upon the introduction of NAC to the solution the response at the BDD electrode shows a new well defined electrochemical signal emerging at +0.5 V which obtains a current plateau at +0.85 V. In contrast, the NAC response obtained at the GC electrode shows ill-defined peak, which increase in the oxidation current at +0.4 V. This current continues to rise with increasing potential but unlike the BDD electrode no defined oxidation wave is observed. Upon reversal of the scan direction no new reductive processes are observed in the potential range studied at each electrode. This is consistent with the electrochemically oxidized species of NAC undergoing a chemically irreversible reaction.

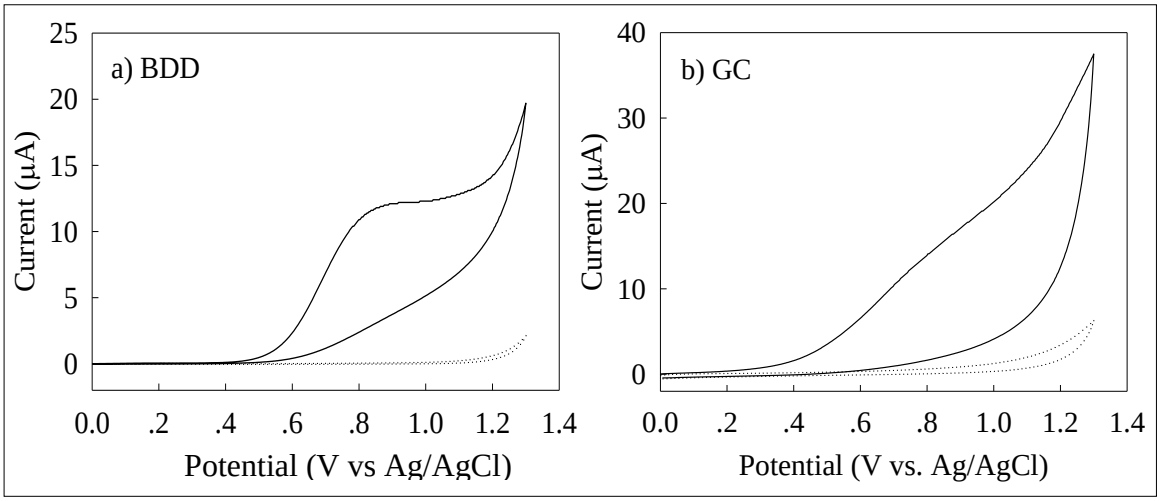

Figure 3.1 Cyclic voltammograms for a) BDD and b) GC versus Ag/AgCl in 1.0 mM NAC in 0.1 M phosphate buffer pH 9 (solid lines) and 0.1 M phosphate buffer pH 9 (dashed lines) Sweep rate, 50 mV/s; area of electrode, 0.07cm^2.

3.3.2 Effect of pH Value on the Electrochemical Behavior of NAC

In order to obtain the optimum electrochemical responses of NAC, it is important to examine the effect of buffer pH. Phosphate buffer, 0.1 mol/L, was used as the supporting electrolyte for investigating the electrochemical property of NAC. The experiments were performed at pH 2.5, 5.0, 6.0, 7.0, 8.0, and 9.0. The obtained results showed that NAC can be oxidized in neutral and alkali medium. The peak potential was shifted towards to more negative when the pH value increased (data not shown). This remark can be explained using the electrooxidation of sulfur-containing compounds at BDD electrode. It involved the dissociation of the proton from the thiol group, followed by the electrochemical oxidation of NAC anion. So at higher pH value, NAC is easy to lose the proton and to produce more stable reduced from. The highest oxidation current peak was obtained from using phosphate buffer pH 9. Thus, this pH was selected as the suitable pH for all subsequent experiments.

3.3.3 Scan Rate and Concentration Dependence

In order to verify that this oxidative reaction is diffusion controlled, a study into the effects of scan rate on the electrochemical signal was undertaken. The corresponding voltammetric responses varied with scan rate with the current plateau increasing linearly with the square root of the scan rate (R^2 = 0.9993) as shown in Figure 3.2. Such dependence indicates that the oxidation of NAC is indeed diffusion controlled. Using the information obtained from the linear regression of the inset shown in Figure 2. (y = 30.269x + 0.1649), Andrieux and Savèant theoretic model (Equation 1) [90] can be used to calculate a diffusion coefficient (D_o). The D_o obtained was found to be 2.096 x 10^{-6} cm^2 s^{-1}. This value is in close agreement with that obtained from previous work [91].

$$I_p = 0.496FAC_sD_o^{1/2}(F/RT)^{1/2}v^{1/} \qquad (1)$$

C_s is the NAC concentration (1 x 10^{-6} mol cm^{-3}), D_o is the diffusion coefficient of NAC, F is Faraday constant, R = 8.31447 J mol^{-1} K^{-1}, T = 298 K and *A* = 0.07 cm^2.

From the cyclic voltammogram, the oxidation of NAC is an irreversible process. Thus, the Randles-Sevcík relationship (Equation 2) can be used to determine the number of electron involved.

$$J_p = (2.99\times10^5)n[(1-\alpha)n_\alpha]^{1/2}]D_o^{1/2}C_s^{1/2} \qquad (2)$$

In order to estimate the value of *n*, it is first necessary to calculate the value of $(1-\alpha)n_\alpha$. In irreversible systems, an approximate calculation is based on the linear relationship between the anodic peak potential (E_p) and log*v* (y = 0.1255x + 0.9894). Using Equation 3, the relationship between the slope and the factor $(1-\alpha)n_\alpha$ was found to be 0.235.

$$0.1255 = 1.15RT/[(1-\alpha)n_\alpha]F \qquad (3)$$

After calculating the value of $(1-\alpha)n_\alpha$, using Equation 2 and the previously estimated NAC diffusion coefficient, it was possible to calculate the number of electrons involved in the electrooxidation of NAC is *n* = 2.15 ≈ 2 which accordance with previous literature [91]. Next, the analytical utility of using the BDD electrode

was examined. The variation in the voltammetric currents was analyzed as a function of the NAC concentrations. The response of the BDD electrode was found to be linear over the concentration range 0.01 – 3.0 mmol/L and produced a limit of detection at S/B ≥ 3 of 50 µmol/L. The data was illustrated in Figure 3.3.

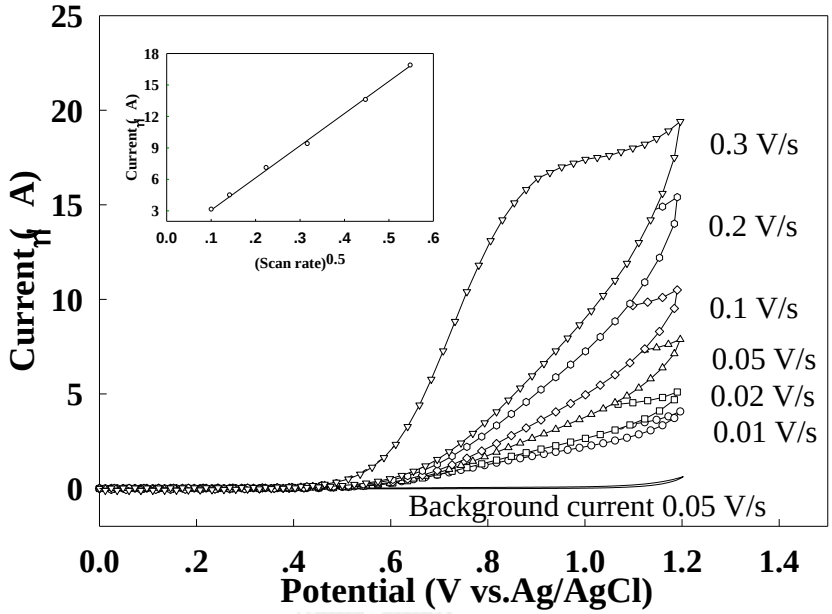

Figure 3.2 Cyclic voltammogram for 1 mM NAC in 0.1 M phosphate buffer (pH 9) at boron-doped diamond electrode for a series of potential sweep rates; area of electrode, 0.07 cm^2. The calibration curve of relationship between current (µA) and $(\text{sweep rate})^{0.5}$ was also in the inset of this figure.

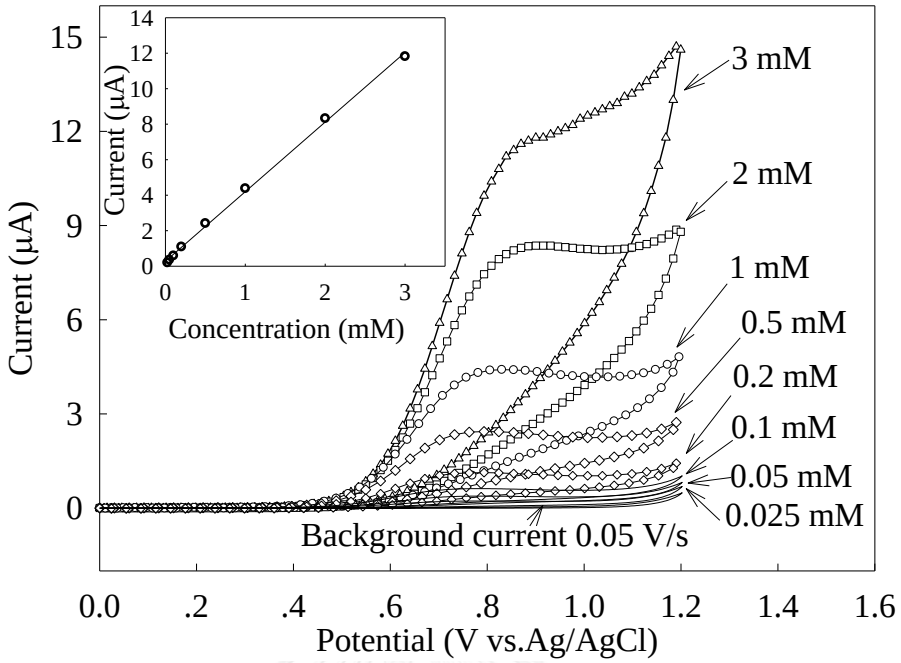

Figure 3.3 Cyclic voltammogram for NAC in 0.1 M phosphate buffer (pH 9) at boron-doped diamond electrode for a series of NAC concentrations. The potential sweep rate was 50mV/s; area of electrode, 0.07 cm^2. The calibration curve is shown in the inset.

3.3.4 Hydrodynamic voltammetry

Hydrodynamic voltammetry is a suitable method to obtain the appropriate potential applied to the FIA/amperometic detection. In this study, standard solution of NAC was repetitively injected while the FIA/amperometry operating potential was increased from 0.5 V to 1.0 V in 0.1 V increments over the range from 0.5 - 0.8 V and in 0.5 V increment for 0.8 - 1.0 V, respectively. Figure 3.4a displayed the hydrodynamic voltammogram of the standard solution containing 100 μmol/L NAC. When the applied potential increased the current response of NAC also increased, and no reached to maximum value. Hence, the S/B ratio was calculated from the Figure 3.4a at each point to create a graph as a function of S/B ratios and applied potential (Figure 3.4b) to obtain the maxima potential point. To get the best sensitivity and signal to noise ratio, +0.85 V was chosen as an optimal detection potential.

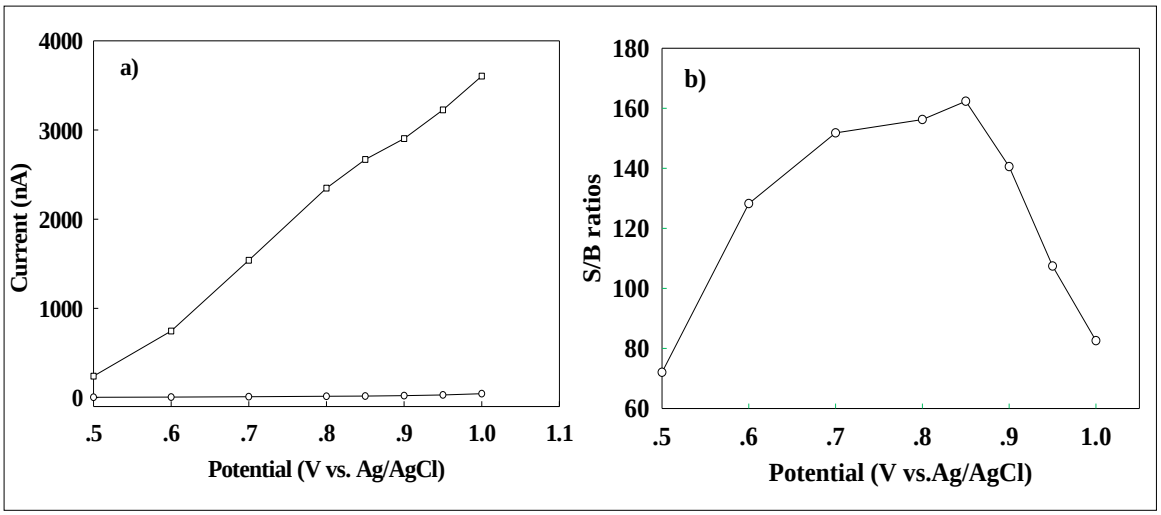

Figure 3.4 (a) Hydrodynamic voltammogram of (-○-) 0.1 M phosphate buffer (pH 9, background current) and (-□-) 100 μM of NAC in 0.1 M phosphate buffer (pH 9) with four injections of analysis, using 0.1 M phosphate buffer (pH 9) as a carrier solution. (b) Hydrodynamic of signal- to- background ratio. The flow rate was 1 mL/ min.

3.3.5 Flow injection analysis with amperometric detection

After optimizing the suitable detection potential for the FIA procedure, amperometric measurements were carried out in phosphate buffer (pH 9) containing different NAC concentration in order to obtain the analytical curve. The FI current-time response for different NAC concentrations showed linear relationship between the current values (at +0.85 V) obtained and the NAC concentrations exhibited from 0.5 μmol/L to 50 μmol/L with a correlation coefficient of 0.9989. To higher concentrations than 50μmol/L occurs the deviation of linearity. The detection limit obtained from experiment was found to be 10 nmol/L (S/N = 3). Compared to previously published works, particularly those that using the chemically modified electrodes [78-85], the proposed method provided the lowest detection limit. This indicates that a BDD electrode is ultrasensitive for the detection of NAC.

3.3.6 Detection of NAC in commercially available drugs

In order to investigate the analytical of proposed method, FIA amperometric procedure was applied for the determination of NAC in commercially available drug samples. The NAC content was determined by standard addition method that also shown in Figure 3.5. The recovery of this method was determined by measuring the percentage of recovery after sample solutions have been spiked with known amounts of standard compounds. Table 1 showed the recovery for intra-day and inter-day from the determination of NAC using this proposed method.

The precision of the method was obtained on the basis of intra-assay. Three concentrations of added solution (0.33, 0.67, 1.31 μg/mL) were chosen for investigation in order to check the results obtained from low, medium and high concentrations with respect to the probable range of interest in samples. Results obtained from ten injections were within 3.7 % of the relative standard deviation (RSD). The RSD values for day-to-day assays of NAC were also investigated. It was found that in the same laboratory within one week the RSD values did not different more than 4.1 %. These results implied that BDD detection exhibited a high reproducibility and accuracy. Moreover, we have tested BDD electrodes for long-term stability under continuous operation (50 injections). They exhibited highly reproducible responses from day to day; also, the response was reproducible after several days of exposure to the laboratory atmosphere. Recoveries obtained from the proposed method were found over the ranges of 94.4 - 103.6% for intra-day, while the inter-day recovery of NAC varied over the range of 93.0 - 102.7%, respectively.

This quantitative measurement revealed that the experimentally calculated values closely matched the manufacturer's claim in all five supplements examined shown in Table 2. These results were compared to those obtained by the HPLC-UV method [8] and statistically analyzed using the paired *t*-test at the 95% confidence interval. The paired two-tail test gave calculated *t* values (0.997) below the critical *t*-value (2.447), therefore agreeing the null hypothesis. The data, summarized in Table 2, reveal that the results of FIA coupled with BDD amperometry are of comparable

accuracy to, and not significantly different from, those values obtained by the traditional HPLC-UV method.

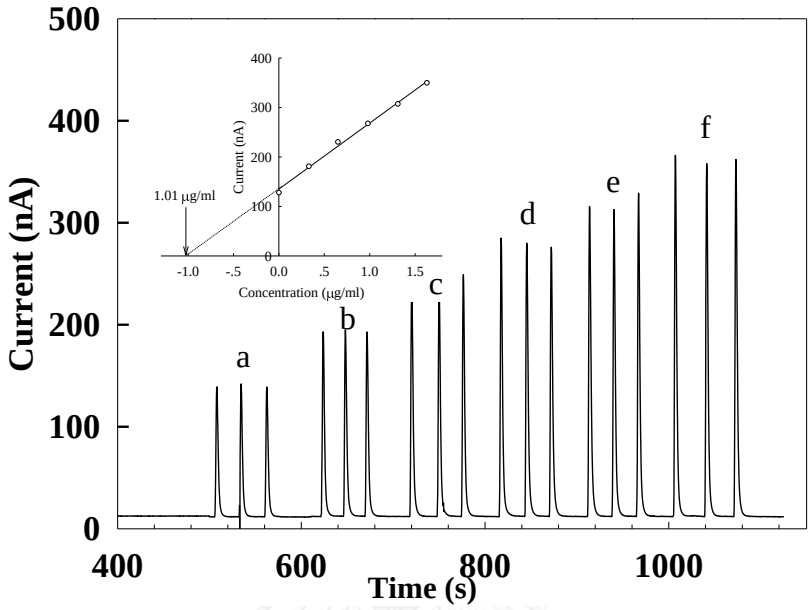

Figure 3.5 Flow injection analysis results for determination of NAC in commercially available tablets. Using the standard addition for the added NAC: (a) 0.00 µg/mL, (b) 0.33 µg/mL, (c) 0.65 µg/mL, (d) 0.98 µg/mL, (e) 1.31 µg/mL, (f) 1.63 µg/mL.

3.4 Conclusions

The results of this investigation show that BDD electrode is attractive material for further investigations concerning the determination of NAC. Cyclic voltammetric studies show the superiority of BDD electrode over GC electrode in terms of reproducibility, sensitivity and low background current (capacitive current). The anodic peak currents increase compared with that on a GC electrode. The effect of the scan rate on the peak current shows that the electrochemical process of NAC on BDD electrode was controlled by the diffusion of the species.

Experiments in FIA were performed to characterize the BDD electrode as an amperometric sensor for the detection of NAC. It can be successfully adopted to detect NAC. The method showed to be fast, simple, precise and highly sensitive among other interesting features of the method proposed which make it applicable

to NAC analysis and quality control of pharmaceutical samples. The results indicated that this method has been satisfactorily applied to the determination of NAC in commercially available drug with corresponding to the label and standard method. In conclusion, FIA coupled with BDD amperometry provides an attractive alternative method for the determination of NAC in drug samples, among others, and may also be useful for biomedical and clinical investigation of NAC levels.

CHAPTER IV

IMPROVEMENT OF SENSITIVITY AND SELECTIVITY FOR ELECTROCHEMICAL SENSOR BASED ON ELECTRODE MODIFICATION

There are two parts for this chapter. Past I presents sensitive and selective electrochemical sensor using silver nanoparticles modified glassy carbon electrode for determination of cholesterol in bovine serum. Past II reports bimetallic Pt–Au nanocatalysts electrochemically deposited on boron-doped diamond electrodes for nonenzymatic glucose detection.

Part I:

Sensitive and selective electrochemical sensor using silver nanoparticles modified glassy carbon electrode for determination of cholesterol in bovine serum

Siriwan Nantaphol [a], Orawon Chailapakul [a,b] and Weena Siangproh [c*]

[a] Department of Chemistry, Faculty of Science, Chulalongkorn University, Patumwan, Bangkok 10330, Thailand

[b] National Center of Excellent of Petroleum, Petrochemicals and Advanced Materials, Chulalongkorn University, Patumwan, Bangkok 10330, Thailand

[c] Department of Chemistry, Faculty of Science, Srinakharinwirot University, Sukhumvit 23, Wattana, Bangkok 10110, Thailand

* Corresponding author

Sensors and Actuators B: Chemical 207 (2015): 193 – 198

Abstract

For the first time, a newly sensitive and simple method for the determination of cholesterol based on coupling of enzymatic assay and electrochemical detection has been developed. Silver nanoparticles modified glassy carbon electrode (AgNPs/GCE) was fabricated by electrochemical deposition technique and used as the working electrode. The electrochemical performances were investigated by cyclic voltammetry and chronoamperometry. Under the optimized conditions, a linear relationship between the reduction current and cholesterol concentration was found in the range of 3.9 mg/dL to 773.4 mg/dL with a detection limit of 0.99 mg/dL. The proposed method was applied to determine cholesterol in bovine serum. The recoveries obtained were within the range of 99.6-100.7%, which indicated that the presented method is applicable to determine cholesterol in bovine serum. In addition this electrochemical sensor displayed very high specificity to cholesterol with no observed interference from easily oxidizable species such as ascorbic acid and uric acid. All these excellent performances of the developed sensor indicated that this sensing platform could be easily extended to the detection of other important biomarkers.

4.1 Introduction

Cholesterol is an important biomarker for various diseases. It acts as a major structural constituent of plasma membranes and is a precursor of biological substances, such as bile acid, vitamin D and steroid hormones [8]. High cholesterol level in blood serum is a major factor for several diseases, such as coronary heart disease, myocardial infarction and arteriosclerosis hypertension, while low cholesterol level may result in hypolipoproteinemia, anemia, septicemia, malnutrition, hyperthyrea and hepatopathy [92]. The normal total plasma cholesterol for an individual is less than 5.2 mM (200 mg/dL), with a high level being considered as more than 6.2 mM (240 mg/dL) [93]. Hence, accurate, sensitive and fast monitoring of cholesterol levels is of great importance in clinical analysis/diagnosis. In addition, the development of quantitative methodology for determination of cholesterol is significant and challenging to develop reliable cholesterol sensors.

The analytical methods for cholesterol determination can be classified into two groups: nonenzymatic and enzymatic methods. In general, the enzymatic method provides more selectivity than nonezymatic method and has been employed in routine clinical laboratory. The determination of cholesterol by enzymatic method is based on the following mechanism [9];

$$\text{Cholesterol ester} + H_2O \xrightarrow{\text{ChE}} \text{cholesterol} + \text{fatty acids}$$

$$\text{Cholesterol} + O_2 \xrightarrow{\text{ChOx}} \text{4-cholestene-3-one} + H_2O_2$$

The cholesterol ester will be hydrolyzed by cholesterol esterase (ChE) to produce free cholesterol and fatty acids. Then free cholesterol is oxidized by oxygen in the presence of cholesterol oxidase (ChOx) to produce 4-cholestene–3–one and hydrogen peroxide (H_2O_2). The measurement of H_2O_2 can be used for the indirect quantification of cholesterol.

Up to now, several cholesterol determination techniques have been published including colorimetric [94], spectrophotometric [95], high performances liquid chromatography (HPLC) [96] and electrochemical method [42, 97].

Electrochemical method is the most frequency applied for cholesterol determination via the monitoring of oxygen consumption or the production of H_2O_2 during the enzymatic reactions. Amperometric measurement of H_2O_2 is the most frequently monitored and proposed. However, the suffering from some easily oxidized species such as ascorbic acid and uric acid at high overvoltage will be occurred at the same time. Therefore, the accuracy of method is limited. To overcome the weak point, the possible interference from easily oxidizable species in biological samples can be minimized using modified working electrode with selective catalyst or using the reduction of H_2O_2 at low applied potential instead of oxidation of H_2O_2.

In recent years, metal nanoparticles have been used in wide applications in electrochemical sensors. Among the metal nanoparticles, silver nanoparticles (AgNPs) are one of the most well-developed materials and have been used to modify the surface of working electrodes because they are inexpensive in relative comparison with those other materials, possess good chemical and physical properties, providing excellent electron transfer rates, and greatly decrease the overpotential of oxidizing or reducing agents produced from enzymatic products. In previous studied, AgNPs were shown excellent electrocatalytic activity for H_2O_2 and size distribution of AgNPs played an important role in their electrocatalytic activity [11, 15-17].

Electrochemical cholesterol biosensor based on electron transfer between an electrode and immobilized cholesterol oxidase has been focused for cholesterol research because they show advantages such as high sensitivity, selectivity and suitable for real time detection [10, 98]. However the use of enzyme immobilized on electrode surface had limitations because the enzyme is easily denature during its immobilization procedure. In addition, the reduction of substrate-enzyme complex formation due to steric hindrance and high cost of the supporting material or its immobilized procedure were reported. Moreover, the activity of enzyme is often to be affected by pH, temperature, humidity and toxic chemicals [99]. In addition, the reduction of substrate-enzyme complex formation due to steric hindrance and high cost of the supporting material or its immobilized procedure were reported.

Moreover, the activity of enzyme is often to be affected by pH, temperature, humidity and toxic chemicals [99].

To overcome those problems, the use of coupling between the enzymatic assay and electrochemical detection has been demonstrated [10]. ChOx were added in the solutions instead of the immobilization on electrode surface to catalyst the reaction of cholesterol and generated H_2O_2 will be recorded immediately. In this work, we report a sensitive, selective and simple method using silver nanoparticles modified glassy carbon electrode (AgNPs/GCE) to achieve a new nanosensor for the determination of cholesterol. AgNPs possess the catalytic activity of H_2O_2 reduction occurred at low overpotential. The proposed method showed high selectivity for cholesterol detection without disturbance from interference such as ascorbic acid and uric acid.

To the best our knowledge, there is no record for the using of AgNPs/GCE to detect cholesterol in real samples. The results show AgNPs/GCE displayed excellent performance, wide linear range, and low detection limit of cholesterol detection.

4.2 Experimental

4.2.1 Apparatus

All electrochemical experiments were performed with a model PGSTAT 101 Autolab Electrochemical System controlled with the NOVA software package (Kanaalweg 29-G 3526 KM Utrecht, The Netherlands). Three-electrode system was used, where an Ag/AgCl (3 M KCl) electrode served as the reference electrode, a platinum wire electrode served as the auxiliary electrode and AgNPs/GC electrode served as working electrode.

4.2.2 Reagents and solutions

Cholesterol, cholesterol oxidase (ChOx) from *Streptomyces* sp. (25U/mg) and lipid cholesterol rich from adult bovine were purchased from Sigma (St. Louis, MO). Potassium dihydrogen phosphate (KH_2PO_4) was purchased from Carlo

ErbaReagenti-SDS (Val de Reuil, France). Hydrogen peroxide (H_2O_2), disodium hydrogen phosphate (Na_2HPO_4), potassium chloride (KCl) and boric acid (H_3BO_3) were purchased from Merck (Darmstadi, Germany). Silver nitrate ($AgNO_3$) was purchased from POCH S.A. (Poland). Glacial acetic acid (CH_3COOH) was purchased from Fisher Scientific (Pittsburgh, PA). Phosphoric acid (H_3PO_4, 85%) was purchased from Carlo Erba (Rodano, MI, USA). Stock solution of cholesterol was daily prepared by dissolving cholesterol in the mixture of triton X-100 and isopropanol. This stock solution was further diluted to make difference concentrations of cholesterol in 0.05 M phosphate buffer pH 7.4 containing 0.1 M KCl. The solution was stirred with magnetic bar at 60 ℃ to obtain a homogeneous solution. Stock solution of ChOx was prepared freshly by dissolving in 0.05 M phosphate buffer (pH 7.4). All standard and sample solutions were prepared by using high purity water from MilliQ Water System (Millipore, USA, R ≥ 18.2 MΩ cm). All chemical were of analytical reagent grade and used without further purification.

4.2.3 Preparation of AgNPs/GC electrode

The procedure for preparation of silver nanoparticles modified glassy carbon electrode was adapted from Ref. [100]. Prior to use, glassy carbon electrode (GCE, diameter 3 mm) was polished with 1.0 and 0.2 μm alumina powder, respectively and sonicated in ethanol and then in deionized water for 1 min each. Silver nanoparticles (AgNPs) have been deposited onto glassy carbon electrode surface from a solution of $AgNO_3$ in Britton-Robinson (pH 2.0) which prepared by mixing of 0.04 M H_3BO_3, 0.04 M H_3PO_4 and 0.04 M glacial acetic acid and adjust with 0.2 M sodium hydroxide. Electrodeposition was carried out by applying an accumulation potential during a time with stirring.

4.2.4 Electrochemical measurements

Cholesterol oxidase was pipetted into the electrochemical cell containing 1 mL standard/sample solution and stirred for 1 min. Three-electrode system was immersed in the solution. Then, the measurement using

chronoamperometry at -0.5 V for 50 s was performed. All experiments were performed at room temperature.

4.2.5 Bovine serum analysis

The labeled concentration of cholesterol in adult bovine serum was used to represent the biological sample. The serum sample was prepared by dissolving of adult bovine serum powder in triton X-100 and isopropanol, and then diluted with 0.05 M phosphate buffer pH 7.4 containing 0.1 M KCl. The solution was stirred with magnetic bar at 60 ℃.

4.3. Results and discussion

4.3.1 Electrochemical detection of standard H_2O_2 and standard cholesterol

For an electrochemical determination of cholesterol, the measurement of the H_2O_2 produced from cholesterol oxidation can be used for the indirect quantification of cholesterol [101]. In this study, silver nanoparticles modified glassy carbon electrode (AgNPs/GCE) was fabricated by deposition of silver at -0.6 V for 200 s using solution of 5 mM $AgNO_3$ in Britton-Robinson (pH 2.0). The experiment was start from using 1 mM standard H_2O_2 in 0.05 M phosphate buffer pH 7.4 containing 0.1 M KCl to investigate the electrochemical response of H_2O_2 using cyclic voltammetry. The cyclic voltammograms of standard H_2O_2 measured on the AgNPs/GCE and on unmodified GCE were shown in Figure 4.1a. At AgNPs/GCE the reduction of H_2O_2 is observed at the potential about -0.4 V. In contrast, no significant voltammetric currents were observed at unmodified electrode. The results indicated that this modified electrode could be a promising sensor for sensitive detection of H_2O_2. Subsequently, the cyclic voltammograms of H_2O_2 produced from the reaction between cholesterol and ChOx measured at AgNPs/GCE was shown in Figure 4.2b. This indicated that the proposed AgNPs/GCE can be used as a newly sensor for cholesterol detection.

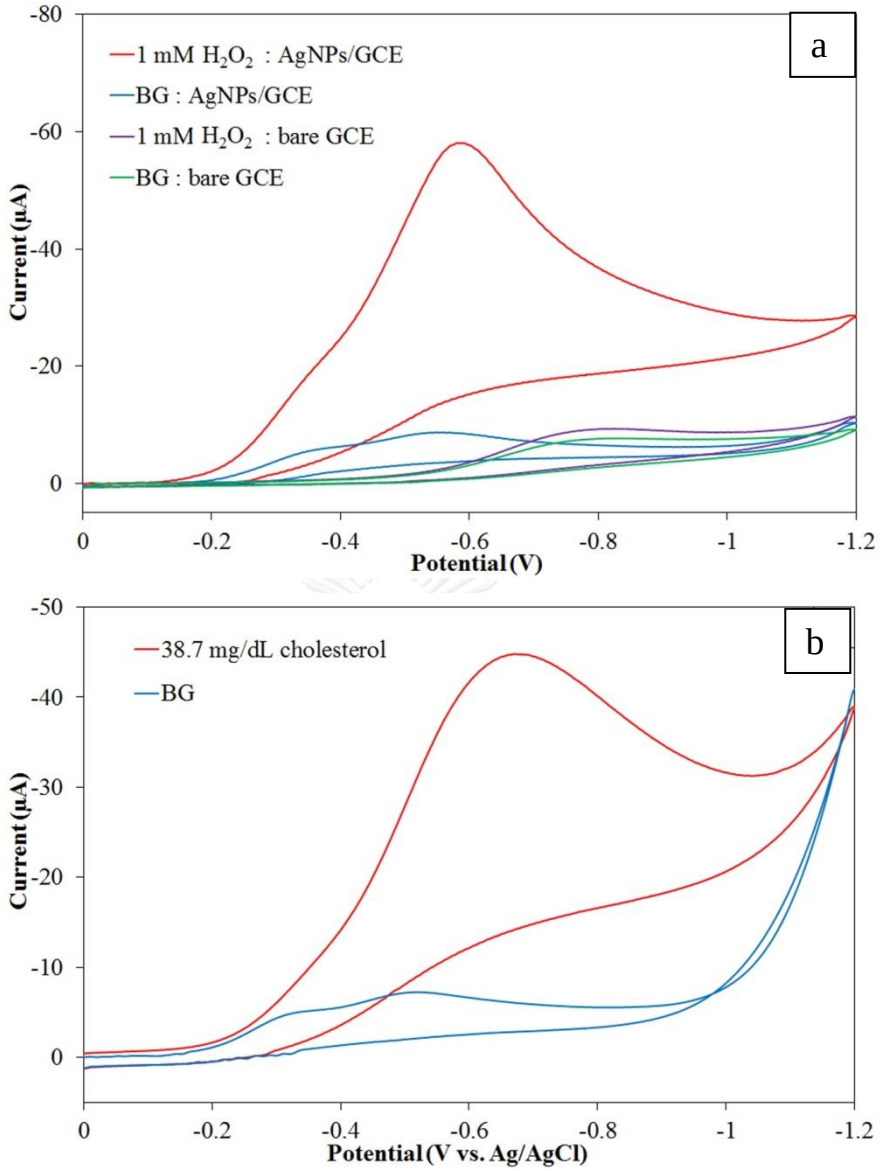

Figure 4.1 (a) Cyclic voltammograms of 1 mM standard hydrogen peroxide (H_2O_2) in 0.05 M phosphate buffer pH 7.4 containing 0.1 M KCl measured on AgNPs/GC electrode and bare GC electrode under scan rate was 100 mV/s. (b) Cyclic voltammograms of 1 mM cholesterol measured on AgNPs/GC electrode.

4.3.2 Optimization of the conditions for modified electrode

To obtain a good electrochemical response for the reduction of H_2O_2, concentration of $AgNO_3$, deposition potentials and deposition times were investigated. First, the deposition potentials were optimized, the cathodic peak

currents of H_2O_2 is gradually increased from -0.5 V to -0.6 V and then decreased with the potentials shifting negatively to -1 V. The highest peak intensity was reached at the deposition potential at -0.6 V. Next, the effect of deposition times on the peak currents was investigated in the range from 100 s to 350 s. The cathodic peak current is maximum at the deposition time is 200 s. Moreover, the effect of $AgNO_3$ concentrations was also studied. The optimized value for the concentration is 0.6 mM $AgNO_3$. In summary, the optimal conditions for modified electrode are -0.6 V deposition potential, 200 s deposition time and using 0.6 mM $AgNO_3$.

4.3.3 Effect of type and concentration of chloride salts

From literature reviews, the addition of mixture of chloride salts into the supporting electrolyte had a significant impact on the sensitivity of methodology. Therefore, the optimization of type and concentration were carried out for the electrochemical detection of H_2O_2. The effects of several salts such as NaCl, KCl, mixture of NaCl + KCl and K_2SO_4 were tested by using all concentrations at 0.1 M. The peak current was taken into consideration in order to choose the salts. Among these, KCl gave the best response; hence, KCl was selected as a suitable salt added into supporting electrode for all experiments.

Next, the effect of concentration of KCl on the current was investigated. The concentration values were examined in the range of 0.025-0.5 M using solution containing 1 mM H_2O_2. The maximum peak current was achieved at concentration of 0.1 M KCl. Decrease in the current responses was observed when the concentrations of KCl were greater than 0.1 M. Therefore, the 0.1 M KCl was selected as the optimum concentration for the proposed method.

4.3.4 Effect of ChOx concentration for cholesterol detection

The effect of ChOx concentration on the cholesterol detection was studied within the range from 0.08 to 0.56 U/mL ChOx using 38.7 mg/dL of cholesterol substrate. Figure 4.2 showed that the rapid increase of cathodic current was

obtained when the amount of enzyme increased from 0.08 U/mL to 0.4 U/mL and then reached a plateau. Therefore, the optimum concentration of ChOx was determined as 0.4 U/mL and used for all experiment.

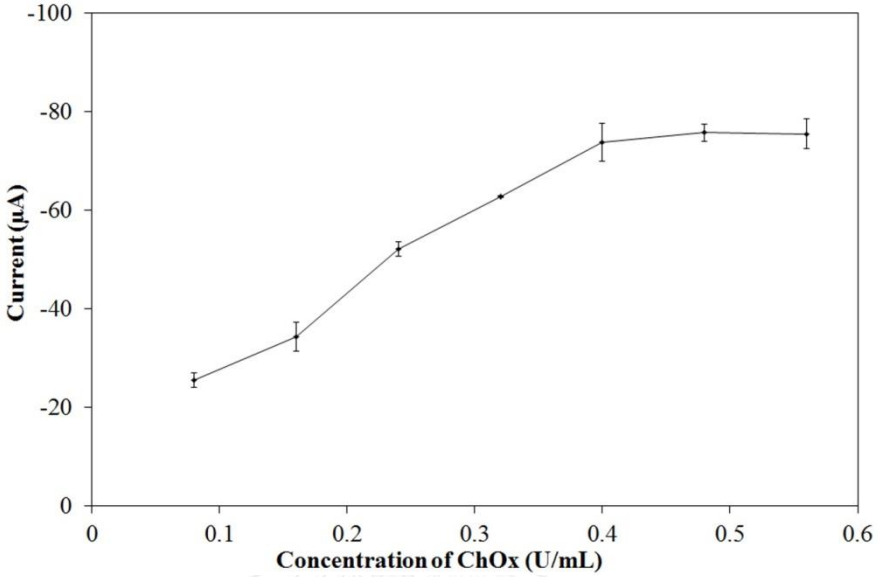

Figure 4.2 Effect of the cholesterol oxidase for determining 38.7 mg/dL cholesterol in 0.05 M phosphate buffer pH 7.4 containing 0.1 M KCl.

4.3.5 Effect of dissolved oxygen into solution for electrochemical detection

Owing to this system, the experiment was recorded by monitoring the reductive peak of H_2O_2. Thus, it is necessary to check the effect of dissolved oxygen into solution after enzyme reaction occurred on the electrochemical reduction of H_2O_2. From the results, it can be observed that comparing the net reductive currents (after subtraction of background) obtained from purge and without purge N_2 before analysis, there are no significantly different. It means that there is no effect of oxygen on the reduction of H_2O_2 for this assay. Then, the measurement of H_2O_2 produced from reaction can be carried out under the atmospheric environment.

4.3.6 Chronoamperometric study for cholesterol determination

Chronoamperometry was selected for electrochemical quantitation of cholesterol due to its high sensitivity and wide applications. The sensitivity and selectivity of electrochemical detection depended on the selection of the applied potentials. In order to obtain a good analytical performance for allowing cholesterol determination, the effect of detection potential on the reduction of H_2O_2 at AgNPs/GCE was optimized in the range of -0.4 V to -0.8 V. The results shown in Figure 4.3a, cathodic currents increased as the negative detection potential increased, but the background current also increased because the reduction of oxygen occurred at the potential more than -0.5 V [101]. On the basic of sensitivity and selectivity, a hydrodynamic voltammogram of signal-to-background ratios (S/B) were investigated instead of using only reduction currents. The current signal was shown in Figure 4.3b. The S/B ratio measured at -0.5 V provided a maximum signal, therefore, an applied potential of -0.5 V was chosen for further chronoamperometric measurement.

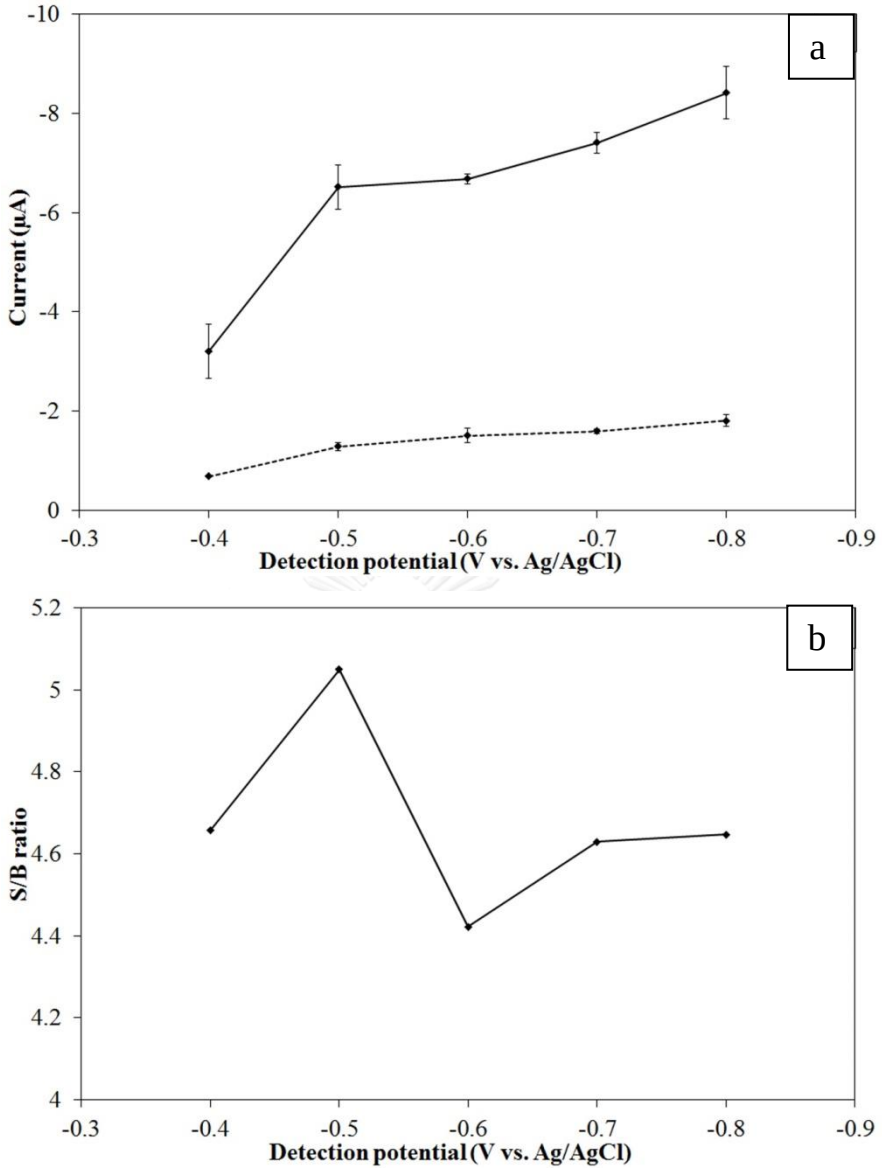

Figure 4.3 (a) Hydrodynamic voltammograms of 38.7 mg/dL cholesterol (blue line) and background (blue line) for 50 s sampling time. (b) Hydrodynamic voltammogram of signal-to-background ratios extracted from the data shown in part a.

4.3.7. Analytical performance

AgNPs/GCE was used as working electrode for measurement of different cholesterol concentrations and the amperometric current responses were recorded at a steady state current of 50 s as shown in Figure 4.4a. A calibration curve was obtained from relationship between cholesterol concentrations versus the current

response as showed in Figure 4.4b. The signals were proportional to the concentration of cholesterol over the range of 3.9 mg/dL to 773.4 mg/dL with a correlation coefficient of 0.9966. The detection limit (LOD) was calculated as the concentrations which produced the signal at 3 times of the standard deviation of a blank and found to be 0.99 mg/dL. The results obtained from the proposed method covered a wide range of cholesterol concentrations. The apparent Michaelis-Menten constant (K_m), which gives an indication of the enzyme-substrate kinetics, can be estimated from the Lineweaver-Burk equation:

$$\frac{1}{I_{ss}} = \frac{1}{I_{max}} + \frac{K_m}{I_{max}} \times \frac{1}{C}$$

where I_{ss} is the steady-state current, I_{max} is the maximum current measured under saturated substrate condition, and C is the cholesterol concentration. The K_m value was determined by the analysis of the slope and intercept for the plot of the reciprocals of steady-state current versus cholesterol concentration and found to be 64.2 mg/dL (1.66 mmol/L). From the Km values, this work gave the higher value, which means that the affinity between cholesterol and cholesterol oxidase is relatively small as compared to that mentioned in other works. The major reason is that the cholesterol oxidase functioning in this work is not fixed on the electrode, and the affinity between cholesterol and cholesterol oxidase is so weak that it does not give high current. Nevertheless, the proposed method provided a relatively high sensitivity and a low detection limit. In addition, a linear range covers the applicable region which makes the measurement of sample can be performed without dilution.

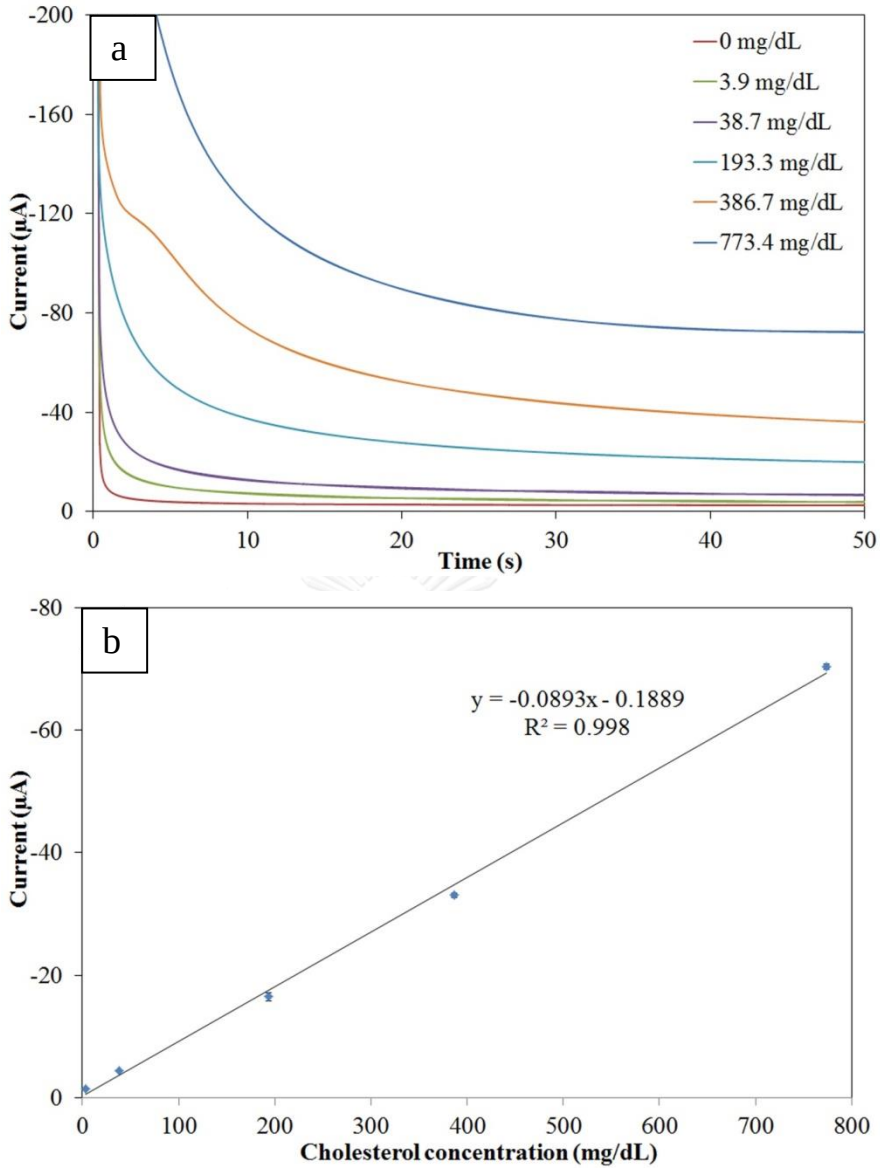

Figure 4.4 (a) Chronoamperograms of 0-773.4 mg/dL cholesterol determination at -0.5 V vs. Ag/AgCl. (b) The calibration graph of cholesterol over the concentration range of 3.9 mg/dL to 773.4 mg/dL.

The performance of proposed cholesterol sensor compared to previously report was shown in the Table 4.1. It is confirmed that the presented cholesterol sensor exhibited good sensing performance. Our sensor offers the wide detection range and lower detection limit, except the use of ChOx-IL/PB/GCE. However, the proposed sensor still has advantage in term of easily preparation of sensor. It did not

require to immobilize enzyme into the sensor. This indicated that the proposed is simple and suitable to apply for the determination of cholesterol in clinical diagnostics.

Table 4.1 Comparison of different modified sensors for cholesterol determination

Electrode	Linear range	Detection limit	Ref.
ChOx/PANI/ITO	25-400 mg/dL	25 mg/dL	[102]
AuE/dithiol/AuNPs/MUA/ ChOx	0.04–0.22 mM	34.6 μM	[103]
$NiFe_2O_4$/CuO/FeO-CH/ChOx	5–500 mg/dL	31.3 mg/dL	[104]
ChOx-IL/PB/GCE	0.01–0.4 mM	4.4 μM	[105]
(PAH–MCNTs–GNPs/HRP)$_4$/(PAH–MCNTs–GNPs/ChOx)$_4$	0.18-11 mM	0.02 mM	[106]
Nafion/ChOx/-Fe_2O_3/Ag	0.1-8.0 mM	18 μM	[107]
AgNPs/GCE	3.9-773.4 mg/dL (0.1-20 mM)	0.99 mg/dL (25.8 μM)	This work

4.3.8 Bovine serum analysis

As mentioned, cholesterol is an important part of a healthy body. In order to verify the reliability of method for cholesterol determination in clinical diagnostics, the proposed sensor, AgNPs/GCE, was applied to determine cholesterol in bovine serum. The label cholesterol concentrations were 50, 100, 150 and 250 mg/dL, respectively. The concentration of cholesterol in bovine serum sample was calculated from standard calibration curve. The results were listed in the Table 4.2. It can be observed that the determined values are highly correlated with the labeled

values. The relative errors are less than 1%. The values of the recovery obtained were in the range of 99.6-100.6 %. The results demonstrated that this proposed method was successful used for determination of cholesterol in bovine serum without any sample preparation. This indicated that the proposed method could be applied for biological samples.

Table 4.2 Determination of cholesterol in bovine serum samples

Sample	Labeled concentration (mg/dL)	Determined value* (mg/dL)	%RSD	Relative error (%)	% Recovery
A	50	49.8±3.6	7.2	-0.3	99.6
B	100	100.7±5.1	5.0	+0.7	100.7
C	150	151.3±8.2	5.4	+0.8	100.8
D	250	251.5±11.3	4.5	+0.6	100.6

4.4. Conclusions

In summary, we have demonstrated the use of simple electrochemical method for cholesterol determination in bovine serum sample for the first time. The determination of hydrogen peroxide produced from cholesterol reaction can be used for the indirect quantification of cholesterol. Electrochemical deposition technique was performed to create AgNPs/GCE and used as working electrode for measurement the reduction of hydrogen peroxide. The catalyst of silver nanoparticles possesses the catalytic activity of hydrogen peroxide reduction, which no observed interference from easily oxidizable species such as ascorbic acid and uric acid. In addition, the main advantages for the use of AgNPs/GCE are in term of high sensitivity, high accuracy, and simple fabrication. Reproducible signal from %RSD for intra- and inter-day were below 7.5%. These results indicated that the high reproducibility was obtained using this system for long time.

Part II:

Bimetallic Pt–Au nanocatalysts electrochemically deposited on boron-doped diamond electrodes for nonenzymatic glucose detection

Siriwan Nantaphol,[a] Takeshi Watanabe,[b] Naohiro Nomura,[b] Weena Siangproh,[c] Orawon Chailapakul,[a]* and Yasuaki Einaga[b,d]*

[a] Department of Chemistry, Faculty of Science, Chulalongkorn University, Patumwan, Bangkok 10330, Thailand

[b] Department of Chemistry, Keio University, 3–14–1 Hiyoshi, Yokohama 223–8522, Japan

[c] Department of Chemistry, Faculty of Science, Srinakharinwirot University, Wattana, Bangkok 10110, Thailand

[d] JST-ACCEL, 3–14–1 Hiyoshi, Yokohama 223–8522, Japan

* Corresponding author

Biosensors and Bioelectronics, (in press), 2017

Abstract

The enormous demand for medical diagnostics has encouraged the fabrication of high-performance sensing platforms for the detection of glucose. Nonenzymatic glucose sensors are coming ever closer to being used in practical applications. Bimetallic catalysts have been shown to be superior to single metal catalysts in that they have greater activity and selectivity. Here, we demonstrate the preparation, characterization, and electrocatalytic characteristics of a new bimetallic Pt/Au nanocatalyst. This nanocatalyst can easily be synthesized by electrodeposition by sequentially depositing Au and Pt on the surface of a boron-doped diamond (BDD) electrode. We characterized the nanocatalyst by scanning electron microscopy (SEM), X-ray diffraction (XRD), and voltammetry. The morphology and composition of the nanocatalyst can be easily controlled by adjusting the electrodeposition process and the molar ratio between the Pt and Au precursors. The electrocatalytic characteristics of a Pt/Au/BDD electrode for the nonenzymatic oxidation of glucose were systematically investigated by cyclic voltammetry. The electrode exhibits higher catalytic activity for glucose oxidation than Pt/BDD and Au/BDD electrodes. The best catalytic activity and stability was obtained with a Pt:Au molar ratio of 50:50. Moreover, the presence of Au can significantly enhance the long-term stability and poisoning tolerance during the electro-oxidation of glucose. Measurements of glucose using the Pt/Au/BDD electrode were linear in the range from 0.01 to 7.5 mM, with a detection limit of 0.01 mM glucose. The proposed electrode performs selective electrochemical analysis of glucose in the presence of common interfering species (e.g., acetaminophen, uric and ascorbic acids), avoiding the generation of overlapping signals from such species.

4.5 Introduction

Owning to the recent increase in the number of people suffering from diabetes, the development of highly sensitive glucose sensors with high reliability, fast response, and excellent selectivity has become more urgent. In general, electrochemical techniques hold great promise for the construction of glucose sensors since these techniques have the advantages of simplicity, high sensitivity, high accuracy, and a low power requirement [108, 109]. There are essentially two categories of electrochemical glucose sensors: enzymatic and nonenzymatic sensors [110-113]. Despite the fact that enzyme-based sensors show good selectivity and are highly sensitive, they are limited by their inadequate long-term stability, which originates from the nature of the enzymes [18, 19, 114]. As a result, there have been enormous efforts made to alleviate these problems. One of the more appealing approaches is the use of nonenzymatic electrochemical sensors based on the direct electrocatalysis of glucose at the electrode. Sensors of this type have some outstanding properties that set them apart; they are simple, reproducible and highly stable [20, 21, 115]. For nonenzymatic glucose sensors, the electrochemical performance much depends on the catalytic activity of the catalysts toward glucose oxidation. With this perspective, the search for electroactive materials with the ability to electro-oxidize glucose with fast kinetics and at a low overpotential is foremost. Various catalytic materials such as the noble metals (Au [18, 116], Pd [114], and Pt [117-119]), and the transition metal (Ni [20, 120, 121], Cu [122, 123], and Co [124]) and their oxides ($NiO/Ni(OH)_2$ [125-127], CuO [128], and Co_3O_4 [22, 129, 130]) have been applied. The transition metals and their oxides have good catalytic properties and are highly sensitive to glucose oxidation. However, an alkaline solution is frequently required for these and thus they are impractical for clinical diagnosis. Pt is a special metal in view of its high electrocatalytic activity toward glucose oxidation in neutral media. However, the loss of catalytic activity due to the accumulation of chemisorbed intermediates from the glucose oxidation process is a critical limitation that prevents the direct application of Pt in the fabrication of glucose sensors.

Development of bimetallic Pt-based materials is thought to be an effective way of addressing this limitation. In many cases, bimetallic catalysts have proven to have superior catalytic efficiency than single metal catalysts. The synergistic effect on the performance of heterometallic nanocatalysts is subject to the surface electronic states, which are greatly affected by changes in the geometric parameters of the catalysts, and are related in particular to the local strain and the effective atomic coordination number on the surface [23, 24, 131]. Great efforts have been dedicated to modifying Pt surfaces by adding metals such as Ru, Pb, Cu, and Ni to them [23, 115, 132-134]. Compared to monometallic Pt, bimetallic Pt has distinct synergistic characteristics and offers electrodes with highly desirable electronic and catalytic properties. It has been demonstrated that a bimetallic alloy of Pt_2Pb catalyzed glucose oxidation not only at a more negative potential than a pure Pt electrode but also with a much higher current response [133]. In addition, the atomic ratio between Pt and Pb also affected the catalytic ability and the sensitivity for sensing glucose [112]. Au is another interesting metal that also displays catalytic activity toward the oxidation of glucose in neutral media. As a result of its filled d orbitals, it is more stable toward oxidation and poisoning during experiments than Pt [18]. In another previously published report, Au clusters were shown to have a stabilizing effect on an underlying Pt surface under highly oxidizing conditions and to suppress Pt dissolution during potential cycling, without decreasing the catalytic activity [135].

The key idea of this work is to combine Pt and Au to improve the electrocatalytic activity and the tolerance to poisoning. A BDD electrode modified with a bimetallic Pt/Au nanocatalyst (Pt/Au/BDD) was used as an effective non-enzymatic glucose sensor. BDD was used for the substrates for the electrodes because of its superior electrochemical properties such as the wide potential window, high resistance to fouling, and low background current. Bimetallic Pt/Au is easily prepared using electrodeposition techniques by sequential depositing Au and Pt on the BDD electrode surface. The electrocatalytic activities of the modified electrodes toward glucose oxidation were studied. The effects of various electrodeposition processes and the composition of the Pt-Au catalyst in preparing

the modified BDD electrodes on the electrocatalytic activity and the sensitivity for glucose oxidation were also investigated. The linearity, LOD, the sensitivity, and the selectivity obtained from these electrodes were compared to Pt/BDD and Au/BDD electrodes, and a commercial flat Pt electrode. We found that significant improvements in the response to glucose improvements were obtained with the Pt/Au/BDD electrode as well as excellent stability, selectivity and reproducibility.

4.6 Experimental section

4.6.1 Chemicals

Potassium tetrachloroaurate(III) ($K[AuCl_4]$), potassium tetrachloroplatinate(II) ($K_2[PtCl_4]$) and glucose were purchased from Wako Chemicals. All the chemicals were used as received without any further purification. Deionized water (18.2 MΩ cm) was used in all the experiments.

4.6.2 Preparation of the modified electrodes

The BDD electrodes were grown on Si (111) wafers using a microwave plasma-assisted chemical vapor deposition system (Astex Corp.) Acetone and $B(OCH_3)_3$ were used as the carbon and boron sources, respectively, with an atomic ratio of B/C = 1%. Electrodeposition was used to prepare the modified electrodes. $K[AuCl_4]$ and $K_2[PtCl_4]$ were each dissolved in solutions of 0.2 M H_2SO_4. One-step electrodeposition was performed in a mixture of 1 mM $K[AuCl_4]$ and 1 mM $K_2[PtCl_4]$ by applying an accumulation potential of -0.5 V for 180 s. The modified electrode was then rinsed with water to remove physically adsorbed substances. This modified electrode is denoted as the AuPt/BDD electrode. For two-step sequential electrodeposition, two types of modified electrodes were prepared. The first is a Pt/Au/BDD electrode. This was prepared by depositing Au onto the BDD surface using the 1 mM $K[AuCl_4]$ solution. Then, Pt was deposited onto the Au layer using the 1 mM $K_2[PtCl_4]$ solution. The second is an Au/Pt/BDD electrode. To prepare this, the order in which the metals were deposited was reversed; the Pt was deposited first, and the Au second. Au/BDD and Pt/BDD electrodes were also prepared using one-step electrodeposition

procedures with 1 mM $K[AuCl_4]$ and 1 mM $K_2[PtCl_4]$ solutions, respectively. These were used for comparison.

4.6.3 Apparatus and Electrochemical Measurements

The modified electrodes were characterized by field-emission scanning electron microscopy (FESEM, JEOL JSM-7610F at 15 kV) and X-ray diffraction (XRD, Bruker AXS D8 DISCOVER). Electrochemical experiments were performed on an ALS852D (ALS/CH Instruments) electrochemical analyzer at room temperature (25 °C). A three-electrode cell with a sample volume of 80 µL, a Ag/AgCl reference electrode, a Pt wire as a counter electrode, and the modified BDD as a working electrode, was employed.

4.7 Results and discussion

4.7.1 Characterization of the modified electrodes

FE-SEM images of the different nanomaterials are shown in Figure 4.5a-e. For the Au/BDD electrode, the Au nanospheres are evenly dispersed across the BDD surface, as shown in Figure 4.5a. The image of the Pt/BDD electrode in Figure 4.5b clearly shows that direct electrodeposition of Pt^{2+} on the bare BDD surface has led to the aggregation of thin Pt sheets to form a flower-like morphology. The AuPt/BDD, shown in Figure 4.5c, displays a flower-like structure comprising numerous small nanoparticles. In the case of the Pt/Au/BDD electrode, shown in Figure 4.5d, for which the Pt particles were deposited onto the layer of Au particles, a thin sheet of uniformly dispersed Pt particles with high density can be seen. For the Au/Pt/BDD electrode, for which the Au particles were deposited onto the Pt particles, the FE-SEM image shows an aggregate of many tiny Au and Pt particles leading to the formation of flower-like structures of various sizes (Figure 4.5e).

The crystalline structures of the Au-Pt nanostructures on the BDD electrode surfaces were verified by XRD analysis as shown in Figure 4.5f. For the Pt/BDD and Au/BDD electrodes, major characteristic peaks at *c.a.* 39.81° (line a) and 38.31° (line b) were observed, indicating the crystalline nature of Pt and Au, respectively.[136] For

AuPt/BDD (line c), the diffraction peak has shifted to a higher 2θ value than pure Pt but smaller than that of pure Au, confirming the formation of a AuPt alloy.[137] The Pt/Au/BDD (line d) and Au/Pt/BDD (line e) electrodes both have large and small diffraction peaks at the same positions as pure Pt and Au, respectively. These results indicate that the formation of the Au-Pt nanostructures on the Pt/Au/BDD and Au/Pt/BDD electrodes, are in the form of a bimetallic mixture rather than an alloy.

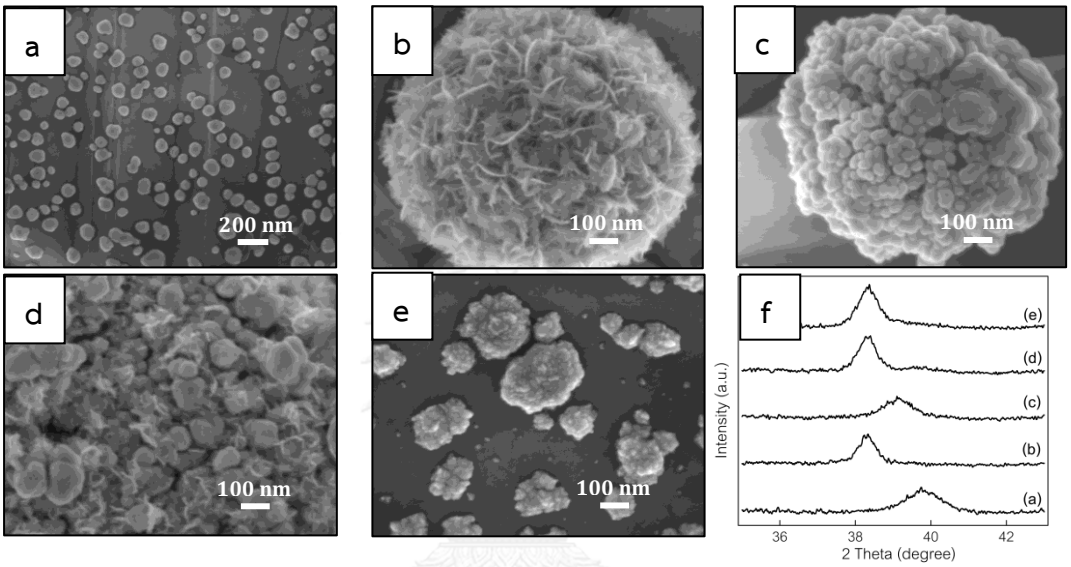

Figure 4.5 FE-SEM images of (a) Au/BDD, (b) Pt/BDD, (c) AuPt/BDD, (d) Pt/Au/BDD, and (e) Au/Pt/BDD electrodes, respectively. (f) XRD patterns of Au/BDD (line a), Pt/BDD (line b), AuPt/BDD (line c), Pt/Au/BDD (line d), and Au/Pt/BDD (line e), respectively.

4.7.2 Electrocatalytic Activity toward Glucose Oxidation in Neutral Media

The nonenzymatic oxidation of glucose at unmodified BDD, Pt/BDD, Au/BDD and Pt/Au/BDD electrodes was studied using cyclic voltammetry, and their electrocatalytic characteristics were compared. For the simple BDD electrode (Figure 4.6a), no redox peaks in the potential range from 0 to 1.2 V were observed in the absence and presence of 5 mM glucose in 0.1 M PBS (pH 7.4) containing 0.1 M NaCl. In contrast, the CV curve for the Pt/Au/BDD electrode (Figure 4.6b) without glucose displays hydrogen adsorption/desorption peaks at negative potentials, a flat double layer region at intermediate potentials, and metal oxide formation/reduction peaks

at positive potentials. After adding 5 mM glucose, an anodic peak appears at a potential of around -0.087 V. This is marked as the onset of glucose oxidation. During the positive scan, multiple oxidation peaks were observed. The first anodic peak can be attributed to the electrochemical adsorption of glucose on the surface, forming a layer of glucose intermediates. On moving the potential to more positive values, the adsorbed glucose was oxidized, resulting in an oxidation peak above 0.2 V. In the negative scan, a reduction peak at 0.1 V appears. This can be attributed to reduction of the surface oxide, which had grown at the high positive potential. With reduction of the surface oxide, more surface-active sites became available for the oxidation of glucose, resulting in a large and broad oxidation peak. These phenomena were in accordance with those reported in previous publications [138, 139]. The anodic current observed after adding glucose to the supporting solution demonstrates the electrocatalytic activity of the Pt/Au/BDD electrode for glucose oxidation. For comparison, the electrochemical responses for glucose oxidation at the Pt/BDD (Figure 4.6c) and Au/BDD (Figure 4.6d) electrodes were also investigated. The CV curves obtained for these electrodes displayed similar characteristics for glucose oxidation as the Pt/Au/BDD electrode, but the peak current obtained with the Pt/Au/BDD electrode was larger than that obtained with the Pt/BDD and Au/BDD electrodes. In addition, the oxidation peak potential with the Pt/Au/BDD electrode (-0.087 V) was lower than that with the Pt/BDD (-0.065 V) and Au/BDD (-0.045 V) electrodes, demonstrating that the Pt/Au/BDD electrode providesthe highe st catalytic activity toward glucose oxidation in neutralmedia compared with BDD electrodes modified with Pt or Au only.

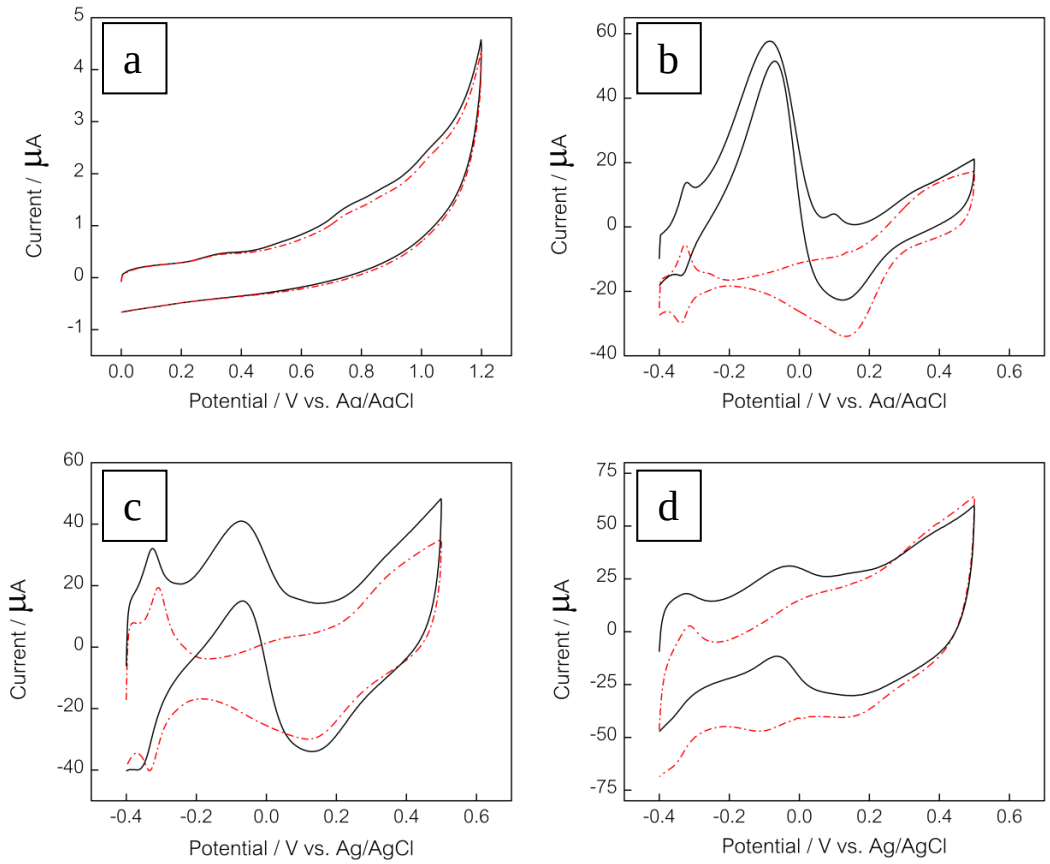

Figure 4.6 Cyclic voltammograms for (a) unmodified BDD, (b) Pt/Au/BDD, (c) Pt/BDD, and (d) Au/BDD electrodes in the absence (red dashed line) and presence of 5 mM glucose (black solid line) in 0.1 M PBS (pH 7.4) containing 0.1 M NaCl. Scan rate: 50 mV/s.

We also investigated the influence on glucose oxidation of the different electrodeposition procedures for forming the bimetallic electrodes. Figure 4.7 shows the CVs recorded in 5 mM glucose using the Pt/Au/BDD, Au/Pt/BDD, and AuPt/BDD electrodes. The glucose oxidation peak for the Pt/Au/BDD electrode is the highest, demonstrating that the nanocatalyst with Pt nanoparticles on top of Au nanoparticles had higher electrocatalytic activity for glucose oxidation than nanocatalysts in the form of a bimetallic alloy of AuPt, or with Au nanoparticles on top of Pt nanoparticles. Thus, the catalytic performance of the electrode depends on

the process by which the Pt and Au nanostructure is formed on the surface of the BDD electrode.

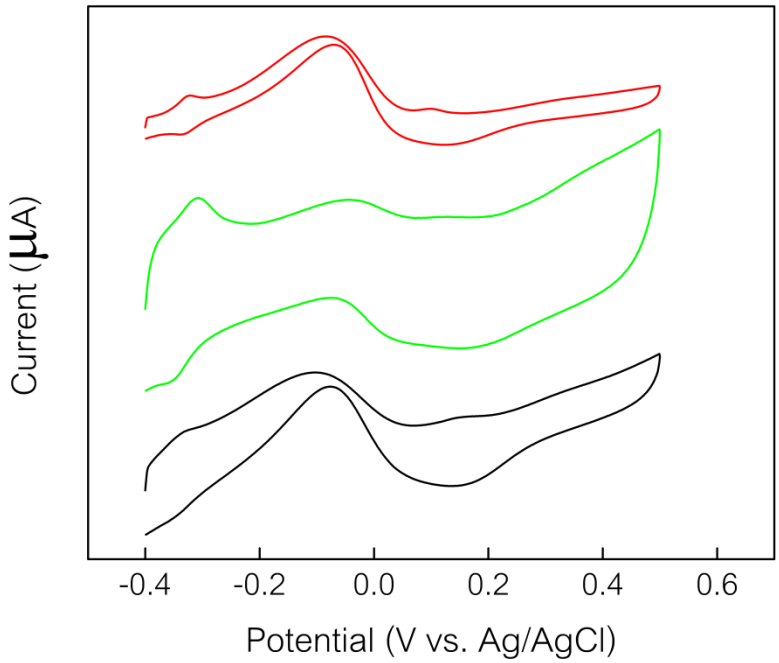

Figure 4.7 Cyclic voltammograms for 5 mM glucose in 0.1 M PBS (pH 7.4) containing 0.1 M NaCl at AuPt/BDD (black line), Au/Pt/BDD (green line), and Pt/Au/BDD (red line) electrodes. Scan rate: 50 mV/s.

4.7.3 Optimization parameters

On the basis of the above discussion, it is clear that the Pt/Au/BDD electrode has the best performance for the electro-oxidation of glucose. Here, we focus on optimizing this bimetallic nanomaterial. The electrodeposition parameters including the deposition potentials, the total concentration and the molar ratio of the Au and Pt precursors may be important aspects for fabricating sensors with the best electrocatalytic properties. The effect of the deposition potentials for Au and Pt on the glucose oxidation current are shown in Figure 4.8a and 4.8b, respectively. The increase in deposition potential has resulted in a significant increase in the glucose current response, which can be attributed to the increase in the amount of metal

electrodeposited on the electrode surface. This may be related to the increase in film thickness as well as the increase in nucleation during the electrodeposition process. However, at more negative deposition potentials, beyond -0.4 V for Au and -0.5 V for Pt, the Pt/Au/BDD electrodes have lower analytical performance. This may be because that large amount of metal has aggregated leading to a decrease in catalytic performance.

The total concentration and molar ratio of the Pt and Au precursors were also investigated. The concentrations of $K[AuCl_4]$ and $K_2[PtCl_4]$ were examined at a fixed molar ratio of 1:1 for the $K[AuCl_4]$ and $K_2[PtCl_4]$. The relationships between the current and the number of measurements and the concentration were considered. The number of measurements is defined as the number of cycles before the current signal decreases by 7% from the first cycle. As shown in Figure 4.8c, the maximum current and the highest number of measurements were obtained at 1 mM concentrations of $K[AuCl_4]$ and $K_2[PtCl_4]$ (i.e., the total concentration was 2 mM). Subsequently, the molar ratio of $K[AuCl_4]$ and $K_2[PtCl_4]$ was examined (the total concentration was kept at 2 mM). As shown in Figure 4.8d, the signal current increases with increasing Pt:Au molar ratio, indicating the catalytic activity depends mainly on the amount of Pt. However, for both high and low molar ratios, the response of electrode was unstable which might be due to the loss of activity as a result of the accumulation of chemisorbed intermediates leading to the electrocatalyst blocking the surface. On the other hand, with a molar ratio of 50:50, the electrode not only gave high current but was also highly stable. Interestingly, it has been reported that the presence of Au might address the poisoning problem of Pt catalysts, changing the electronic band structure of Pt by modifying the strength of the surface adsorption, which is an essential factor for improving the catalytic performance and efficiency of Pt catalysts.[140]

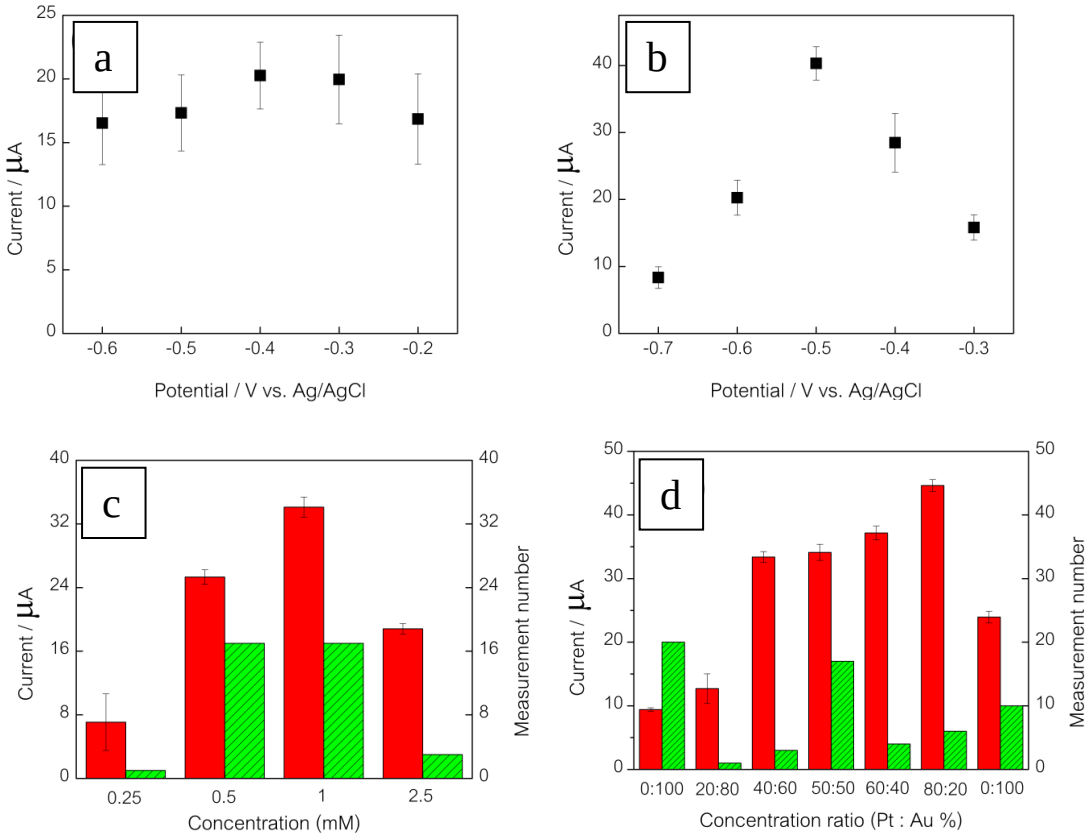

Figure 4.8 Effect of electrodeposition conditions on nonenzymatic glucose oxidation. Dependence of the current on (a) the deposition potential of Au, (b) the deposition potential of Pt, (c) the concentration of the Au and Pt precursors and (d) the molar ratio of Au and Pt precursors.

4.7.4 Analytical performance

After characterizing the modified electrodes with cyclic voltammetry, the analytical performances were examined using chronoamperometry, because this is more sensitive, leading to lower detection limits. In addition, for long-term applications, it is an easier detection method to implement [56]. First, optimization of the applied potential to achieve the greatest sensitivity for glucose oxidation was carried out. The applied potential was studied in the range from 0 to -0.25 V. The highest signal current was achieved at a potential of -0.15 V. Therefore, this was selected for further experiments.

The chronoamperometric response for glucose at the surfaces of the Pt/Au/BDD (Figure 4.9a), Pt/BDD (Figure 4.9b) and Au/BDD (Figure 4.9c) electrodes, and that of a commercial flat Pt (Figure 4.9d) electrode in 0.1 M PBS (pH 7.4) containing 0.1 M NaCl were studied, and their analytical performances were compared. With increasing glucose, the oxidation peak currents increase gradually suggesting that these peaks were indeed due to the oxidation of glucose. Calibration curves derived from the chronoamperometric data are shown in Figure 4.10. This indicates that the Pt/Au/BDD electrode has the best analytical performance. The response of this electrode is linear in the concentration range from 0.01-7.5 mM with an experimental limit of detection (LOD) of 0.01 mM. The Pt/BDD electrode had higher sensitivity but a narrower linear range than the bulk Pt electrode. This smaller linear range may have been caused by poisoning; the accumulation of intermediates on the electrode surface may have blocked some active surface sites resulting in the short linear response. The sensitivity of the Au/BDD electrode was poor, due to the low catalytic activity for glucose oxidation. The linear range, detection limit and the sensitivity of the electrodes are summarized in Table 1. The lower and upper limits of the linear range of the Pt/Au/BDD electrode cover the physiological range (3.5 – 6.1 mM) [115], suggesting that this is a very promising electrode configuration for analytical applications.

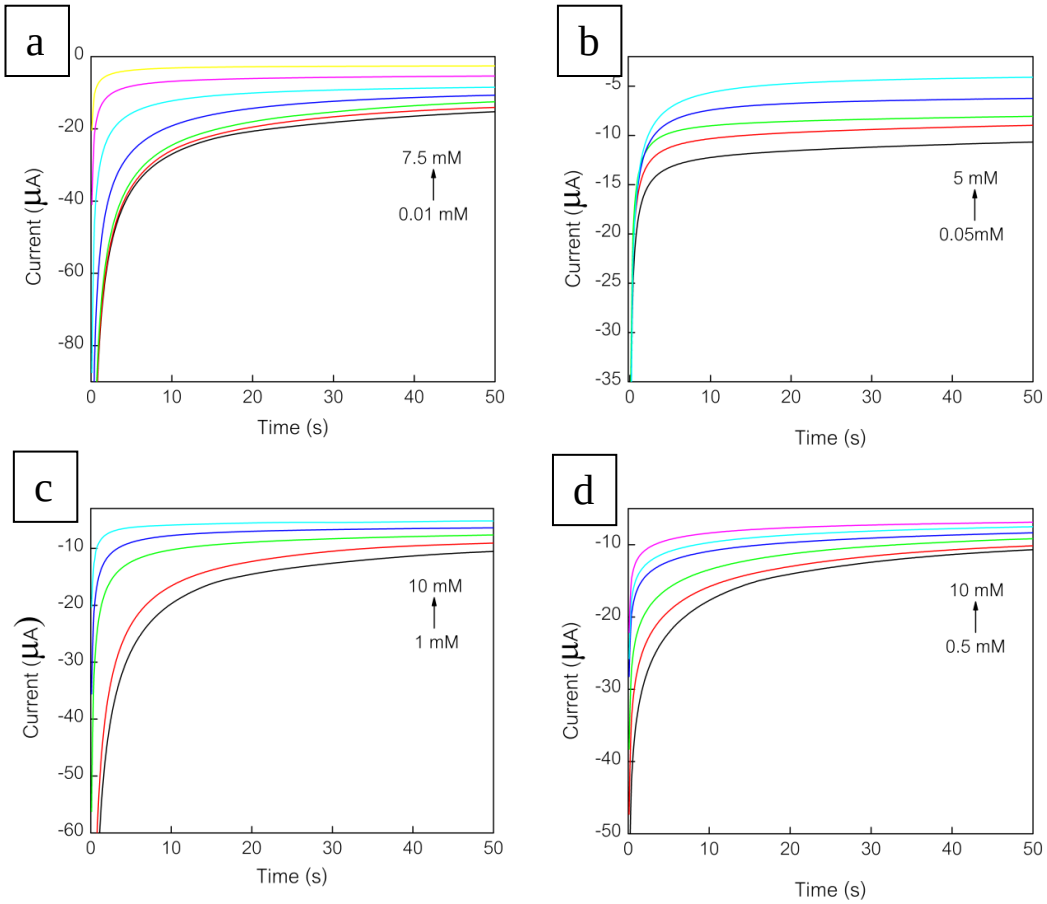

Figure 4.9 Chronoamperograms for different concentrations of glucose in 0.1 M PBS (pH 7.4) containing 0.1 M NaCl with (a) a Pt/Au/BDD electrode, (b) a Pt/BDD electrode, (c) a Pt electrode, and (d) a Au/BDD electrode. The applied potential in each case was -0.15 V.

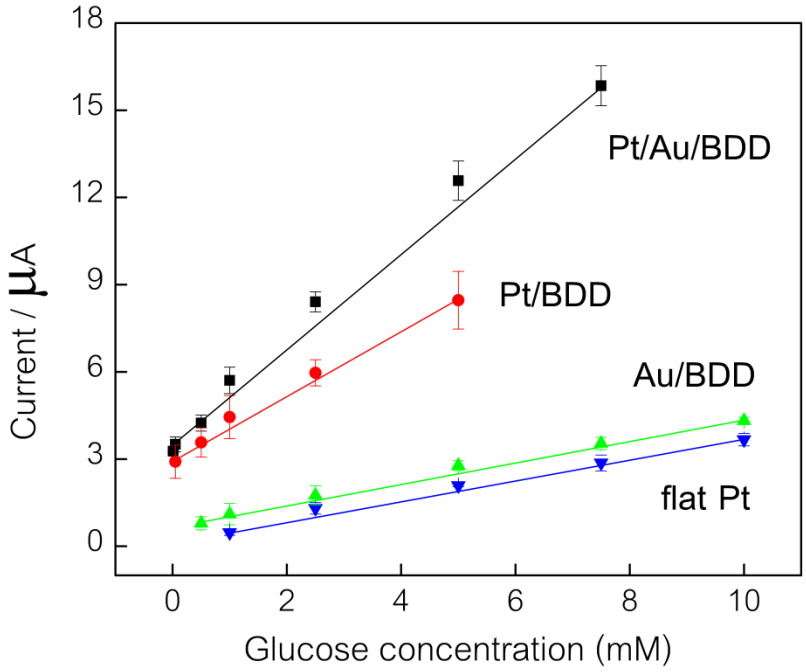

Figure 4.10 Calibration curves for the chronoamperometric tests shown in Figure S1. The working electrodes are a commercial flat Pt (blue) electrode, and Au/BDD (green), Pt/BDD (red) and Pt/Au/BDD (black) electrodes. The applied potential was -0.15 V with a sampling time of 50 s.

Table 4.3 Summary of the performances of the electrodes

Electrode	Linear equation	Linear range (mM)	Detection limit (mM)
commercial flat Pt	y = 0.3426x + 0.299	1-10	1
Au/BDD	y = 0.3685x + 0.7539	0.5-10	0.5
Pt/BDD	y = 0.3685x + 0.7539	0.05-5	0.05
Pt/Au/BDD	y = 1.6962x + 3.6369	0.01-7.5	0.01

4.7.5 Effects of chloride ions

Chloride ions may have a serious poisoning effect on metal or alloy electrocatalysts leading to loss of activity for the oxidation of glucose [141]. Thus, the influence of chloride ions was examined by cyclic voltammetry. Different concentrations of NaCl were added to the supporting electrolyte (0.1 M PBS). The results show that chloride ions (0.05-1 mM) lead to only minimal changes in current for 5 mM glucose compared to that recorded in the absence of chloride ions (Figure 4.11). In addition, the oxidation peak potential remains unchanged with the presence of chloride ions. This means that chloride ions have no noticeable poisoning effect on the Pt/Au catalyst, and the sensor can be used for glucose sensing even in the presence of high concentrations of chloride ions.

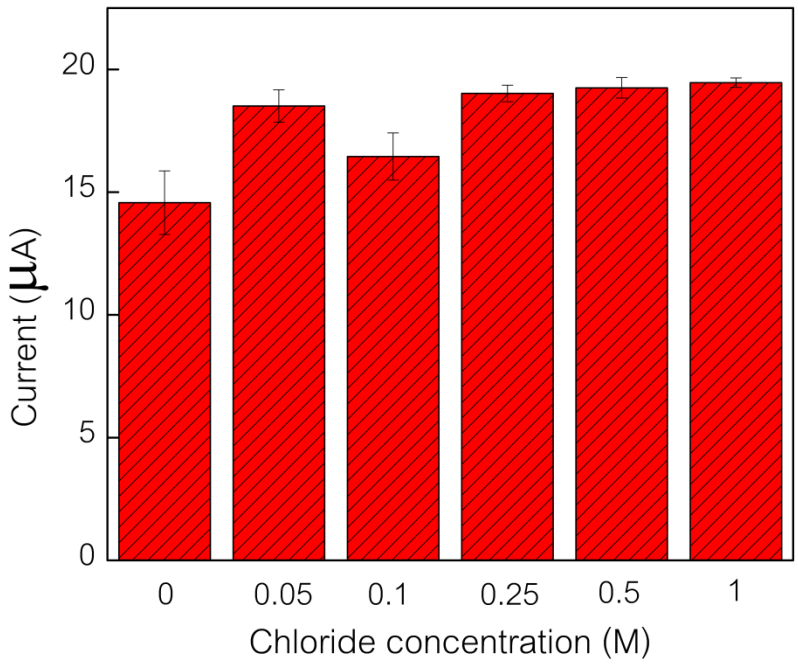

Figure 4.11 The electrochemical response of 5 mM glucose in 0.1 M PBS (pH 7.4) containing different concentrations of NaCl

4.7.6 Selectivity

An important parameter for a biosensor is its ability to distinguish between interfering species and the target analyte in physiological environments. Although the normal physiological level of glucose (3.5-6.1 mM) is much higher than that of other redox-active interfering species such as ascorbic acid (AA) (~0.1 mM) uric acid (UA) (~0.02 mM), and AP (~0.1 mM), their electron transfer rates are higher than that of glucose. As a result, the oxidation current for them is comparable to that of glucose. Therefore, AA, UA, and AP are major interfering species for the detection of glucose. The CV scans of 5 mM glucose, 0.1 mM AA, 0.2 mM AP, and 0.5 mM UA with different types of electrodes were investigated. The CVs obtained with the Pt/Au/BDD and Pt/BDD electrodes, and the commercial flat Pt electrode, are shown in Figure 4.12a-c, respectively. For these modified electrodes, the onset potential for glucose oxidation is much lower than the one recorded for AA, UA, and AP oxidation. On the other hand, the CV scans with the Au/BDD electrode showed overlapping between the glucose and AA oxidation peaks (Figure 4.12d). To confirm the results, the amperometric responses of glucose and the interfering species were further investigated. The results are shown in Table 4.4. For the Pt/Au/BDD, Pt/BDD and Pt electrodes, the interfering species led to only minimal changes relative to the response current to 5 mM glucose, generally less than ±5.0%, compared to that recorded in the absence of the interfering species. This means that these substances did not interfere in the determination of glucose, and the sensors have high selectivity. In contrast, the current when using the Au/BDD electrode increased by 20% after adding AA, demonstrating that the selectivity between glucose and AA was poor for this electrode.

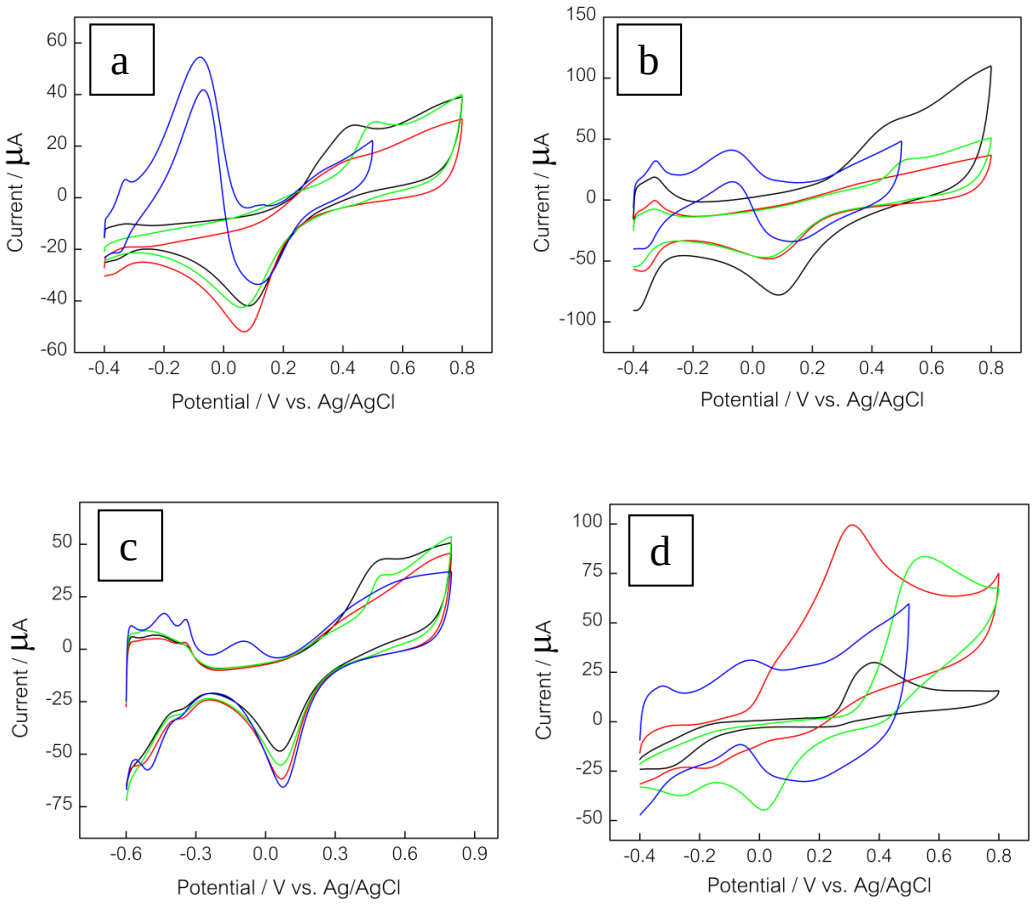

Figure 4.12 Cyclic voltammograms for the oxidation of 5 mM glucose (blue), 0.1 mM AA (red), 0.5 mM UA (black), and 0.2 mM AP (green) obtained with the Pt/Au/BDD electrode (a), the Pt/BDD electrode (b), the commercial flat Pt electrode (c), and the Au/BDD electrode (d).

Table 4.4 The effect of interfering species on glucose determination for the modified electrodes.

Electrode	Glucose + interference	$(I_{glucose+interference}/I_{glucose})\times100$
Pt	Glucose + UA	103.42
	Glucose + AA	101.14
	Glucose + AP	98.86
Pt/BDD	Glucose + UA	97.71
	Glucose + AA	96.58
	Glucose + AP	101.34
Au/BDD	Glucose + UA	103.36
	Glucose + AA	122.39
	Glucose + AP	104.73
Pt/Au/BDD	Glucose + UA	100.44
	Glucose + AA	96.19
	Glucose + AP	99.27

4.7.7 Reproducibility and repeatability

The reproducibility of the electrode is expressed in terms of the relative standard deviation (RSD) for six Pt/Au/ BDD electrodes under the same conditions and concentration of glucose (5 mM) using six prepared electrodes in parallel. It was found that the six electrodes, made independently, had acceptable reproducibility

with a relative standard deviation of 3.2%. To test the repeatability of the Pt/Au/BDD electrode, we performed 15 successive measurements at a glucose concentration of 5 mM. The relative standard deviation was 3.6%, revealing an acceptable repeatability.

4.8 Conclusions

In summary, a novel modified BDD electrode with bimetallic Pt/Au can be conveniently prepared using a simple electrodeposition process. This electrode is especially suited for use as a nonenzymatic glucose sensor owing to its high electrocatalytic activity for glucose oxidation in physiological conditions, its high resistance to poisoning by chloride ions, and its high selectivity for the detection of glucose. It is capable of sensing glucose chronoamperometrically at a negative potential of -0.15 V (Ag/AgCl), where the interference from the oxidation of common interfering species such as AA, AP, and UA are effectively avoided. A wide linear range of 0.01 mM to 7.5 mM and a low detection limit of 0.01 mM were obtained. This novel catalytic material has the potential to be used in catalysis, for sensors and so on.

CHAPTER V

DEVELOPMENT OF BORON DOPED DIAMOND ELECTRODE FOR PAPER-BASED ANALYTICAL DEVICE

There are two parts for this chapter. Past I reports a novel paper-based device coupled with a silver nanoparticle-modified boron doped diamond electrode for cholesterol detection. Past II presents boron doped diamond paste electrodes for microfluidic paper-based analytical devices.

Part I:

A novel paper-based device coupled with a silver nanoparticle-modified boron-doped diamond electrode for cholesterol detection

Siriwan Nantaphol [a], Orawon Chailapakul [a,b*] and Weena Siangproh [c**]

[a] Electrochemistry and Optical Spectroscopy Research Unit, Department of Chemistry, Faculty of Science, Chulalongkorn University, 254 Phayathai Road, Pathumwan, Bangkok 10330, Thailand

[b] Center for Petroleum, Petrochemicals and Advanced Materials, Chulalongkorn University, 254 Phayathai Road, Pathumwan, Bangkok 10330, Thailand

[c] Department of Chemistry, Faculty of Science, Srinakharinwirot University, Sukhumvit 23, Wattanna, Bangkok 10110, Thailand

* Co-corresponding author:

** Corresponding author

Analytica Chimica Acta 891 (2015): 136-143

Abstract

A novel paper-based analytical device (PAD) coupled with a silver nanoparticle-modified boron-doped diamond (AgNP/BDD) electrode was first developed as a cholesterol sensor. The AgNP/BDD electrode was used as working electrode after modification by AgNPs using an electrodeposition method. Wax printing was used to define the hydrophilic and hydrophobic areas on filter paper, and then counter and reference electrodes were fabricated on the hydrophilic area by screen-printing in house. For the amperometric detection, cholesterol and cholesterol oxidase (ChOx) were directly drop-cast onto the hydrophilic area, and H_2O_2 produced from the enzymatic reaction was monitored. The fabricated device demonstrated a good linearity (0.39 mg dL^{-1} to 270.69 mg dL^{-1}), low detection limit (0.25 mg dL^{-1}), and high sensitivity (49.61 µA mM^{-1} cm^{-2}). The precision value for ten replicates was 3.76 % RSD for 1 mM H_2O_2. In addition, this biosensor exhibited very high selectivity for cholesterol detection and excellent recoveries for bovine serum analysis (in the range of 99.6-100.8 %). The results showed that this new sensing platform will be an alternative tool for cholesterol detection in routine diagnosis and offers the advantages of low sample/reagent consumption, low cost, portability, and short analysis time.

5.1 Introduction

Cholesterol is an essential component of the mammalian cell membrane and is a precursor of bile acid and steroid hormones. However, abnormal cholesterol levels are related to several diseases, such as hypertension, coronary heart disease, arteriosclerosis, brain thrombosis, lipid metabolism dysfunction and myocardial infarction [92]. Thus, the monitoring of the cholesterol level is very important for disease control and prevention. Various analytical strategies for cholesterol assays have been developed that can be sub-classified into two groups, including a chemical and an enzymatic method [142-145]. Currently, the enzymatic method has received greater attention for cholesterol analysis because it provides greater sensitivity and selectivity than the chemical method. The well-known principle of an enzyme-based cholesterol sensor is typically based on the reaction between cholesterol and the cholesterol oxidase (ChOx) enzyme. Free cholesterol is oxidized by cholesterol oxidase to produce 4-cholestene-3-one and hydrogen peroxide (H_2O_2), and the H_2O_2 generated can be used for indirect quantification of cholesterol [9, 10, 146]. The electrochemical method, especially the electrochemical biosensor, is extremely attractive for the determination of cholesterol because the electrochemical biosensors provide high sensitivity, require inexpensive instrumentation, and are suitable for real-time analysis. Previously, several methods have been used to immobilize the enzyme onto an electrode, such as entrapment in a polymer [147], covalent linkage with glutaraldehyde [148] or a polymer [149], and electrostatic adsorption [150]. Although these sensing platforms provide good performance for cholesterol detection, limitations still remain in terms of time consumption, detection performance and the ease with which the enzyme is denatured during its immobilization. To overcome this drawback, it is necessary to design and fabricate a new cholesterol sensor that offers simple fabrication, an easy immobilization step, and a short analysis time.

Recently, filter paper has received interest as a potential material for sensor applications due to its large surface area and low cost. In 2009, electrochemical detection on a paper-based analytical device (PAD) was first developed by Dungchai and coworkers [56]. This platform became a new alternative analytical device and

was applied in many application areas [151-156]. Their simplicity of fabrication, portability and disposability coupled with the small volume of reagent/sample solution required for PADs make them suitable and very appealing for the development of new clinical diagnostic tools. Moreover, the biocompatibility of filter paper makes it suitable for immobilization of enzymes or other bioreceptors [61, 157, 158]. However, the traditional paper-based electrochemical devices with a three-electrode system (consisting of a working electrode (WE), a counter electrode (CE), and a reference electrode (RE)) still have some limitations, including low sensitivity because of a small electrode area and the use of carbon ink as a working electrode [56, 159].

To solve these problems, the use of a commercial electrode coupled with PAD was considered. Boron-doped diamond (BDD) thin films are novel carbon-based materials that have very attractive properties compared to other conventional electrodes in terms of (i) wide electrochemical potential window; (ii) low and stable background current; (iii) resistance to electrode fouling; (iv) high response reproducibility and long-term response stability; and (v) biocompatibility. As advantages, we can conclude that the BDD electrodes provide the potential for electroanalysis application with high sensitivity [160-162]. To eliminate possible interference from easily oxidizable species in biological samples, cholesterol detection and measurement via the monitoring of H_2O_2 reduction is proposed in this work. Unfortunately, the reduction of H_2O_2 cannot be observed on a bare BDD electrode. Therefore, silver nanoparticle (AgNP) has been considered as the modifier for modification of the BDD surface because they have a large specific surface area, excellent conductivity and extraordinary electrocatalytic activity. Moreover, AgNP also show an excellent electrocatalytic activity for H_2O_2 reduction [11, 15, 16, 101].

On this basis, we have developed a novel cholesterol biosensor based on a silver nanoparticle-modified boron-doped diamond (AgNP/BDD) electrode with PAD. An electrodeposition method was used to deposit AgNP onto the BDD electrode surface. The resulting device possessed the advantages of simple fabrication, small sample volume/reagent requirements, low cost and short analysis time. In addition, the AgNP/BDD electrode exhibited a highly sensitive and selective response to detect

cholesterol without disturbance from interfering compounds such as ascorbic acid, uric acid, and glucose. To the best of our knowledge, this the first report of the coupling of an AgNP/BDD electrode with PAD to fabricate a cholesterol biosensor. The results show that this device displayed excellent performance, a wide linear range, and a low detection limit for cholesterol detection.

5.2 Experimental

5.2.1 Chemicals and materials

Cholesterol and cholesterol oxidase (ChOx) from *Streptomyces* sp. (25 U/mg) and lipid cholesterol enriched from adult bovine serum were purchased from Sigma (St. Louis, MO). Potassium dihydrogen phosphate (KH_2PO_4) was purchased from Carlo Erba Reagenti-SpA (Val de Reuil, France). Hydrogen peroxide (H_2O_2), disodium hydrogen phosphate (Na_2HPO_4), potassium chloride (KCl) and boric acid (H_3BO_3) were purchased from Merck (Darmstadt, Germany). Silver nitrate ($AgNO_3$) was purchased from POCH S.A. (Poland). Glacial acetic acid (CH_3COOH) was purchased from Fisher Scientific (Pittsburgh, PA). Phosphoric acid (H_3PO_4, 85%) was purchased from Carlo Erba (Rodano, MI, USA). Carbon ink and silver/silver chloride (Ag/AgCl) ink were obtained from Gwent Group (Torfaen, United Kingdom). Filter paper grade no. 1 (size, 46 x 57 cm^2) was purchased from Whatman. A stock solution of cholesterol was prepared daily by dissolving cholesterol in a mixture of Triton X-100 and isopropanol. This stock solution was further diluted to make different concentrations of cholesterol in 0.05 M PBS pH 7.4. The solution was stirred with a magnetic bar at 60 °C to obtain a homogeneous solution. Stock solution of ChOx was freshly prepared by dissolving in 0.05 M phosphate buffer (pH 7.0). All chemicals were used without further purification.

5.2.2 Sample preparation

The labeled concentration of cholesterol in adult bovine serum was used to represent the serum sample. The serum samples were prepared by dissolving adult

bovine serum powder in Triton X-100 and isopropanol, and diluting with 0.05 M PBS pH 7.4. The solution was stirred with a magnetic bar at 60 °C.

5.2.3 Preparation of AgNP/BDD electrode

A simple one-step electrodeposition method was used for the electrode modification. A three-electrode system (Ag/AgCl (3 M KCl) electrode as the reference electrode (RE), a platinum wire as the counter electrode (CE) and a BDD electrode as the working electrode (WE)) was used in this work. Electrodeposition of AgNPs onto the BDD electrode surface was accomplished by dipping the electrode in a solution of $AgNO_3$ in Britton-Robinson buffer (pH 2) and applying a potential with stirring. The electrode was then rinsed with water to remove any physically adsorbed substances on the electrode.

The electrodeposition parameters for the modification of the electrode including deposition potentials, deposition times, and concentrations of $AgNO_3$ could affect the performance of the electrochemical response for the H_2O_2 reduction, which should be optimized to increase the sensitivity. The ranges of each parameter optimized are shown in Table 5.1.

Table 5.1 Summary of the experimental parameters for modification of electrode

Parameters	Range tested	Optimum value
deposition potentials (V vs Ag/AgCl)	(-0.3) - (-0.7)	-0.5
deposition times (s)	25 - 300	150
concentrations of $AgNO_3$ (mM)	0.25 - 10	5

5.2.4 Fabrication of cholesterol sensor and analytical procedure

In this work, wax printing and filter paper (Whatman No. 1) were selected for the construction of the devices according to a previously reported method[28]. The

patterned PAD was designed by the Adobe Illustrator, and then the patterns were printed onto paper using a wax printer (Xerox Color Qube 8570, Japan). The printed PAD was heated on the hot plate at 175 °C for 50 s to melt the printed wax so that it penetrated through the paper to form the hydrophobic and hydrophilic patterns. Screen-printing in-house was used to fabricate CEs and REs. Carbon ink was used for the CE. Ag/AgCl ink was used for the RE and conductive pads. The screen block was designed using Adobe Illustrator software and constructed by Chaiyaboon Co. (Bangkok, Thailand). The CE and RE were screened onto the hydrophilic area on the top of the PAD. The double-sided adhesive tape was punched to create a 1.0 cm diameter hole. This double-sided adhesive tape was used to attach the bottom of the PAD and the AgNP/BDD electrode to complete the device. For the determination of cholesterol, an optimal volume of ChOx was drop-cast and dried onto the hydrophilic zone of the PAD. Then, 10 µL of standard/sample cholesterol solution was dropped, and electrochemical measurements were performed with a model PGSTAT 101 Autolab Electrochemical System controlled with the NOVA software package (Kanaalweg 29-G 3526 KM Utrecht, The Netherlands) at room temperature (22 ± 1 °C). The overall fabrication and analytical procedure for the determination of cholesterol are shown in Figure 5.1.

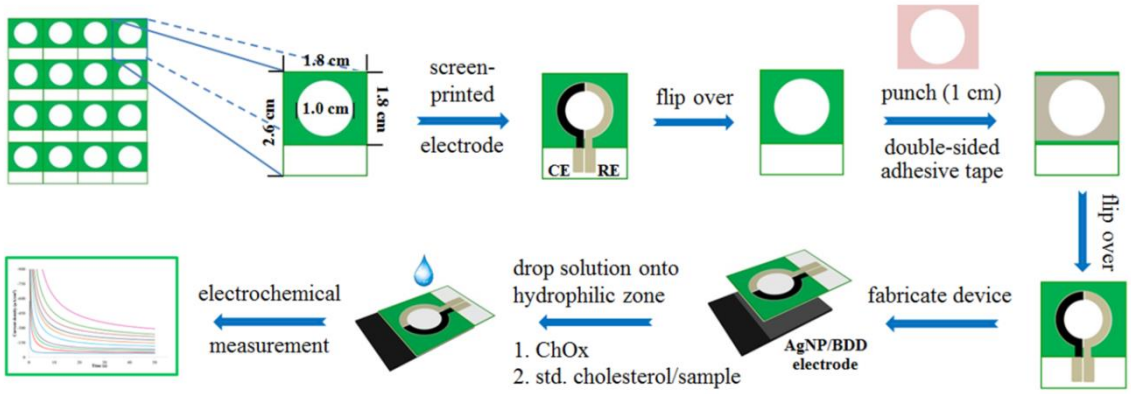

Figure 5.1 Schematic representation of the fabrication and analytical procedure for the cholesterol sensor based on the coupling of the AgNP/BDD electrode with PAD

5.3. Results and discussion

5.3.1 Device design

The coupling of the AgNP/BDD electrode with PAD for the fabrication of a cholesterol biosensor was designed to improve the electrochemical performance of the PAD using the BDD electrode as the WE instead of the traditional carbon screen-printed electrode. A low background current at the BDD electrode can enhance the sensitivity for the cholesterol detection. Moreover, the device that we have designed can reduce the consumption of standard/reagent solution and reduce the time required for the enzyme immobilization step by direct drop-casting of ChOx onto the hydrophilic zone of the PAD. The enzyme is immobilized on the filter paper by the adsorption process. After addition of the cholesterol solution, ChOx catalyzes the oxidation of cholesterol to generate H_2O_2 and cholest-4-en-3-one. The electrochemical reduction of H_2O_2 occurs at the modified electrode after a suitable potential is applied. The cathodic currents of H_2O_2 are recorded and used to determine the concentration of the cholesterol in the samples. The mechanism of cholesterol detection is shown in Figure 5.2.

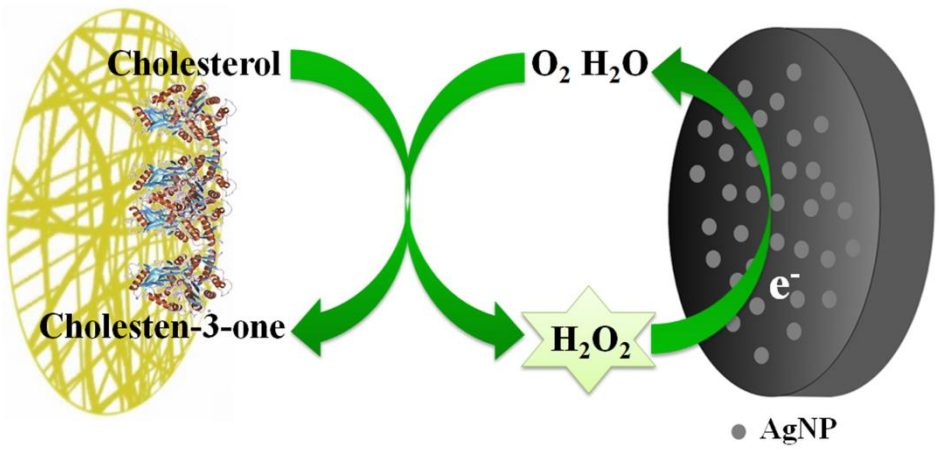

Figure 5.2 Schematic representation for the cholesterol detection processes on the AgNP/BDD electrode coupled with PAD

5.3.2 Surface morphology of AgNP/BDD electrode

Scanning electron microscope (SEM) was used to characterize the surface morphology of bare BDD electrode and AgNP/BDD electrode as shown in Figure 5.3a and Figure 5.3b, respectively. After electrodeposition of AgNPs, a number of nanoparticles were clearly seen. The size of AgNPs was in the nanoscale. Some bigger particles may be possibly caused by the aggregation. The distribution of AgNPs on the electrode surface led to increase the surface area and improve the electrochemical sensitivity of the modified electrode.

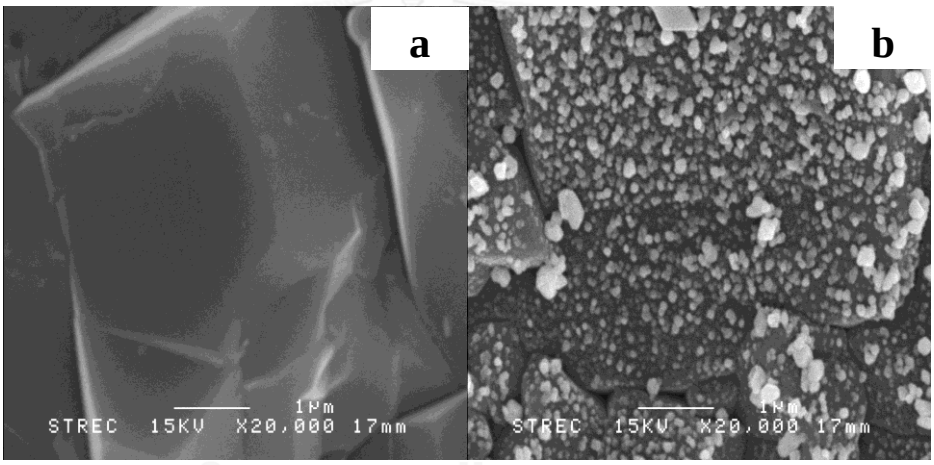

Figure 5.3 SEM images of (A) bare BDD electrode and (B) AgNP/BDD electrode prepared by electrodeposition at a potential of −0.5 V during 50 s from a pH 2 Britton-Robinson containing 5 mM $AgNO_3$

5.3.3 Electrochemical behavior of standard H_2O_2 and cholesterol on the AgNP/BDD electrode coupled with PAD

Cyclic voltammetry was initially employed to investigate the electrochemical behavior of H_2O_2 on the AgNP/BDD electrode coupled with PAD. The cyclic voltammograms (CVs) in the absence and presence of 1 mM H_2O_2, recorded at the bare BDD electrode and the AgNP/BDD electrode, corresponding to the background

at the scan rate of 100 mV s^{-1} are shown in Figure 5.4a. The cathodic peak of H_2O_2 did not appear at the bare BDD electrode, supporting the observation that this electrode has no electrochemical activity toward H_2O_2. For the AgNP/BDD electrode, a well-defined cathodic peak of H_2O_2 can be observed at a potential of approximately -0.61 V vs. Ag/AgCl, suggesting that the use of the BDD electrode modified with AgNPs can promote the electron transfer in the H_2O_2 reduction.

Subsequently, the electrochemical behavior of the H_2O_2 produced from the reaction between cholesterol and ChOx was investigated on an AgNP/BDD electrode coupled with the PAD. The results are shown in Figure 5.4b. The cathodic peak of the H_2O_2 that was produced appeared at a potential of approximately -0.71 V. The reduction peak potential of the H_2O_2 that was produced shifted to a more negative value compared to the reduction peak potential of standard H_2O_2 because of the effect of the Triton X-100 that was used as the surfactant for dissolving the cholesterol. The results indicated that the proposed device can be used as a new biosensor for cholesterol detection. Then, the effect of the enzyme volume on the cathodic current of 38.7 mg/dL of cholesterol was investigated in the range of 0.2-1.0 µL. The optimum volume of enzyme was 0.8 µL, and this volume was used for all experiments.

In addition, the effect of dissolved oxygen in the solution was investigated by monitoring the reduction current of H_2O_2 in this system, because the effect of O_2 during the electrochemical measurements is an area of concern. From the results, the net reduction currents (after the subtraction of the background) from before and after the N_2 purge were not significantly different, which agrees with the previous literature [51]. Thus, the cholesterol detection can be carried out in an atmospheric environment.

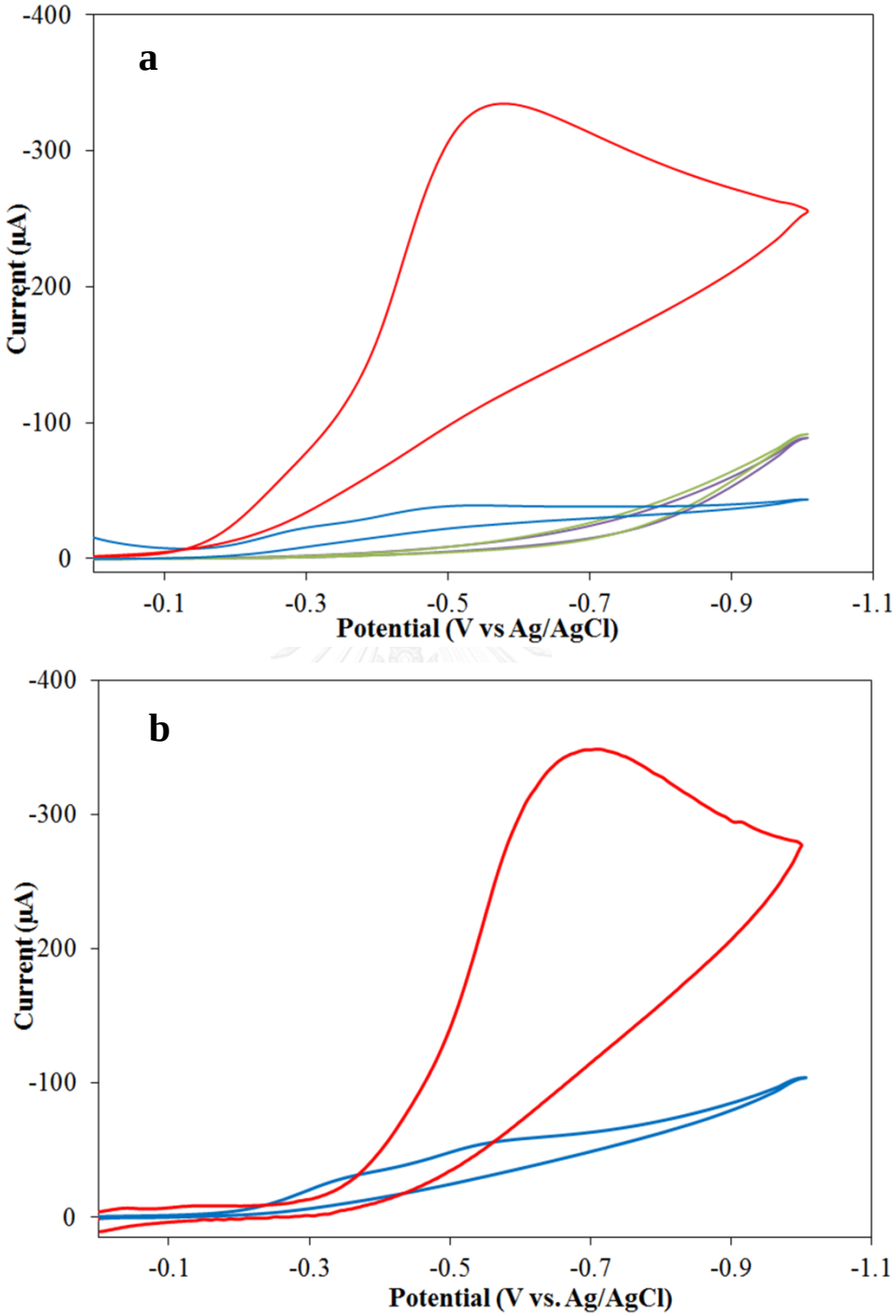

Figure 5.4 (a) CVs of the bare BDD electrode (purple line) and the AgNP/BDD electrode (blue line) in 0.05 M PBS, pH 7.4. CVs of reduction of 1 mM H_2O_2 at the bare BDD electrode (green line) and AgNP/BDD electrode (red line). Scan rate: 100 mV s^{-1}. (b) CVs of the AgNP/BDD electrode in the absence (blue line) and presence of 38.7 mg/dL cholesterol.

5.3.4 Effect of the scan rate

The effect of the scan rate is the most important experimental parameter for evaluating the mass transfer of the reactant toward the electrode via diffusion or adsorption control. Figure 5.5 shows cyclic voltammograms of 1 mM H_2O_2 in the potential range of 0 V to -1 V vs. Ag/AgCl with different scan rates at the AgNP/BDD electrode coupled with PAD. At the scan rate from 10 to 100 mV s^{-1}, the peak current (i_p) of H_2O_2 was proportional to the square root of the scan rate ($v^{1/2}$) (inset, Fig. 2; linear regression equation: y = -23.158x + 27.895 with R^2 = 0.9946). The results suggested that the mass transfer in this system was a diffusion-controlled process.

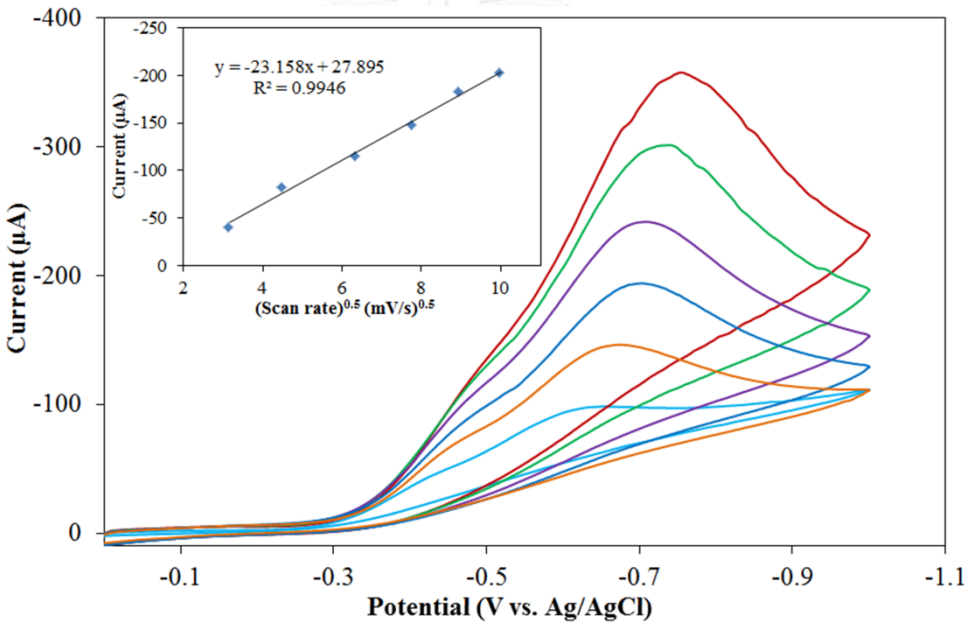

Figure 5.5 CVs for 1 mM H_2O_2 in 0.05 M PBS (pH 7.4) at the AgNP/BDD electrode coupled with PAD for a series of scan rates (10, 20, 40, 60, 80, and 100 mV s^{-1}). The relationship between cathodic current (µA) and $(\text{scan rate})^{0.5}$ is shown in the inset.

5.3.5 Selection of applied potential

Due to its high sensitivity and wide applicability, chronoamperometry was selected for the electrochemical determination of cholesterol. The sensitivity and selectivity of electrochemical detection depended on the selection of the applied

potential. To achieve the lowest detection limit and highest selectivity, the dependence of the current response of the fabricated biosensor on H_2O_2 reduction at applied potentials ranging from -0.5 to -1 V vs. Ag/AgCl was examined in 0.05 M PBS (pH 7.4) containing 1 mM H_2O_2. Figure 5.6a shows the *i-E* curve of the reduction current of 1 mM H_2O_2 and the background current at each potential. The reduction current of H_2O_2 and the background current were significantly increased by increasing the detection potentials. On the basis of sensitivity and selectivity, a hydrodynamic voltammogram of signal-to-background (S/B) ratios was considered instead of using only reduction currents. The results are shown in Figure 5.6b. The signal ratio reached a maximum at the detection potential of -0.7 V vs. Ag/AgCl. Therefore, an applied potential of -0.7 V vs. Ag/AgCl was selected for the chronoamperometric measurement in the following experiments.

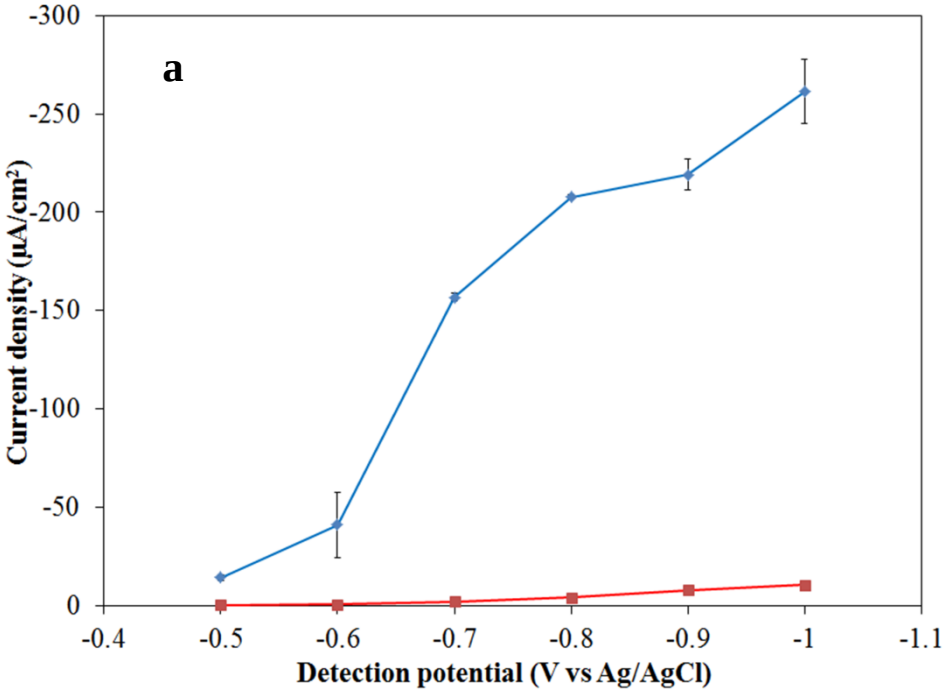

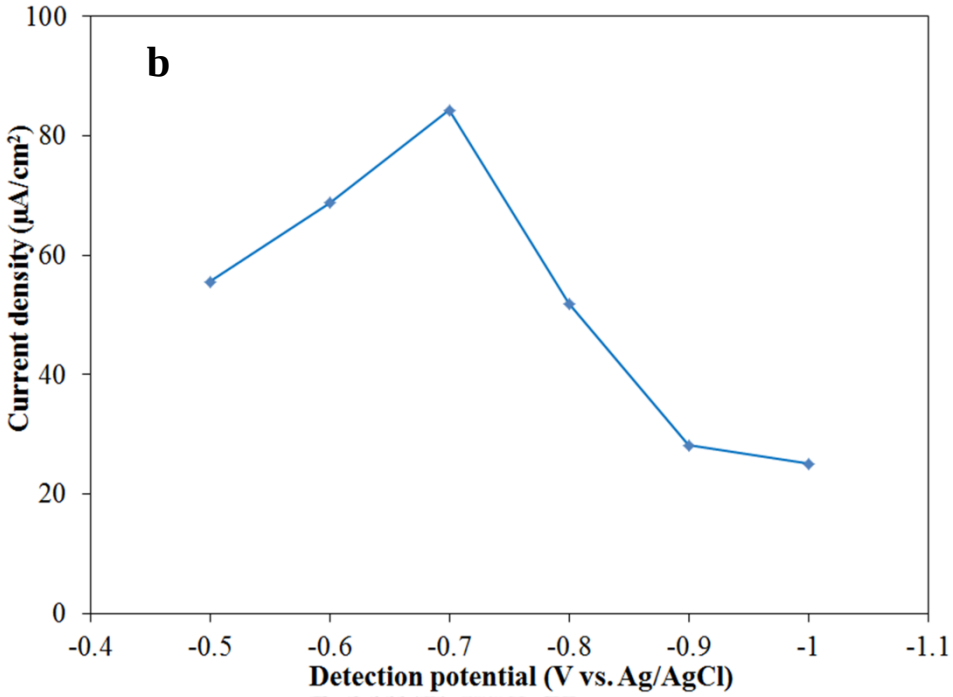

Figure 5.6 (a) Hydrodynamic voltammograms of 38.7 mg/dL cholesterol (blue line) and background (blue line) for 20 s sampling time. (b) Hydrodynamic voltammogram of signal-to-background ratios extracted from the data shown in part a.

5.3.6 Analytical performance

The relationship between the cathodic current and the concentration of cholesterol was examined at the optimal detection potential of -0.7 V vs. Ag/AgCl and recorded at the apparent steady state current of 20 s. Figure 5.7 shows the chronoamperograms of cholesterol calibration using the fabricated biosensor. The cathodic current increased with increasing cholesterol concentration due to the reduction of H_2O_2 generated by the enzymatic reaction. The linearity of the calibration curve is shown in the inset. The cathodic currents exhibited a linear correlation with the cholesterol concentration across the range from 0.39 to 270.69 mg dL^{-1} (correlation coefficient of R^2 = 0.9967) with a sensitivity of 49.61 μA mM^{-1} cm^{-2}, which was calculated by dividing the slope of the calibration curve by the electrode surface area. The limit of detection (LOD) was estimated as the concentration that produced three times the standard deviation of the blank sample and was found to be 0.25 mg dL^{-1}. Previously, the national cholesterol education

program (NCEP) has reported that the normal level of total blood cholesterol in a human is lower than 5.18 mM (200 mg dL^{-1}) [93]. This information shows that the fabricated biosensor covers a wide range of cholesterol concentrations and can be applied for cholesterol detection in the clinical diagnostics. The apparent Michaelis–Menten constant (K_M) that gives an indication of the enzyme-substrate kinetics can be estimated based on the Lineweaver–Burk equation: $1/I_{ss} = (K_M/I_{max})(1/C) + 1/I_{max}$, where I_{ss} is the steady-state current, I_{max} is the maximum current measured under the saturated substrate conditions, and C is the cholesterol concentration. The K_M value of the system in this work was found to be 6.48 mM or 250.43 mg dL^{-1}. The performance of the proposed cholesterol biosensor compared to the previously reported value is shown in Table 5.2. The results confirm that the proposed novel cholesterol biosensor exhibited excellent sensing performance. Moreover, our proposed biosensor offers the advantages of a simple and fast immobilization process.

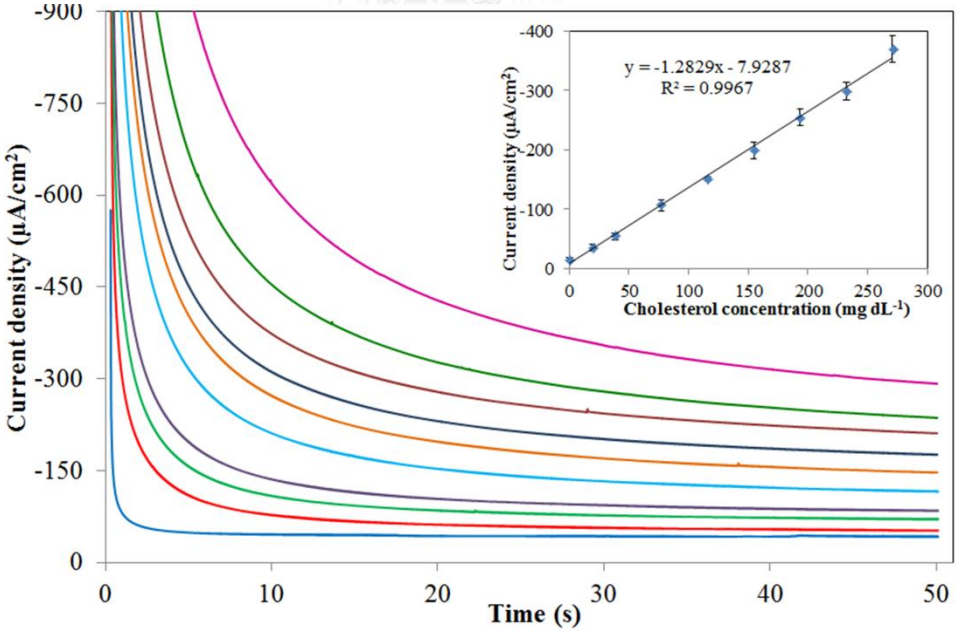

Figure 5.7 Chronoamperograms of cholesterol (0, 0.4, 19.3, 38.7, 77.3, 116.0, 154.7, 193.4, 232.0, and 270.69 mg dL^{-1}) determination at -0.7 V vs.Ag/AgCl. The calibration plot of the cathodic currents at 20 s of sampling time for the determination of cholesterol is shown in the insert.

Table 5.2 Comparison of analytical performances of different electrochemical biosensors for the determination of cholesterol

Cholesterol biosensor	Immobilization method	Linear range (mM)	LOD (μM)
GCE/PTH/ChOx/HRP [163]	covalent linking	0.025-0.125	6.3
Nafion/ChOx/-Fe_2O_3/Ag [107]	co-immobilized with α-Fe_2O_3 micro-pine shaped hierarchical structures	0.1-8.0	18
ChOx/Pt–Au@ZnONRs/CS-MWCNTs/GCE [164]	adsorption	0.0001-0.7593	0.03
ChOx/AuPt–Ch–IL/GCE [165]	cross-linking	0.05-6.2 and 6.2-11.2	10
ChOx–CS/Hb–CS/GCE [166]	encapsulation	0.01-0.6	9.5
AuE/dithiol/AuNPs/MUA/ChOx [103]	covalent attachment	0.04-0.22	34.6
(PAH–MCNTs–GNPs/HRP)$_4$/(PAH–MCNTs–GNPs/ChOx)$_4$ [106]	electrostatic interaction	0.18-11	20
G/PVP/PANI nanocomposites [42]	adsorption	0.05–10	1
AgNPs/BDDE coupled with PAD (this work)	adsorption	0.39-270.69 mg dL^{-1} or 0.01-7 mM	6.5

The repeatability of the sensor was evaluated. One fabricated sensor was evaluated by repeating the measurement of 1 mM H_2O_2 ten times. The relative standard deviation (RSD) was 3.76%, indicating that the biosensor measurement was highly repeatable. Moreover, the reproducibility of the sensor was also evaluated using chronoamperometric detection of 37.8 mg/dL cholesterol. The RSD of five different sensors under the same conditions was found to be 3.5%, indicating that the fabricated biosensor had acceptable precision.

5.3.7 Interference study

The selectivity is an important factor for evaluating the performance of sensors. The effects of common interfering molecules that coexist with cholesterol in serum, such as glucose (Glu), ascorbic acid (AA), and uric acid (UA) were investigated. Glu (1 mM), AA (0.2 mM), and UA (0.2 mM) were added into 38.7 mg dL^{-1} cholesterol standard solution separately and then measured by the fabricated biosensor. The results showed the negligible effect of these interferences on the current response of the fabricated cholesterol sensor as shown in Figure 5.8. The current ratios between the presence and absence of the interferences were found to be 1.02, 1.01, and 0.99 for glucose, AA, and UA, respectively. Thus, highly selective detection of cholesterol was obtained using the proposed method. All the above results demonstrated that the use of the AgNP-modified BDD electrode facilitates the low potential amperometric detection of cholesterol and enhances the selective ability of the biosensor.

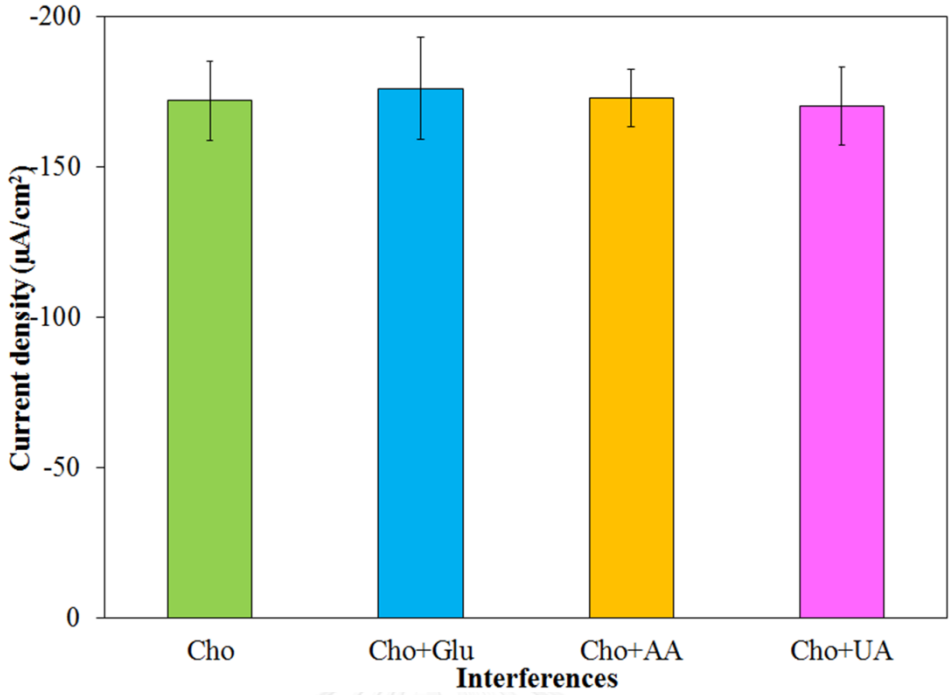

Figure 5.8 The interference effect of 1 mM Glu, 0.2 mM AA, and 0.2 mM UA in the detection of 1 mM cholesterol in 0.05 M PBS, pH 7.4.

5.3.8 Sample analysis

To demonstrate the possible clinical applications, the cholesterol sensor was used to determine the cholesterol level in bovine serum. The results are listed in Table 5.3. The cholesterol concentrations determined by the fabricated sensor are in good agreement with the concentration of the cholesterol labeled in the bovine serum sample. The values of the recoveries obtained were in the range of 99.6-100.8 %. These results clearly indicate that the proposed method can be applied to measure cholesterol in bovine serum.

Table 5.3 Determination of cholesterol in bovine serum samples

Sample	Labeled concentration (mg/dL)	Determined value (mg/dL)	%RSD	Relative error (%)	% Recovery
A	40	40.6±1.4	3.4	+1.5	99.6
B	60	61.3±1.8	3.0	+2.1	100.7
C	80	79.4±1.0	1.0	-0.3	100.8
D	100	99.6±1.0	1.3	-0.7	100.6

5.4 Conclusion

In summary, we have demonstrated a novel design for an electrochemical paper-based analytical device based on an AgNP-modified BDD electrode with PAD for use as a cholesterol biosensor. This novel cholesterol biosensor offers the advantages of simple fabrication, no requirement for an enzyme immobilizing step, low consumption of reagents/sample, low cost, and short analysis time. The most significant characteristics of this cholesterol biosensor are its wide linear range, low limit of detection, high sensitivity, good reproducibility, and freedom from interference from easily oxidizable species such as glucose, ascorbic acid, and uric acid. In addition, this fabricated biosensor was successfully applied to the determination of cholesterol in bovine serum.

Part II:

Boron doped diamond paste electrodes for microfluidic paper-based analytical devices

Siriwan Nantaphol,[a] Robert B. Channon,[b] Takeshi Kondo,[c] Weena Siangproh,[d] Orawon Chailapakul,[a]* and Charles S. Henry[b]**

[a] Department of Chemistry, Faculty of Science, Chulalongkorn University, Patumwan, Bangkok 10330, Thailand

[b] Department of Chemistry, Colorado State University, Fort Collins, CO, 80523, United States

[c] Department of Pure and Applied Chemistry, Faculty of Science and Technology, Tokyo University of Science, 2641 Yamazaki, Noda, Chiba 278–8510, Japan

[d] Department of Chemistry, Faculty of Science, Srinakharinwirot University, Sukhumvit 23, Wattana, Bangkok 10110, Thailand

** Corresponding author

* Co-corresponding author

Analytical Chemistry 89(7) (2017): 4100–4107

Abstract

Boron doped diamond (BDD) electrodes have exemplary electrochemical properties; however, widespread use of high-quality BDD has previously been limited by material cost and availability. In the present article, we report the use of a BDD paste electrode (BDDPE) coupled with microfluidic paper-based analytical devices (μPADs) to create a low-cost, high-performance electrochemical sensor. The BDDPEs are easy to prepare from a mixture of BDD powder and mineral oil and can be easily stencil-printed into a variety of electrode geometries. We demonstrate the utility and applicability of BDDPEs through measurements of biological species (norepinephrine and serotonin) and heavy metals (Pb and Cd) using μPADs. Compared to traditional carbon paste electrodes (CPE), BDDPEs exhibit a wider potential window, lower capacitive current, and are able to circumvent the fouling of serotonin. These results demonstrate the capability of BDDPEs as point-of-care sensors when coupled with μPADs.

4.5 Introduction

Since microfluidic paper-based analytical devices (μPADs) were first reported in 2007 for multiplexed diagnostic detection [167], they have emerged as a promising technology to address the growing need for simple, quantitative, and point-of-need assay platforms. μPADs provide the advantages of low cost, low sample consumption, ease of use, portability, and ease of disposability, making them ideal sensors for resource-limited settings [54]. Moreover, flow can be generated via capillary forces, precluding the need for mechanical or electrical pumps [168]. The hydrophobic barriers which constrain the flow can be easily manufactured by a variety of methods, such as wax printing [63], photolithography [56], or printing of hydrophobic polymers [25, 57]. Furthermore, μPADs are compatible with many classical detection motifs such as colorimetry [59, 63], electrochemistry [56, 169], electrochemiluminescence [60, 170], chemiluminescence [61, 171], and fluorescence [62, 172].

Electrochemical detection is a particularly attractive partner for μPADs, due to its instrumental simplicity, fast analysis times, high sensitivity, high accuracy, simple instrumentation, and low power requirements. Electrochemical paper-based analytical devices (ePADs), first reported in 2009 by Dungchai et al. [56], have used various electrode materials (e.g., carbon, metals, microwires, and nanoparticles) and fabrication techniques (e.g., screen/stencil-printing, pencil/pen drawing, inkjet-printing, and wire placement) [42, 159, 173-178]. Carbon electrodes, especially screen-printed carbon paste electrodes (CPE), have been extensively employed in ePADs due to their easy fabrication, low cost, and potential for large-scale production [179, 180]. Despite these advantages, CPEs are prone to surface fouling, which negatively impacts on analyte adsorption, electron-transfer kinetics, and electrocatalysis, resulting in poor limits of detection and a reduced device lifetime [29, 30, 181]. The electrochemical response of the CPEs is also heavily dependent on the manufacturing process, where key small technical details are difficult to include in publications or reports. Furthermore, commercial CPE are often more expensive than their homemade counterparts, and are limited by the available geometries and

functionalities of the electrodes. Finally, though other electrode materials have been employed as disposable electrodes, such as sputtered Au or Pt, these are often more difficult in terms of time and cost to make, and are significantly more prone to surface fouling than CPEs, limiting their applicability.

Boron doped diamond (BDD) is a carbon-based p-type semiconductor, which exhibits quasi-metallic conductivity at boron doping concentrations of around 1 boron atom per 1700 carbon atoms [31]. The attractive features of BDD electrodes include remarkably low background currents, high mechanical robustness, stability in strong alkaline and acidic media, very wide potential window, and a high resistance to fouling [182-184]. As with the vast majority of carbon-based electrode materials, the particular properties of the BDD depend on the synthesis and processing. For example, freestanding BDD electrodes exhibit very low background currents and a particularly wide potential window, due to the minimal sp^2 carbon content, but are often difficult and costly to manufacture and process, requiring highly specialized machinery and techniques for polishing and sealing [185]. In contrast, thin-film BDD electrodes are easier to manufacture; they are typically grown by chemical vapor deposition on a silicon wafer substrate [21, 186]. However, the electrochemical cell is typically clamped to the thin-film electrode [187], which limits the available electrode and cell geometries and applications. Freestanding and thin-film BDD electrodes have been previously coupled with microfluidic devices to combine the electrochemical advantages of BDD with the higher sensitivities and lower detection limits afforded through convective flow [188, 189], and this remains an active research area in the field [190, 191], However, currently available commercial and academic BDD electrodes are incompatible with point-of-care sensors, in terms of limited geometry, manufacturing time, and cost.

Conductive BDD powder was first demonstrated by Fischer and Swain in 2005 [192]. The BDD powder is easily prepared from an insulating diamond powder substrate (8–12 μm diameter) through microwave plasma-assisted chemical vapor deposition (MPCVD). Combination of the BDD powder with a conducting ink, followed by screen printing, yields a BDD paste electrode (BDDPE), which can potentially

overcome the aforementioned limitations of conventional BDD electrodes [35, 49, 193]. Specifically, these BDDPE are an attractive alternative to conventional BDD electrodes in terms of lower cost, simpler and faster electrode fabrication, and are ideal as a disposable and portable platform. Additionally, previous investigations with a simple BDDPE have demonstrated reduced electrode fouling for dopamine electrooxidation compared to CPEs, suggesting that the BDDPE will outperform conventional CPEs [49].

In this work, we demonstrate the use of BDD powder for the fabrication of disposable BDDPEs in a μPAD platform. Electrode performance is contrasted with conventional CPEs and traditional BDD electrodes. To demonstrate the scope of this device, the BDDPE ePADs are employed for two applications; the quantitative detection of norepinephrine (NE) and serotonin (5-hydroxytryptamine, 5-HT) and the anodic stripping voltammetry of heavy metals. The simultaneous determination of NE and 5-HT is of great importance, as low levels of NE and 5-HT have been related to several disorders, including depression, migraine, and anxiety [194]. However, previous investigations with CPEs have found significant electrode fouling with 5-HT [170, 195]. BDD is expected to alleviate this problem due to the chemical inertness of the surface, as has been previously shown on conventional freestanding and thin-film electrodes [196, 197]. Additionally, NE and 5-HT have similar electrooxidation potentials on carbon electrodes, making co-detection challenging [198]. Therefore, an electrochemically reduced graphene oxide (ERGO)-modified BDDPE is used herein for simultaneous NE and 5-HT detection due to its high electroactive surface area, rapid electron transfer, and small charge-transfer resistance. In addition, we further demonstrate the application of BDDPEs in a flow-through μPAD, for the simultaneous determination of two heavy metals, Cd(II) and Pb(II). The presence of these toxic elements in the environment is of particular concern due to their adverse effects on ecosystems and human health [199, 200]. Using a flow-through design, coupled with square-wave anodic stripping voltammetry (SWASV), preaccumulation can be carried out online, enhancing the efficiency for the metal deposition and, consequently, improving the detection sensitivity. Aside from their individual importance as

analytical targets, NE, 5-HT, Cd(II), and Pb(II) are important analytes as they allow direct comparison to other studies which have previously investigated these species using CPEs, freestanding BDD electrodes, and thin-film BDD electrodes, in order to demonstrate the significant potential of BDDPE as point-of-care sensors.

5.6 Experimental section

5.6.1 Materials, Equipment, and Chemicals

BDD powder was prepared through a previously reported procedure [49]. In short, natural diamond powder (Micron+SND, Element Six, particle diameter <500 nm) was washed in aqua regia and 30% hydrogen peroxide at 60 °C for 30 min to remove possible metallic contaminants, followed by rinsing with Milli-Q water and drying. To grow BDD on the substrate powder surface, the pretreated diamond powder was spread on a molybdenum susceptor and subjected to MPCVD for 8 h, using previously described conditions [49]. Finally, the BDD powder was ground using a mortar and pestle and oxidized in air using a muffle furnace at 425 °C for 5 h to remove graphitic impurities, resulting in an oxygen-terminated surface [201].

Graphene oxide (GO) was acquired from XF Nano, Inc. (Nanjing, China). 5-HT was acquired from Alfa Aesar (WardHill, MA). NE, potassium phosphate monobasic, sodium phosphate dibasic, and standard solutions of all metals Cd(II), Pb(II), and Bi(III) were acquired from Sigma-Aldrich (St. Louis, MO). Acetic acid, sodium acetate, and light mineral oil were acquired from Fischer Scientific (New Jersey). Potassium ferrocyanide ($Fe(CN)_6^{4-}$) was acquired from Mallinckrodt (St. Louis, MO). All chemicals were analytical grade and used as received, and all solutions were prepared by using purified water (18.2 MΩ cm) from a Milli-Q Millipore water purification system. Whatman 1 chromatography paper was acquired from Fisher Scientific (Pittsburgh, PA). A XEROX Phaser 8860 printer was used to print wax patterns on μPADs following established protocols. An Isotemp hot plate from Fischer Scientific, set at 150 °C, was used to melt the wax on the paper. Ag/AgCl ink from Gwent Group (Torfaen, U.K.) was used to construct the conducting pads and reference electrode (RE). Carbon ink

from Ercon Incorporated (Wareham, MA) was used for the construction of the counter electrode (CE).

5.6.2 Device Fabrication

Wax printing and Whatman 1 chromatography paper were selected for the construction of the devices following previously reported methods [41]. The CE, RE, and conducting pads on wax-printed paper were stencil printed in-house. For fabrication of the BDD paste working electrode (WE), stencil-printed Ag/AgCl on a transparency sheet substrate was prepared as a conducting pad. To minimize BDD paste consumption, a second stencil containing three smaller openings (0.1 mm × 2 mm rectangles) was fabricated using a laser engraving system (Epilog, Golden, CO). The BDD paste WE was prepared by mixing BDD powder and mineral oil (70:30, w/w) and stencil-printed onto the mask. A photograph of the BDDPEs is shown in Figure 5.9a. Double-sided tape was used to attach the CE (stencil-printed carbon) and RE (stencil-printed Ag/AgCl) section to the WE section. Figure 5.9b shows the device design for NE and 5-HT detection, which was carried out by pipetting a 50 µL aliquot atop the BDDPE. For heavy metal analysis, a flow-through pattern µPAD was designed, consisting of a sample zone (where a 50 µL sample aliquot was added), an electrochemical detection zone, and a hydrophilic area at the outlet of the paper channel, as shown in Figure 5.9c.

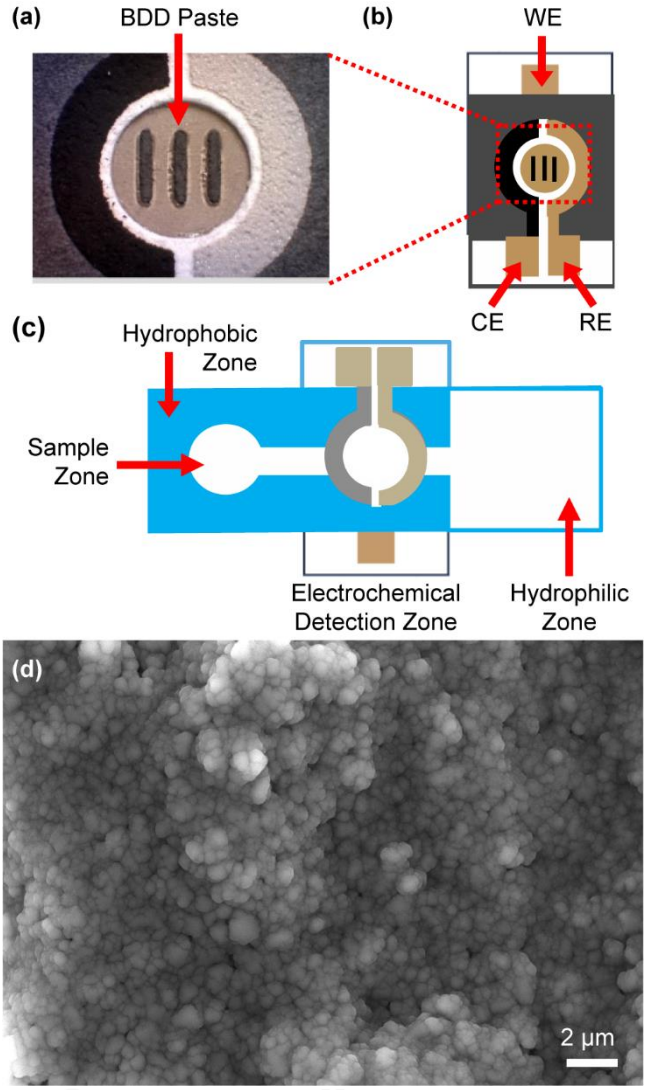

Figure 5.9 Device design for BDDPE, (a) photograph of the BDDPE, (b) ePAD design for NE and 5-HT analysis, (c) µPAD design for the measurement of Pb and Cd, (d) SEM image of BDDPE.

Further details of the fabrication procedures are provided in the Figure 5.10. Wax printing and Whatman #1 chromatographic paper were selected for the construction of the devices. Paper-based microfluidic patterns were designed by computer-aided design software (Adobe Illustrator). Figure 5.10a shows the preparation of paper-based device for NE and 5-HT analysis. The black portion is hydrophobic while the white part is hydrophilic. The wax patterns were printed on Whatman #1 paper sheet using a solid ink printer (XEROX Phaser 8860 or 8870). The

printed paper was heated between the two metal plates placed on a hot plate at 150 °C for 2 min, which caused the wax to permeate through the paper, forming the three-dimensional hydrophobic barriers that confined liquid flow. After hydrophobic barrier creation, in-house screen-printing was used for fabricating CE, RE and conducting pads. The screen-printing blocks were designed using Adobe Illustrator and constructed by Chaiyaboon Co. (Bangkok, Thailand). Firstly, the silver ink was screened on the hydrophilic circle of 8 mm in the center of the square to fabricate RE and conducting pads and dried at 65 °C for 30 min. After that, the carbon ink was screened to fabricate the CE. Finally, the screen-printed electrodes were dried at 65 °C for 30 min to remove any remaining solvent.

Figure 5.10b shows the fabrication of the working electrode (WE). Stencil-printing in-house was used for the construction of the conducting pads by stenciling the Ag/AgCl ink onto the transparency sheet. Three layers including the top layer of double-side sheet tape (for attaching the WE layer with CE and RE layer), the middle layer of transparency sheet, and the bottom layer of double-sided sheet tape (for attaching the laser mark with conducting pad), was used to fabricate the WE mask. The three channels (100 μm × 2 mm per each) were drawn using CorelDRAW X5 and created on the three-layer sheet using laser engraving system (30W Epilog, Golden, CO) (Figure 5.10c). After that, the laser mask was positioned on the conducting pad of transparency sheet. The BDD paste prepared by mixing BDD powder and mineral oil (70:30, w/w) was then filled into the channels. Finally, to complete the device, the double-side tape was used to attach the RE and CE part with WE part, as shown in Figure 5.10d.

The preparation of device for metals analysis is shown in Figure 5.10e. The fabrication procedure is similar to the fabrication of device for NE and 5-HT analysis but uses a different wax-pattern design. The wax-printed paper for metals analysis consisted of the sample zone, the electrochemical detection zone, and the hydrophilic area at the outlet of paper channel to wick solution over the working electrode. The electrochemical detection zone consists of three layers: (i) CE and RE fabricated on the hydrophilic area of the wax pattern paper, (ii) Whatman #1 paper

piece inserted between the stencil-printed electrodes paper layer and WE layer to improve the efficiency for the flow of solution on the channel, and (iii) the BDD paste electrodes.

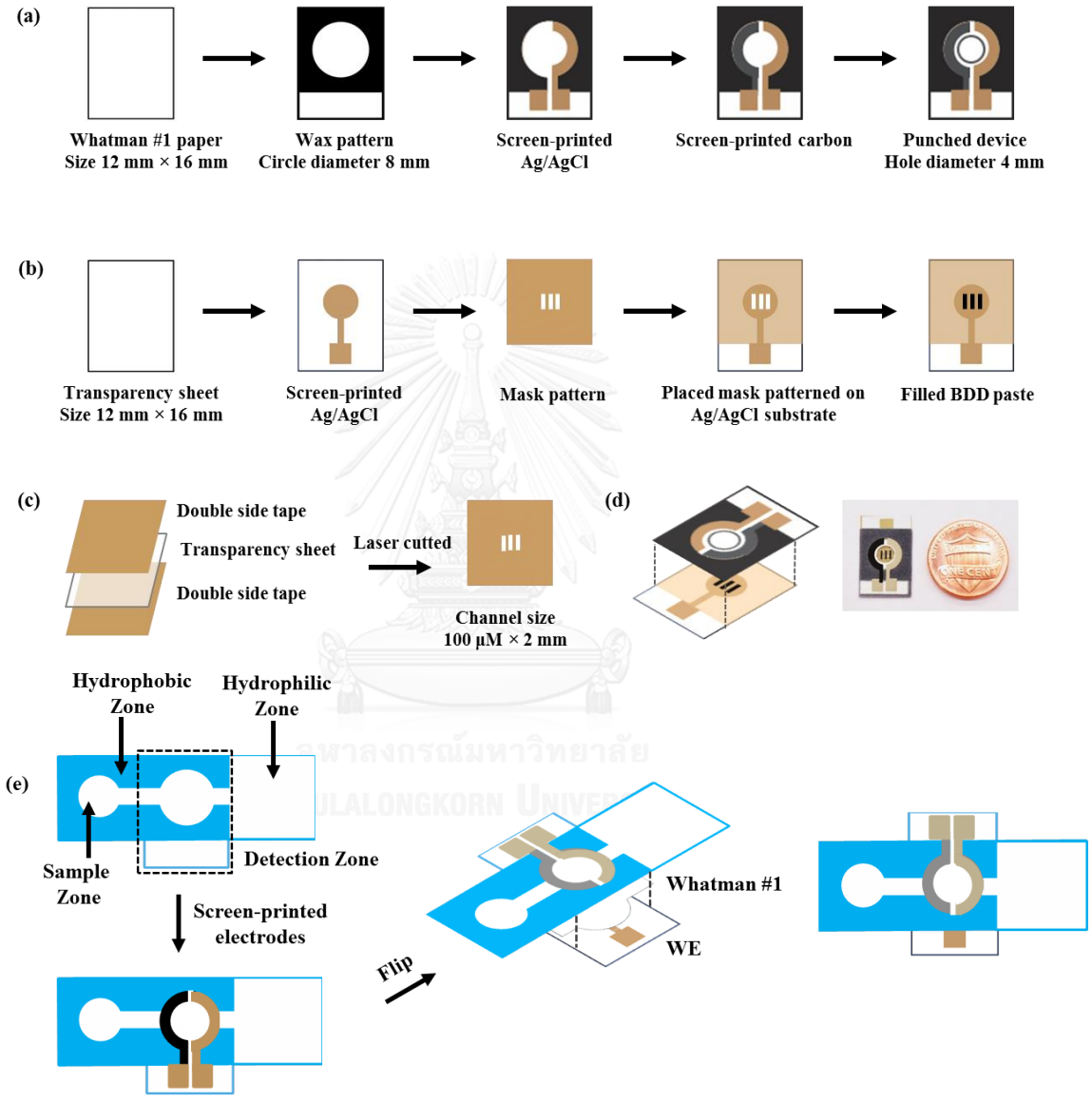

Figure 5.10 (a) The preparation of wax-patterned paper for NE and 5-HT analysis, and the fabrication of CE and RE. (b) The preparation of BDDPE. (c) The preparation of mask pattern for WE. (d) Combination of the BDDPE with RE and CE for the device construction and the photograph of device. (e) The preparation of device for metals analysis.

5.6.3 Electrochemical Detection

All electrochemical experiments were performed with a model 660B potentiostat (CH Instruments, Austin, TX) at room temperature (22 ± 1 °C). For NE and 5-HT detection, an ERGO-modified BDDPE was used as the WE. Standard solutions of NE and 5-HT were prepared in 0.1 M phosphate buffer (PBS) pH 8.0, and a 50 µL aliquot was used for the experiments. For differential pulse voltammetry (DPV), an amplitude of 60 mV, potential increment of 4 Hz, and a pulse width of 0.05 s were used.

For Pb and Cd detection, SWASV was employed with the flow-through device for the simultaneous determination of Cd(II) and Pb(II). All standard metals were prepared in 0.1 M acetate buffer pH 4.5. Bismuth-modified BDDPE were used as WE, prepared by chronoamperometry in a 4 ppm Bi(III) solution at −1.2 V for 20 min. A 50 µL aliquot was added to the sample zone, and SWASV was performed after the solution flowed to electrochemical detection zone (ca. 1 min). SWASV used a frequency of 25 Hz, potential increment of 15 mV, and an amplitude of 50 mV, with an electrochemical deposition step at −1.2 V for 5 min, an equilibration period of 5 s, and a square wave voltammetric stripping range of −1.1 to −0.5 V.

5.6.4 Preparation of ERGO modified BDD paste electrodes

1 mg/mL GO solution was prepared by dissolving 1mg of GO sheet in 1 mL of 0.1 M phosphate buffer solution (PBS) pH 7 with sonication for 1 h to generate a homogeneous solution. Next, 50 µL of GO solution was drop casted onto the electrode surface. Cyclic voltammetry was employed for reducing of GO by applying the potential in the range of 0 to -1.5 V at the scan rate of 50 mV s^{-1} for 20 cycles. Finally, the modified electrode was rinsed with deionized water and kept at the room temperature to dry.

5.7 Results and discussion

5.7.1 Characterization of BDD Paste Electrodes

The BDDPE morphology was characterized by scanning electron microscopy (SEM) as shown in Figure 5.9d. The BDDPE has a homogeneous distribution of ~1 μm sized particles, with a surface roughness of tens of micrometers, which is in agreement with previous studies on BDDPEs [49]. Furthermore, the boron concentration can be estimated from the carrier concentration of the thin-film growth material, through a Hall effect measurement [202], yielding a boron concentration of $\sim 10^{20}$–10^{21} boron atoms/cm^3, suggesting the BDDPEs should have metallic conductivity [203]. The BDDPE quality was then characterized and contrasted with a CPE via double layer capacitance (C_{dl}) and solvent window measurements, as shown in Figure 2, parts a and b, respectively. Cyclic voltammograms (CVs) were run between −0.1 and 0.1 at 0.2 V s^{-1} in 0.1 M KNO_3, and C_{dl} of each electrode was determined at 0 V versus screen-printed Ag/AgCl using [185]

$$C_{dl} = \frac{i_{average}}{vA_{geometry}}$$

where $i_{average}$ is the current average from the forward and reverse sweep in amperes, v is the scan rate in volts per second, and $A_{geometric}$ is the geometric electrode area in square centimeters. The capacitive currents at CPEs and BDDPEs were 61.74 ± 0.36 and 42.29 ± 0.24 μF cm^{-2}, respectively (n = 3 electrodes, Figure 5.11a). The BDDPE capacitance compares favorably with conventional BDD electrodes reported in the literature [185], considering the simple electrode fabrication and application. For example, thin-film BDD electrodes are typically 3.9–381 μF cm^{-2} and freestanding BDD electrodes are typically 2.9–11 μF cm^{-2} [185].

The potential window was recorded for each electrode material using CV in 0.1 M KNO_3 at 0.1 V s^{-1} (Figure 5.11b). Using the definition of BDD solvent window as the anodic and cathodic potential limits to generate a current of ±0.4 mA cm^{-2} from water electrolysis [185], the solvent window of the BDDPE was found to be 2.25 V.

For the CPE, the potential window is much narrower as shown in Figure 5.11b. The solvent window of our BDD electrodes compare well with thin-film BDD electrodes (2.30–1.38 V) and freestanding BDD electrodes (4.11–3.53 V).[185] In addition, a peak was observed at ~+1.5 V in the BDDPE CV, characteristic of non-diamond carbon species (sp^2 carbon) or impurities situated in the grain boundaries of the diamond surface, as is expected for paste or thin-film electrodes [185]. The capacitance and solvent window data confirm that BDDPEs have smaller background currents and wider potential windows than the CPEs typically employed with ePADs, which should translate to improved limits of detection (LOD).

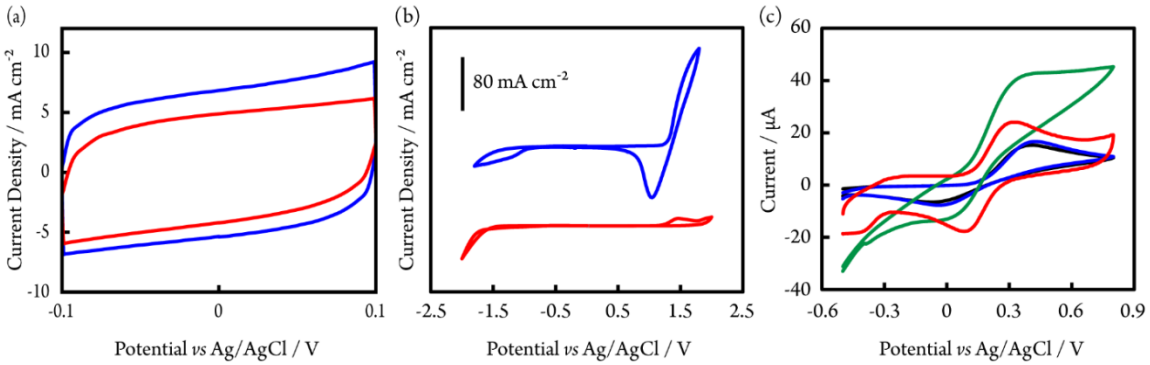

Figure 5.11 (a) CVs in 0.1 M KNO_3 recorded at a *v* of 0.2 V s^{-1} over the potential range -2 to 2 V for the BDDPEs (red line) and -1.8 to 1.8 V for the CPEs (blue line). (b) CVs in aerated 0.1 M KNO_3, recorded at 0.2 V s^{-1} over the potential range -0.1 to 0.1 V for the BDDPEs (red line) and CPEs (blue line). (c) CVs performed with the BDDPEs (blue line), CPEs (black line), ERGO modified BDDPEs (red line), and ERGO modified CPEs (green line), at 0.05 V s^{-1}, using 4 mM $Fe(CN)_6^{4-}$ in 0.1 M KCl.

The electrochemical characteristics of the electrodes were investigated through measurement of the peak currents and peak-to-peak separation (ΔE_p) of the inner-sphere redox couple, $Fe(CN)_6^{4-}$, via CV. As shown in Figure 5.11c, symmetrical voltammograms are observed for $Fe(CN)_6^{4-}$ electrooxidation with BDDPEs and CPEs (ΔE_p = 410 ± 10 and 400 ± 20 mV, respectively, n = 3 electrodes). After modification with ERGO, the ERGO-BDDPEs exhibited symmetrical cathodic and anodic peaks and greater electrochemical reversibility than the ERGO–CPEs, as illustrated through

smaller ΔE_p (200 ± 30 and 280 ± 30 mV, respectively). The large ΔE_p, for the BDDPEs are indicative of ohmic resistive effects, likely originating from the nonohmic contact between the BDD powder and the mineral oil or Ag/AgCl screen-printed contact pad. This hypothesis is supported by ΔE_p of 75 and 89 mV for the outer-sphere couples $FcTMA^+$ and $Ru(NH_3)_6^{3+}$ (1 mM in 0.1 M KNO_3, not shown).

5.7.2 Serotonin and Norepinephrine Detection

The two electron irreversible electooxidation of serotonin (5-HT) is known to produce hydroxylated products, dimers, and other species that can irreversibly adsorb to the electrode, fouling the surface [195]. Electrode fouling decreases sensitivity, making 5-HT determination on carbon electrodes challenging. Previous studies have shown BDD is not as prone to 5-HT fouling due to the relative surface inertness [204]. Parts a and b of Figure 5.12 show CVs for 10 μM 5-HT at a BDDPE and CPE, respectively. Well-defined oxidation peaks were observed for both electrodes for the initial CV. The decrease of oxidation peak current and peak potential shift after the first cycle are indicative of electrode fouling, although the fouling is less severe for BDDPEs compared to CPEs. We attribute this phenomena to the lower adsorption of the organic species on BDDPEs when compared with CPEs [49].

In order to improve resistance to electrode fouling, electrode pretreatment was tested to reactivate the electrode surface. Several methods have been described for the pretreatment of BDD thin-film electrodes. Duran et al. investigated the effect of anodic, cathodic, or a combined anodic and cathodic galvanostatic polarization on the response of a diamond microelectrode for two inner-sphere redox couples, $Fe(CN)_6^{4-}$ and 5-HT. Cathodic pretreatment and combined pretreatment performed by the anodic step followed by the cathodic step were found to be effective for activating a fouled microelectrode [29]. Similarly, Sarada et al. showed the CV of 5-HT at a BDD electrode before and after pretreating the electrode by oxidizing the surface in PBS. Relative to a fresh diamond electrode, the 5-HT oxidation peak potential and current for a diamond electrode after anodic

pretreatment remained unchanged [196]. Therefore, the effect of anodic pretreatment on the electrochemical response of BDDPEs was investigated for 5-HT as shown in Figure 5.12. Figure 5.12c shows the effect of anodic cleaning on the response of fouled BDDPEs by comparing the DPV of 10 μM 5-HT on BDDPE before and after treatment. Three DPVs were performed on the same electrode without a cleaning step, resulting in an oxidation current decrease and positive peak potential shift, likely due to the adsorption of a quinone as the oxidation product of 5-HT [195]. Subsequently, anodic pretreatment was carried out by oxidizing the fouled electrode with at +1.2 V for 5 min in PBS solution, leading to a peak current and peak potential similar to those of the fresh BDDPEs (red dashed line). These results indicate that the BDDPE was returned to its native activity state after anodic treatment, and subsequently anodic treatment was used for all 5-HT and NE measurements.

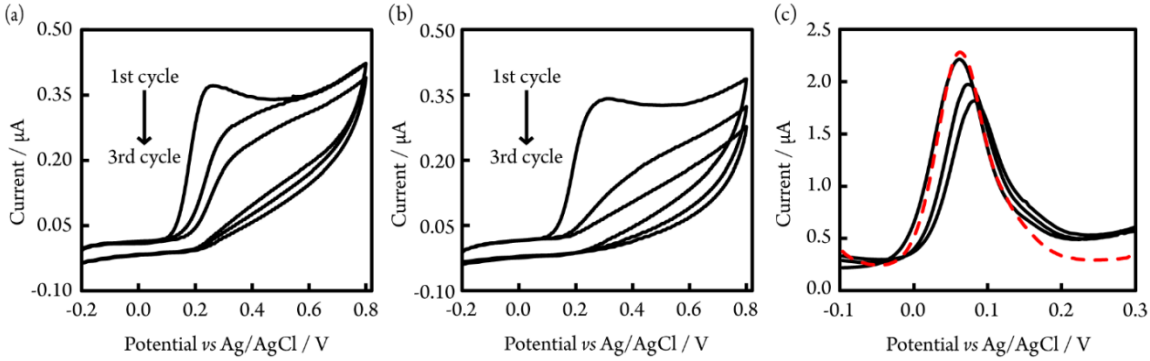

Figure 5.12 Three successive CVs of 10 μM 5-HT for (a) BDDPEs and (b) CPEs in 0.1 M PBS (pH 8.0) at 0.05 V s^{-1}. (c) Three consecutive DPVs of 10 μM 5-HT in 0.1 M PBS (pH 8.0) at a BDDPE before (solid lines) and after (red dashed line) anodic polarization.

Next, the electrochemical behavior of NE and 5-HT on BDDPEs was investigated by CV (Figure 5.13a). Due to their similar oxidation potentials, NE and 5-HT could not be discriminated using bare BDDPEs. Therefore, ERGO was chosen to modify the BDDPEs in an attempt to enable simultaneous detection of both analytes. CVs of BDDPEs and ERGO-BDDPEs at varying scan rates from 0.01 to 0.1 V s^{-1} using $Fe(CN)_6^{4-}$ are shown in Figure 5.14, parts a and b, respectively. ΔE_p at the

unmodified BDDPEs increases from 190 ± 4 mV at 0.01 V s^{-1} to 387 ± 7 mV at 0.1 V s^{-1}, whereas ΔE_p at the ERGO-BDDPEs increases from 120 ± 5 mV at 0.01 V s^{-1} to 280 ± 7 mV at 0.1 V s^{-1}. The lower ΔE_p for the ERGO-BDDPEs implies faster electron-transfer kinetics from the ERGO modification [142]. Figure 5.14c shows a linear dependence of the peak current versus square root of the v for both unmodified and modified electrodes, indicating that the electrochemical processes at both electrodes are diffusion controlled [205].

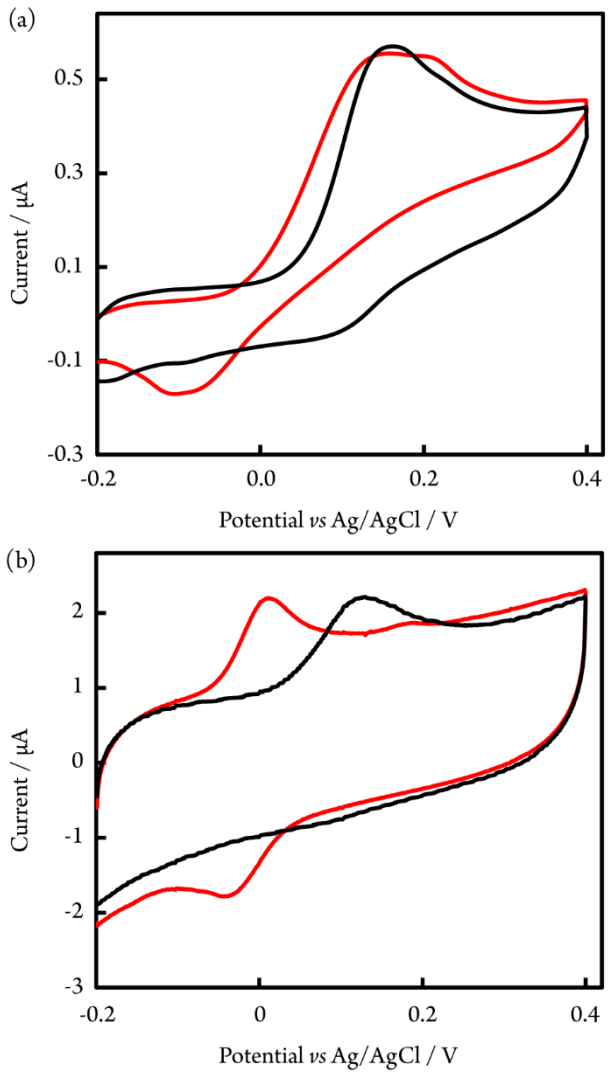

Figure 5.13 CVs performed with bare BDDPEs (a) and ERGO-BDDPEs (b) for the oxidation of 25 μM NE (red line) and 10 μM 5-HT (black line) in 0.1 M PBS (pH 8.0).

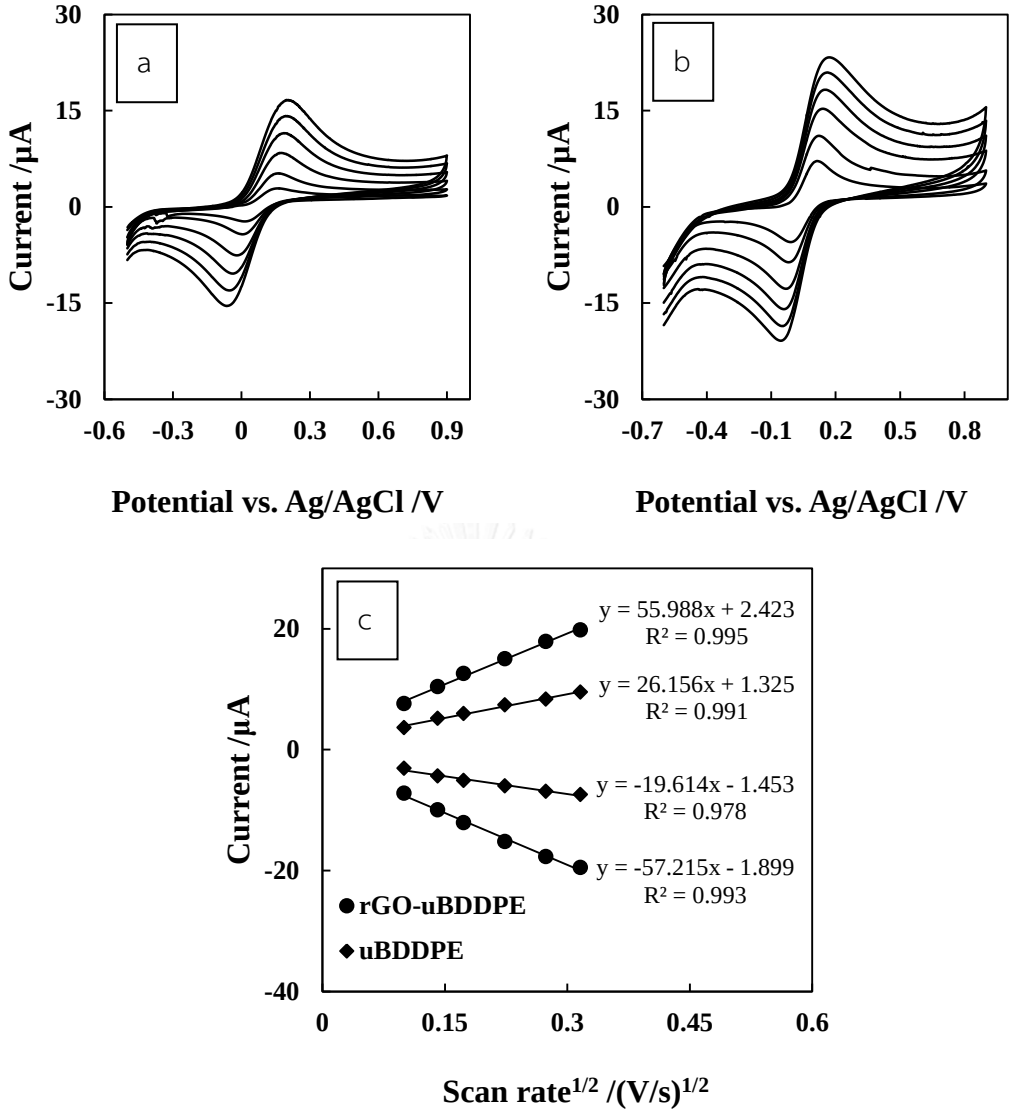

Figure 5.14 CVs for 4 mM $Fe(CN)_6^{4-}$ in 0.1 M KCl at (a) the BDDPE and (b) the ERGO-BDDPE on ePAD for a series of scan rates (0.01, 0.02, 0.04, 0.06, 0.08, and 0.1 V s^{-1}). (c) The relationship between peak current and $(\text{scan rate})^{1/2}$.

The surface area of the electrodes was determined by using Randles–Sevcik equation [206]:

$$i_{pa}=(2.69\times10^5)n^{2/3}AD_o^{1/2}v^{1/2}C_o^*$$

where i_{pa} is the peak current in amperes, A is the area of the electrode in square centimeters, C_o* is the concentration of electroactive species in millimoles per liter, and D is the diffusion coefficient in square centimeters per second. Given D_o = 7.26 ×

10^{-6} cm^2 s^{-1} for $Fe(CN)_6^{4-}$[207], A for each electrode can be calculated from the slope of the i_p versus $v^{1/2}$ plot. The surface areas (A) of the electrodes were found to be 8.66 × 10^{-2} and 16.7 × 10^{-2} cm^2 for the BDDPEs and ERGO-BDDPEs, respectively. The results demonstrated the ERGO layer is effective at increasing the electroactive surface area.

CVs of NE and 5-HT at the ERGO-BDDPE are shown in Figure 5.13b. Following modification, the E_{pa} of NE decreased from 0.13 ± 0.0047 to −0.006 ± 0.0052 V, while the E_{pa} of 5-HT decreased from 0.14 ± 0.0061 to 0.12 ± 0.0035 V, showing a clear separation in NE and 5-HT oxidation peaks. To evaluate the mass transfer of the analytes toward the electrode, CV was performed at different scan rates. As seen in Figure 5.15, parts a and b, the anodic peak currents of NE and 5-HT oxidation increase with increasing *v* as predicted. Moreover, the peak currents of both compounds are linearly proportional to the square root of *v* in the range of 0.01–0.1 V s^{-1}, suggesting that the electrochemical processes are diffusion-controlled.

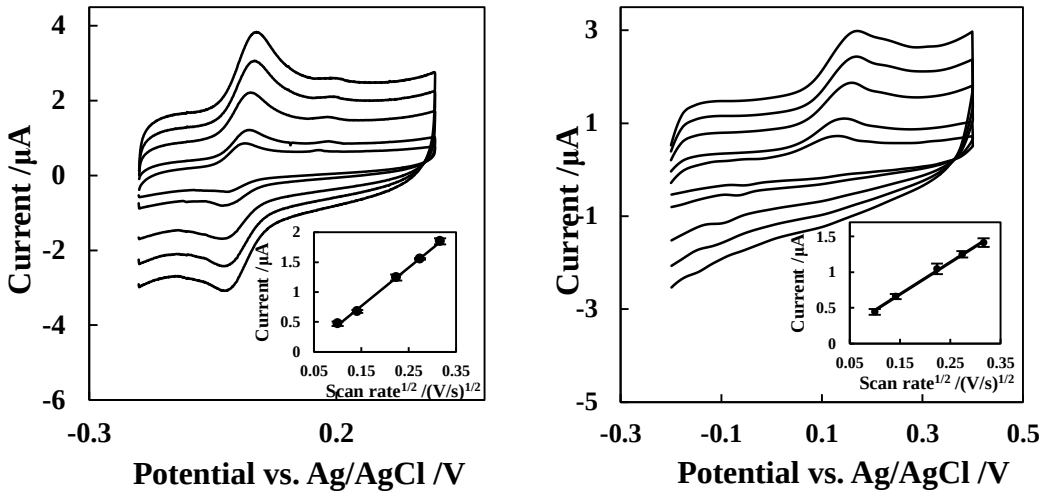

Figure 5.15 CVs for (a) 25 µM NE and (b) 10 µM 5-HT in 0.1 M PBS (pH 8.0) at the ERGO-BDDPE for a series of scan rates (0.01, 0.02, 0.04, 0.06, 0.08, and 0.1 V s^{-1}). The relationship between signal current and $(\text{scan rate})^{1/2}$ (y = 6.449x - 0.202, R^2 = 0.998 for NE and y = 4.491x + 0.015, R^2 = 0.997 for 5-HT) are shown in the inset.

5.7.3 Analytical Performance

Next, DPV was employed for the simultaneous determination of NE and 5-HT. The linear range of NE and 5-HT was studied at ERGO-BDDPEs, with a fixed concentration of the other species. As shown in Figure 5.16, parts a and b, the peak currents of NE or 5-HT increased linearly with the concentration. For NE detection, a linear calibration plot was found over a range of 2.5–100 μM with a sensitivity of 0.030 μA μM^{-1} and correlation coefficient (R^2) of 0.9991. For 5-HT, a linear calibration plot was obtained over a range of 0.5–7.5 μM with a sensitivity of 0.069 μA μM^{-1} and R^2 of 0.9938. The experimental LODs were 2.5 and 0.5 μM for NE and 5-HT, respectively. Although this device exhibits higher LOD values than other BDD electrode materials [196, 204], it has other advantages in terms of ease of use, low cost, and disposability.

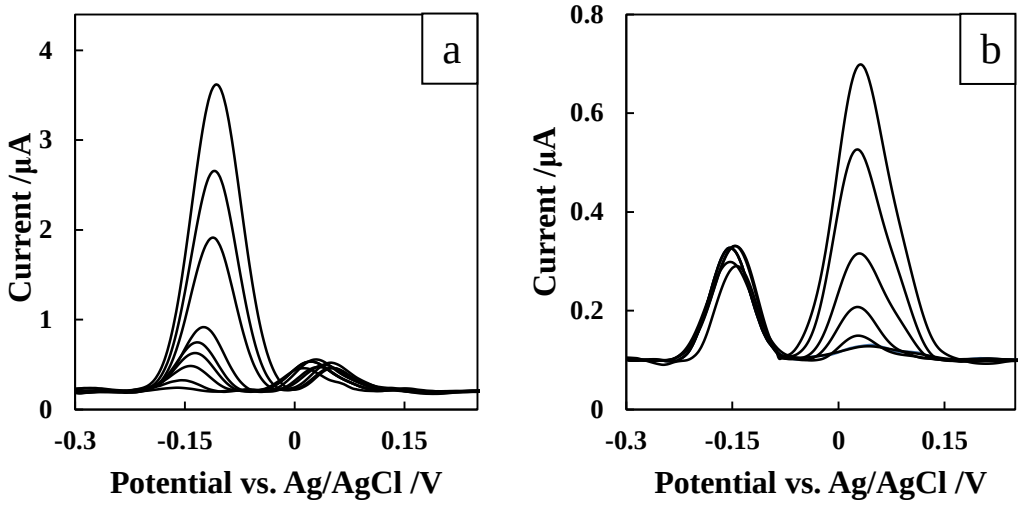

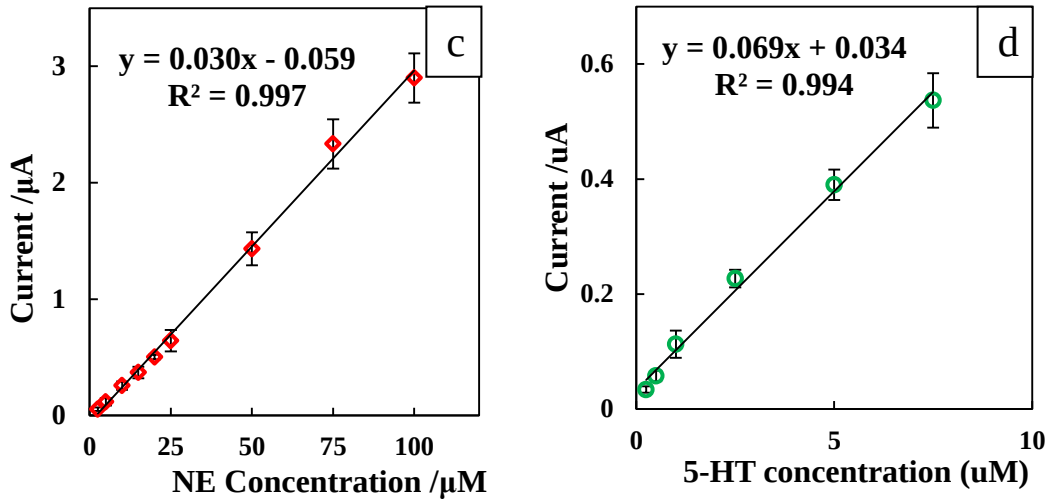

Figure 5.16 (a) DPVs of different concentrations of NE in the presence of 2.5 µM 5-HT in 0.1 M PSB (pH 8.0), NE concentrations are: 2.5, 5, 10, 15, 20, 25, 50, and 100 µM. (b) DPVs of different concentrations of 5-HT in the presence of 10 µM NE in 0.1 M PBS (pH 8.0), 5-HT concentrations are: 0.25, 0.5, 1, 2.5, 5, and 7.5 µM, with corresponding calibration plots of (c) NE and (d) 5-HT.

Next, the device repeatability was evaluated through repeated measurements of 10 µM NE and 5 µM 5-HT (n = 10, not shown). The relative standard deviations (RSDs) were 6.93% and 8.43%, for NE and 5-HT, respectively. The intra-device reproducibility was evaluated using DPV detection of 10 µM NE and 5 µM 5-HT. The RSDs of six different devices under the same conditions were found to be 6.02% and 7.68%, for NE and 5-HT, respectively. All of these values are in line with other ePAD systems.

5.7.4 Detection of Heavy Metals

The contamination of the environment by heavy metals [e.g., Cd(II) and Pb(II)] remains a serious problem because of their environmental persistence and high toxicity [208]. In order to show the scope of the developed sensor, BDDPEs were employed for heavy metal determination. SWASV is a particularly attractive electrochemical technique for trace heavy metal determination, as it greatly reduces

the background noise arising from capacitive charging currents during the potential scan [209]. Conventional ASV measurements consist of two steps: first, in the preconcentration step, metal ions are electrochemically deposited onto the electrode surface, typically under controlled stirring conditions. Then, the stirring is ceased and the deposited metal is oxidized or stripped from the electrode, back into the solution. The resulting anodic diffusion current is then used to determine the concentration of the metal. However, this approach is not ideal for in-field measurements due to the practicality and difficulty of synchronizing stirring and ASV procedures.

To overcome this limitation, BDDPEs on static and flow-through PADs were applied for the simultaneous determination of Cd(II) and Pb(II), using SWASV. For simplicity, the preconcentration step was performed without stirring, which will affect the device sensitivity as preaccumulation of analytes in stripping is limited by diffusion. Therefore, to increase electrode sensitivity, Bi was used to modify BDDPEs, forming a metal–bismuth alloy on the electrode surface, which facilitates the nucleation process during metal ion deposition [210]. The PADs were designed as a flow-through pattern by adding a hydrophilic area in the outlet of a paper channel (Figure 5.9c). This design allows the continuous wicking of solution across the electrodes in the preconcentration step, facilitating the accumulation of metals onto the electrode surface [211]. During the preconcentration step, −1.2 V was applied for 5 min, providing enough time to stop the flow before the stripping step.

Figure 5.17 shows the SWASV for static and flow-through devices for the simultaneous detection of 50 ppb Cd(II) and Pb(II). The voltammogram obtained from the flow-through PADs, in which the sample solution continuously flowed in the paper microchannel, showed well-defined separated peaks for Cd(II) and Pb(II), at −0.93 and −0.67 V versus the Ag/AgCl reference electrode, respectively. In contrast, the voltammogram obtained from the static PAD, in which the sample solution was directly dropped onto the electrodes, showed a much lower current signal. These results demonstrate that the flow-through PADs exhibit a much higher sensitivity than the static system [4.3 and 3.1 times higher for Cd(II) and Pb(II), respectively]. This is

likely due to the increased mass transport as a result of convection through PAD, enhancing the efficiency of the metal accumulation.

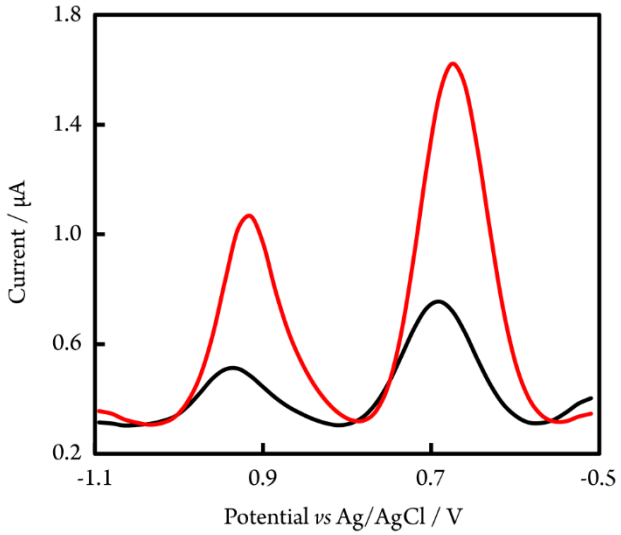

Figure 5.17 SWASV for a 50 ppb solution of Cd(II) and Pb(II) in 0.1 M acetate buffer (pH 4.5), using a static system (black line), and flow through system (red line).

The analytical performance of the flow-through PADs for Cd(II) and Pb(II) determination was evaluated using SWASV under the optimized experimental conditions. SWASV of different concentrations of Pb(II) and Cd(II) are shown in Figure 5.18a. The resulting calibration plots were linear over the concentration range from 1 to 200 ppb for Pb(II) and 25–200 ppb for Cd(II) (Figure 5.18b) with sensitivities of 0.305 and 0.218 μA μM^{-1}, respectively. The experimental LODs were 1 and 25 ppb for Pb(II) and Cd(II), respectively. These results indicate that the devices are not only simple and inexpensive, but also provide the good linearity and LODs compared to alternate methods which are often more expensive and require complicated fabrication procedures [212-214]. While these detection limits are higher than other optimized materials using Bi co-deposition, the LOD value of Pb is below the EPA action limit of contaminants in drinking water and also demonstrate applicability of the system to inorganic as well as organic analytes.

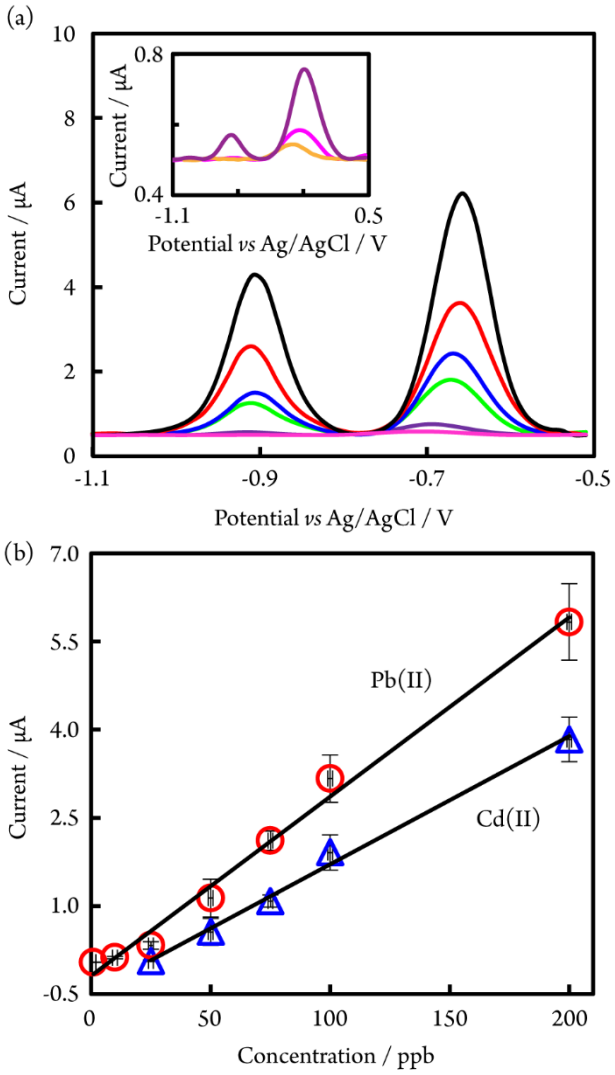

Figure 5.18 (a) SWASV of Cd(II), and Pb(II) from 1-200 ppb, in 0.1 M acetate buffer (pH 4.5) using the flow through μPAD, with low concentrations (1–25 ppb) in the inset. (b) Corresponding calibration curves for increasing concentrations of Pb(II) (1-200 ppb, sensitivity = 0.0305 μA/ppb, R^2 = 0.991) and Cd(II) (25-200 ppb, sensitivity = 0.0218 μA/ppb, R^2 = 0.9938).

The effects of some possible interferences [Mn(II), Cr(III), Fe(III), Zn(II), Cu(II), Ca(II), Na(I), and K(I)] were investigated by adding them into a solution containing 50 ppb of Cd(II) and Pb(II) in 0.1 M acetate butter pH 4.5. The tolerance ratio is defined as the mass ratio of interfering species relative to the target metal that makes a change in peak current of ±5%. By limiting the scanning potential in the system from

−1.1 to −0.5 V, the maximum tolerable concentrations of foreign species are shown in Table 5.4. These findings indicate that the aforementioned common metal ions do not interfere with the determination of Cd(II) and Pb(II).

Table 5.4 Tolerance ratio of interfering metal ions in the electrochemical determination of 50 ppb of Cd(II) and Pb(II) on flow-through devices

Interfering Metals	Tolerance Ratio (by mass)	
	Cd(II)	Pb(II)
Mn(II)	100	100
Cr(III)	50	100
Fe(III)	100	50
Zn(II)	>500	>500
Cu(II)	10	100
Ca(II)	>500	>500

To demonstrate the method applicability, flow-through μPAD devices were used to detect Cd(II) and Pb(II) in spiked drinking water samples. The drinking water samples were bought from a local supermarket (Bangkok, Thailand). For analysis, the drinking water was diluted (1:5) with acetate buffer (pH 4.5) and recovery studies were carried out by spiking Cd(II) and Pb(II) to the drinking water samples at three different concentrations (5, 25, and 59 ppb). The percentages of recoveries were found in a range from 93.01% to 103.10% and the acceptable %RSD (n = 3) was below 4.77% (Table S2). In addition, the unknown samples were determined by both the proposed method and a standard method (inductively coupled plasma optical emission spectroscopy, ICP-OES) (Table S3). The results from the developed method were in good agreement with those from the ICP-OES method. These results clearly indicate the ability to measure Cd(II) and Pb(II) levels in drinking water samples.

5.8 Conclusions

In this work, we report for the first time the fabrication and electrochemical characterization of BDDPE for μPADs. The BDDPE exhibits very useful electrochemical properties such as wide solvent window, low background currents, and resistance to surface fouling, which play an important role in the analytical performance of electrochemical sensors. The BDDPEs demonstrated here can be easily fabricated and integrated with ePADs. In addition, the BDDPEs are cheaper and more amenable to disposable and portable platforms compared with conventional BDD electrodes (the prices are ~$0.1/each and $310/each for BDDPEs and polycrystalline BDD electrodes, respectively). To demonstrate the scope of the BDDPEs, the material is applied in ePAD and μPAD formats for the quantitative detection of biological species and heavy metals. In case of biological species, the ePAD device was capable of simultaneously detecting NE and 5-HT in wide concentration ranges and with low limit of detections. In addition, electrode fouling from 5-HT electrooxidation is easily overcome through anodic electrode treatment, opening this sensor for use with multiple measurements (e.g., testing of 20 different samples in situ with one electrode). For heavy metal quantitation, a flow-through μPAD design with SWASV enhances the efficiency of metal deposition, thereby improving the detection sensitivity compared to a static ePAD system. The developed sensor is applicable to a range of analytes and, through overcoming analytical challenges such as electrode fouling and peak shielding, should open up ePADs and μPAD to wide adoption across a range of fields.

CHAPTER VI

CONCLUSIONS AND FUTURE WORKS

6.1 Conclusions

The conclusions were separated into five parts as follows:

Part I: Ultrasensitive and simple method for determination of *N*-Acetyl-L-Cysteine in drug formulations using a diamond Sensor

A highly sensitive BDD sensor coupled with FIA was firstly reported for determining NAC in drug formulations. The effects of basic experimental parameters including pH, applied potential and scan rate on the response of the BDD electrode were investigated. The FIA amperometric method was applied as a sensitive method for trace detection of NAC. A linear range of 0.5 – 50 µmol/L and a detection limit of 10 nmol/L (S/N=3) were obtained. Single BDD sensor could be used up to 50 times with no problem from electrode fouling. The results of amperometric determinations show a very good reproducibility, and the R.S.D. for the measurement based on 10 measurements was <3.7% and <4.1% for intra- and inter-day, respectively. Additionally, the BDD sensor was also applied for determining NAC in real samples from various pharmaceuticals. The results indicated, as compared with those of conventional methods, the proposed sensor offers the advantages of fast analysis time, simplicity, and no requirement of complicated operational step.

Part II: Sensitive and selective electrochemical sensor using silver nanoparticles modified glassy carbon electrode for determination of cholesterol in bovine serum

A highly selective and sensitive cholesterol sensor based on coupling to enzymatic assay and electrochemical detection was developed. Hydrogen peroxide produced from cholesterol reaction was monitored for the indirect quantification of cholesterol. The working electrode of AgNPs/GCE was fabricated by one-step electrochemical deposition technique. AgNPs possesses the catalytic activity of

hydrogen peroxide reduction, which no observed interference from easily oxidizable species such as ascorbic acid and uric acid. Under the optimized conditions, a linear range was found to be of 3.9 - 773.4 mg/dL with a detection limit of 0.99 mg/dL. In addition, this electrochemical sensor displayed very high sensitivity, high accuracy, simple fabrication, and high reproducibility for measuring cholesterol. The proposed method was successfully applied to determine cholesterol in bovine serum which provided the results in good agreement with label.

Part III: Bimetallic Pt–Au nanocatalysts electrochemically deposited on boron-doped diamond electrodes for nonenzymatic glucose detection

A non-enzymatic glucose sensor was developed using bimetallic Pt/Au modified BDD electrode. Pt/Au nanocatalyst can easily formed using electrodeposition of sequentially depositing Au and Pt on BDD electrode surface. The Pt/Au modified BDD electrode is especially suitable to be used as a nonenzymatic glucose sensor owing to its high electrocatalytic activity for glucose oxidation in physiological conditions, and its high resistance to poisoning by chloride ions. A wide linear range of 0.01 -7.5 mM and a detection limit of 0.01 mM were obtained. Additionally, the proposed electrode displayed selective electrochemical analysis of glucose in the presence of common interfering species (e.g., acetaminophen, uric and ascorbic acids), eliminating overlapping signals from such species. The results demonstrated that this novel catalytic material have had the potential to be used in catalysis for sensors and so on.

Part IV: A novel paper-based device coupled with a silver nanoparticle-modified boron-doped diamond electrode for cholesterol detection

A new electrochemical sensing platform based on the combination of AgNP-modified BDD electrode with PAD was proposed and used as a cholesterol biosensor. The novel cholesterol biosensor offered the advantages of simple fabrication, no requirement of an enzyme immobilizing step, low sample volume, low cost, and short analysis time. A linearity (0.39 mg dL^{-1} to 270.69 mg dL^{-1}), a detection limit (0.25

mg dL^{-1}), sensitivity (49.61 μ A mM^{-1} cm^{-2}), and high precision, were obtained. In addition, the proposed biosensor exhibited very high selectivity for cholesterol detection and excellent recoveries for bovine serum analysis (in the range of 99.6-100.8 %). Therefore, this new sensing platform will be an alternative tool for cholesterol detection in routine diagnosis.

Part V: Boron doped diamond paste electrodes for microfluidic paper-based analytical devices

BDDPE was introduced to be used as a novel working electrode for ePADs. The BDDPE exhibited a wider potential window and lower background current in an aqueous electrolyte, and higher resistance to fouling by serotonin oxidation products when compared with carbon paste electrodes. To demonstrate viability of the proposed electrodes, they were applied for the quantitative detection of biological species and heavy metals. In case of biological species, the device was capable of detecting NE at a concentration range of 2.5-100 µM and 0.5-7.5 µM for 5-HT. In addition, the fouled electrode from an adsorbed quinone which is an oxidized product of serotonin could return to its native state of activity by oxidizing the surface at highly positive potential. For measuring heavy metals, using flow through design with square-wave anodic stripping voltammetry (SWASV) technique could enhance the efficiency of the metal deposition on electrode surface. This approach could improve the sensitivity of detection which exhibited a much higher sensitivity than the normal static system. The results showed that the developed sensors were applicable to a wide range of analytes. This finding demonstrated the overcoming analytical challenges such as electrode fouling and peak shielding, and should open up ePADs and µPAD to various applications.

6.2 Future works

BDDPE is very attractive material for fabrication of working electrode due to there is variety of electrode geometries, and can be easily integrated with low-cost

sensors. Additionally, BDDPE exhibits outstanding electrochemical properties in terms of providing a wide potential window and low capacitive current and also have high fouling resistance. Therefore, BDDPE coupled with uPADs has the tendency to be applied for simultaneously detecting multi-analytes in complicated samples. For example, the designed device will contain various zones for adjusting specific conditions of each analyte. The analysis will be simultaneously performed under its optimized conditions. The proposed device will reduce the complexity of analysis and provide many options to increase sensitivity and selectivity for chemical or biochemical analysis in various fields.

REFERENCES

[1] Toussaint, B., Pitti, C., Streel, B., Ceccato, A., Hubert, P., and Crommen, J. Quantitative analysis of N-acetylcysteine and its pharmacopeial impurities in a pharmaceutical formulation by liquid chromatography-UV detection-mass spectrometry. J Chromatogr A 896(1-2) (2000): 191-9.

[2] Toussaint, B., Ceccato, A., Hubert, P., De Graeve, J., De Pauw, E., and Crommen, J. Determination of l-lysine N-acetylcysteinate and its mono- and dimeric related compounds by liquid chromatography–mass spectrometry. Journal of Chromatography A 819(1–2) (1998): 161-170.

[3] Molnár, B., Fodor, B., Csámpai, A., Hidvégi, E., and Molnár-Perl, I. Structure-related new approach in the gas chromatography/mass spectrometry analysis of cathinone type synthetic drugs. Journal of Chromatography A 1477 (2016): 70-75.

[4] Andreasen, S.Z., et al. Integrating electrochemical detection with centrifugal microfluidics for real-time and fully automated sample testing. RSC Advances 5(22) (2015): 17187-17193.

[5] Zhang, C., Wang, X., Hou, M., Li, X., Wu, X., and Ge, J. Immobilization on Metal–Organic Framework Engenders High Sensitivity for Enzymatic Electrochemical Detection. ACS Applied Materials & Interfaces 9(16) (2017): 13831-13836.

[6] Tsikas, D., Sandmann, J., Ikic, M., Fauler, J., Stichtenoth, D.O., and Frolich, J.C. Analysis of cysteine and N-acetylcysteine in human plasma by high-performance liquid chromatography at the basal state and after oral administration of N-acetylcysteine. J Chromatogr B Biomed Sci Appl 708(1-2) (1998): 55-60.

[7] Maneuf, Y.P., Gonzalez, M.I., Sutton, K.S., Chung, F.Z., Pinnock, R.D., and Lee, K. Cellular and molecular action of the putative GABA-mimetic, gabapentin. Cell Mol Life Sci 60(4) (2003): 742-50.

[8] Aravamudhan, S., Kumar, A., Mohapatra, S., and Bhansali, S. Sensitive estimation of total cholesterol in blood using Au nanowires based micro-fluidic platform. Biosensors and Bioelectronics 22(9–10) (2007): 2289-2294.

[9] Shen, J. and Liu, C.-C. Development of a screen-printed cholesterol biosensor: Comparing the performance of gold and platinum as the working electrode material and fabrication using a self-assembly approach. Sensors and Actuators B: Chemical 120(2) (2007): 417-425.

[10] Ruecha, N., Siangproh, W., and Chailapakul, O. A fast and highly sensitive detection of cholesterol using polymer microfluidic devices and amperometric system. Talanta 84(5) (2011): 1323-1328.

[11] Cui, K., Song, Y., Yao, Y., Huang, Z., and Wang, L. A novel hydrogen peroxide sensor based on Ag nanoparticles electrodeposited on DNA-networks modified glassy carbon electrode. Electrochemistry Communications 10(4) (2008): 663-667.

[12] Kurbanoglu, S., Ozkan, S.A., and Merkoçi, A. Nanomaterials-based enzyme electrochemical biosensors operating through inhibition for biosensing applications. Biosensors and Bioelectronics 89, Part 2 (2017): 886-898.

[13] Merkoçi, A. Nanoparticles Based Electroanalysis in Diagnostics Applications. Electroanalysis 25(1) (2013): 15-27.

[14] Barberis, A., et al. Simultaneous amperometric detection of ascorbic acid and antioxidant capacity in orange, blueberry and kiwi juice, by a telemetric system coupled with a fullerene- or nanotubes-modified ascorbate subtractive biosensor. Biosensors and Bioelectronics 67 (2015): 214-223.

[15] Yin, J., Qi, X., Yang, L., Hao, G., Li, J., and Zhong, J. A hydrogen peroxide electrochemical sensor based on silver nanoparticles decorated silicon nanowire arrays. Electrochimica Acta 56(11) (2011): 3884-3889.

[16] Li, X., et al. A novel nonenzymatic hydrogen peroxide sensor based on silver nanoparticles and ionic liquid functionalized multiwalled carbon nanotube composite modified electrode. Electrochimica Acta 113 (2013): 170-175.

[17] Chen, H., et al. A hydrogen peroxide sensor based on Ag nanoparticles electrodeposited on natural nano-structure attapulgite modified glassy carbon electrode. Talanta 86 (2011): 266-270.

[18] Cheng, T.-M., et al. (110)-Exposed Gold Nanocoral Electrode as Low Onset Potential Selective Glucose Sensor. ACS Applied Materials & Interfaces 2(10) (2010): 2773-2780.

[19] Fang, B., et al. Silver Oxide Nanowalls Grown on Cu Substrate as an Enzymeless Glucose Sensor. ACS Applied Materials & Interfaces 1(12) (2009): 2829-2834.

[20] Watanabe, T. and Einaga, Y. Design and fabrication of nickel microdisk-arrayed diamond electrodes for a non-enzymatic glucose sensor based on control of diffusion profiles. Biosensors and Bioelectronics 24(8) (2009): 2684-2689.

[21] Watanabe, T., Ivandini, T.A., Makide, Y., Fujishima, A., and Einaga, Y. Selective Detection Method Derived from a Controlled Diffusion Process at Metal-Modified Diamond Electrodes. Analytical Chemistry 78(22) (2006): 7857-7860.

[22] Ding, Y., Wang, Y., Su, L., Bellagamba, M., Zhang, H., and Lei, Y. Electrospun Co3O4 nanofibers for sensitive and selective glucose detection. Biosensors and Bioelectronics 26(2) (2010): 542-548.

[23] Cao, X., Wang, N., Jia, S., and Shao, Y. Detection of Glucose Based on Bimetallic PtCu Nanochains Modified Electrodes. Analytical Chemistry 85(10) (2013): 5040-5046.

[24] Singh, A.K. and Xu, Q. Synergistic Catalysis over Bimetallic Alloy Nanoparticles. ChemCatChem 5(3) (2013): 652-676.

[25] Cate, D.M., Adkins, J.A., Mettakoonpitak, J., and Henry, C.S. Recent Developments in Paper-Based Microfluidic Devices. Analytical Chemistry 87(1) (2015): 19-41.

[26] Yang, Y., Noviana, E., Nguyen, M.P., Geiss, B.J., Dandy, D.S., and Henry, C.S. Paper-Based Microfluidic Devices: Emerging Themes and Applications. Analytical Chemistry 89(1) (2017): 71-91.

[27] Chen, W., Fang, X., Li, H., Cao, H., and Kong, J. A Simple Paper-Based Colorimetric Device for Rapid Mercury(II) Assay. Scientific Reports 6 (2016): 31948.

[28] Mentele, M.M., Cunningham, J., Koehler, K., Volckens, J., and Henry, C.S. Microfluidic Paper-Based Analytical Device for Particulate Metals. Analytical Chemistry 84(10) (2012): 4474-4480.

[29] Duran, B., Brocenschi, R.F., France, M., Galligan, J.J., and Swain, G.M. Electrochemical activation of diamond microelectrodes: implications for the in vitro measurement of serotonin in the bowel. Analyst 139(12) (2014): 3160-6.

[30] Chandra, S., Miller, A.D., Bendavid, A., Martin, P.J., and Wong, D.K.Y. Minimizing Fouling at Hydrogenated Conical-Tip Carbon Electrodes during Dopamine Detection in Vivo. Analytical Chemistry 86(5) (2014): 2443-2450.

[31] Hutton, L., Newton, M.E., Unwin, P.R., and Macpherson, J.V. Amperometric Oxygen Sensor Based on a Platinum Nanoparticle-Modified Polycrystalline Boron Doped Diamond Disk Electrode. Analytical Chemistry 81(3) (2009): 1023-1032.

[32] Luong, J.H., Male, K.B., and Glennon, J.D. Boron-doped diamond electrode: synthesis, characterization, functionalization and analytical applications. Analyst 134(10) (2009): 1965-79.

[33] Read, T.L., Bitziou, E., Joseph, M.B., and Macpherson, J.V. In Situ Control of Local pH Using a Boron Doped Diamond Ring Disk Electrode: Optimizing Heavy Metal (Mercury) Detection. Analytical Chemistry 86(1) (2014): 367-371.

[34] Ay, A., Swope, V.M., and Swain, G.M. The physicochemical and electrochemical properties of 100 and 500 nm diameter diamond powders coated with boron-doped nanocrystalline diamond. Journal of the Electrochemical Society 155(10) (2008): B1013-B1022.

[35] Kondo, T., et al. Enhanced Sensitivity for Electrochemical Detection Using Screen-Printed Diamond Electrodes via the Random Microelectrode Array Effect. Analytical Chemistry 88(3) (2016): 1753-1759.

[36] Ciobanu, M., Wilburn, J.P., Krim, M.L., and Cliffel, D.E. 1 - Fundamentals A2 - Zoski, Cynthia G. in Handbook of Electrochemistry, pp. 3-29. Amsterdam: Elsevier, 2007.

[37] Bard, A. and Faulkner, L. Electrochemical Methods: Fundamentals and Applications. John Wiley & Sons, Inc, 2001.

[38] Wang, J. Analytical Electrochemistry. Wiley, 2004.

[39] Skoog, D.A., Holler, F.J., and Crouch, S.R. Principles of Instrumental Analysis. Thomson Brooks/Cole, 2007.

[40] Skoog, D.A., Holler, F.J., and Nieman, T.A. Principles of Instrumental Analysis. Saunders College Pub., 1998.

[41] Nantaphol, S., Chailapakul, O., and Siangproh, W. A novel paper-based device coupled with a silver nanoparticle-modified boron-doped diamond electrode for cholesterol detection. Analytica Chimica Acta 891 (2015): 136-143.

[42] Ruecha, N., Rangkupan, R., Rodthongkum, N., and Chailapakul, O. Novel paper-based cholesterol biosensor using graphene/polyvinylpyrrolidone/polyaniline nanocomposite. Biosensors and Bioelectronics 52 (2014): 13-19.

[43] Chen, S. 2 - Practical Electrochemical Cells A2 - Zoski, Cynthia G. in Handbook of Electrochemistry, pp. 33-56. Amsterdam: Elsevier, 2007.

[44] Nantaphol, S., Channon, R.B., Kondo, T., Siangproh, W., Chailapakul, O., and Henry, C.S. Boron Doped Diamond Paste Electrodes for Microfluidic Paper-Based Analytical Devices. Analytical Chemistry 89(7) (2017): 4100-4107.

[45] Macpherson, J.V. A practical guide to using boron doped diamond in electrochemical research. Phys Chem Chem Phys 17(5) (2015): 2935-49.

[46] Fujishima, A. Diamond Electrochemistry. BKC, 2005.

[47] Ivandini, T.A. and Einaga, Y. Polycrystalline boron-doped diamond electrodes for electrocatalytic and electrosynthetic applications. 53(8) (2017): 1338-1347.

[48] Irkham, Watanabe, T., Fiorani, A., Valenti, G., Paolucci, F., and Einaga, Y. Co-reactant-on-Demand ECL: Electrogenerated Chemiluminescence by the in Situ Production of S2O82– at Boron-Doped Diamond Electrodes. Journal of the American Chemical Society 138(48) (2016): 15636-15641.

[49] Kondo, T., et al. Screen-printed diamond electrode: A disposable sensitive electrochemical electrode. Electrochemistry Communications 13(12) (2011): 1546-1549.

[50] Santana, E.R., de Lima, C.A., Piovesan, J.V., and Spinelli, A. An original ferroferric oxide and gold nanoparticles-modified glassy carbon electrode for the determination of bisphenol A. Sensors and Actuators B: Chemical 240 (2017): 487-496.

[51] Nantaphol, S., Chailapakul, O., and Siangproh, W. Sensitive and selective electrochemical sensor using silver nanoparticles modified glassy carbon electrode for determination of cholesterol in bovine serum. Sensors and Actuators B: Chemical 207, Part A (2015): 193-198.

[52] Ranger, C.B. Flow injection analysis. Principles, techniques, applications, design. Analytical Chemistry 53(1) (1981): 20A-32A.

[53] Bagheri, H., Gholami, A., and Najafi, A. Simultaneous preconcentration and speciation of iron(II) and iron(III) in water samples by 2-mercaptobenzimidazole-silica gel sorbent and flow injection analysis system. Analytica Chimica Acta 424(2) (2000): 233-242.

[54] Martinez, A.W., Phillips, S.T., Whitesides, G.M., and Carrilho, E. Diagnostics for the Developing World: Microfluidic Paper-Based Analytical Devices. Analytical Chemistry 82(1) (2010): 3-10.

[55] Carrilho, E., Martinez, A.W., and Whitesides, G.M. Understanding Wax Printing: A Simple Micropatterning Process for Paper-Based Microfluidics. Analytical Chemistry 81(16) (2009): 7091-7095.

[56] Dungchai, W., Chailapakul, O., and Henry, C.S. Electrochemical Detection for Paper-Based Microfluidics. Analytical Chemistry 81(14) (2009): 5821-5826.

[57] Sameenoi, Y., Nongkai, P.N., Nouanthavong, S., Henry, C.S., and Nacapricha, D. One-step polymer screen-printing for microfluidic paper-based analytical device ([small mu]PAD) fabrication. Analyst 139(24) (2014): 6580-6588.

[58] Nouanthavong, S., Nacapricha, D., Henry, C.S., and Sameenoi, Y. Pesticide analysis using nanoceria-coated paper-based devices as a detection platform. Analyst 141(5) (2016): 1837-1846.

[59] Chaiyo, S., Siangproh, W., Apilux, A., and Chailapakul, O. Highly selective and sensitive paper-based colorimetric sensor using thiosulfate catalytic etching of silver nanoplates for trace determination of copper ions. Analytica Chimica Acta 866 (2015): 75-83.

[60] Gao, C., Su, M., Wang, Y., Ge, S., and Yu, J. A disposable paper-based electrochemiluminescence device for ultrasensitive monitoring of CEA based on Ru(bpy)32+@Au nanocages. RSC Advances 5(36) (2015): 28324-28331.

[61] Wang, S., et al. Paper-based chemiluminescence ELISA: Lab-on-paper based on chitosan modified paper device and wax-screen-printing. Biosensors and Bioelectronics 31(1) (2012): 212-218.

[62] He, M. and Liu, Z. Paper-based microfluidic device with upconversion fluorescence assay. Anal Chem 85(24) (2013): 11691-4.

[63] Jokerst, J.C., Adkins, J.A., Bisha, B., Mentele, M.M., Goodridge, L.D., and Henry, C.S. Development of a Paper-Based Analytical Device for Colorimetric Detection of Select Foodborne Pathogens. Analytical Chemistry 84(6) (2012): 2900-2907.

[64] Zafarullah, M., Li, W.Q., Sylvester, J., and Ahmad, M. Molecular mechanisms of N-acetylcysteine actions. Cell Mol Life Sci 60(1) (2003): 6-20.

[65] Dekhuijzen, P.N. Antioxidant properties of N-acetylcysteine: their relevance in relation to chronic obstructive pulmonary disease. Eur Respir J 23(4) (2004): 629-36.

[66] Akerlund, B., Jarstrand, C., Lindeke, B., Sonnerborg, A., Akerblad, A.C., and Rasool, O. Effect of N-acetylcysteine(NAC) treatment on HIV-1 infection: a double-blind placebo-controlled trial. Eur J Clin Pharmacol 50(6) (1996): 457-61.

[67] Liu, M., Wikonkal, N.M., and Brash, D.E. Induction of cyclin-dependent kinase inhibitors and G(1) prolongation by the chemopreventive agent N-acetylcysteine. Carcinogenesis 20(9) (1999): 1869-72.

[68] Farquhar, J., Finlay, G., Ford, P.A., and Martin-Smith, M. A reversed-phase high-performance liquid chromatographic assay for the determination of N-

acetylcysteine in aqueous formulations. J Pharm Biomed Anal 3(3) (1985): 279-85.

[69] Nozal, M.J., et al. Determination of glutathione, cysteine and N-acetylcysteine in rabbit eye tissues using high-performance liquid chromatography and post-column derivatization with 5,5'-dithiobis(2-nitrobenzoic acid). J Chromatogr A 778(1-2) (1997): 347-53.

[70] Holdiness, M.R., Morgan, L.R., Jr., Gillen, L.E., and Harrison, E.F. High-performance liquid chromatographic determination of N-acetylcysteine in human serum following acetaminophen overdosage. J Chromatogr 382 (1986): 99-106.

[71] Tsikas, D., Sandmann, J., Ikic, M., Fauler, J., Stichtenoth, D.O., and Frölich, J.C. Analysis of cysteine and N-acetylcysteine in human plasma by high-performance liquid chromatography at the basal state and after oral administration of N-acetylcysteine. Journal of Chromatography B: Biomedical Sciences and Applications 708(1–2) (1998): 55-60.

[72] Harada, D., et al. Determination of Reduced, Protein-Unbound, and Total Concentrations of N-Acetyl-l-cysteine and l-Cysteine in Rat Plasma by Postcolumn Ligand Substitution High-Performance Liquid Chromatography. Analytical Biochemistry 290(2) (2001): 251-259.

[73] Tsai, F.Y., Chen, C.J., and Chien, C.S. Determination of the cysteine derivatives N-acetylcysteine, S-car□ymethylcysteine and methylcysteine in pharmaceuticals by high-performance liquid chromatography. Journal of Chromatography A 697(1) (1995): 309-315.

[74] Celma, C., Allue, J.A., Prunonosa, J., Peraire, C., and Obach, R. Determination of N-acetylcysteine in human plasma by liquid chromatography coupled to tandem mass spectrometry. J Chromatogr A 870(1-2) (2000): 13-22.

[75] Seiwert, B. and Karst, U. Simultaneous LC/MS/MS Determination of Thiols and Disulfides in Urine Samples Based on Differential Labeling with Ferrocene-Based Maleimides. Analytical Chemistry 79(18) (2007): 7131-7138.

[76] Gao, Z.-N., Zhang, J., and Liu, W.-Y. Electrocatalytic oxidation of N-acetyl-l-cysteine by acetylferrocene at glassy carbon electrode. Journal of Electroanalytical Chemistry 580(1) (2005): 9-16.

[77] Barus, C., Gros, P., Comtat, M., Daunes-Marion, S., and Tarroux, R. Electrochemical behaviour of N-acetyl-l-cysteine on gold electrode—A tentative reaction mechanism. Electrochimica Acta 52(28) (2007): 7978-7985.

[78] Shahrokhian, S., Kamalzadeh, Z., Bezaatpour, A., and Boghaei, D.M. Differential pulse voltammetric determination of N-acetylcysteine by the electrocatalytic oxidation at the surface of carbon nanotube-paste electrode modified with cobalt salophen complexes. Sensors and Actuators B: Chemical 133(2) (2008): 599-606.

[79] Heli, H., Majdi, S., and Sattarahmady, N. Ultrasensitive sensing of N-acetyl-l-cysteine using an electrocatalytic transducer of nanoparticles of iron(III) oxide core–cobalt hexacyanoferrate shell. Sensors and Actuators B: Chemical 145(1) (2010): 185-193.

[80] Silva, I.S.d., et al. Quantification of N-acetylcysteine in pharmaceuticals using cobalt phthalocyanine modified graphite electrodes. Talanta 83(5) (2011): 1701-1706.

[81] Ensafi, A.A., Karimi-Maleh, H., Mallakpour, S., and Hatami, M. Simultaneous determination of N-acetylcysteine and acetaminophen by voltammetric method using N-(3,4-dihydroxyphenethyl)-3,5-dinitrobenzamide modified multiwall carbon nanotubes paste electrode. Sensors and Actuators B: Chemical 155(2) (2011): 464-472.

[82] Beitollahi, H., Raoof, J.-B., and Hosseinzadeh, R. Fabrication of a nanostructure-based electrochemical sensor for simultaneous determination of N-acetylcysteine and acetaminophen. Talanta 85(4) (2011): 2128-2134.

[83] Beitollahi, H., Mohadesi, A., Mohammadi, S., and Akbari, A. Electrochemical behavior of a carbon paste electrode modified with 5-amino-3′,4′-dimethyl-biphenyl-2-ol/carbon nanotube and its application for simultaneous determination of isoproterenol, acetaminophen and N-acetylcysteine. Electrochimica Acta 68 (2012): 220-226.

[84] Salmanipour, A., Taher, M.A., Beitollahi, H., and Hosseinzadeh, R. New voltammetric strategy for simultaneous determination of N-acetylcysteine and folic acid using a carbon nanotube modified glassy carbon electrode. Colloids and Surfaces B: Biointerfaces 102 (2013): 385-390.

[85] Beitollahi, H., Taher, M.A., Mirrahimi, F., and Hosseinzadeh, R. Electrochemical sensor for selective determination of N-acetylcysteine in the presence of folic acid using a modified carbon nanotube paste electrode. Materials Science and Engineering: C 33(3) (2013): 1078-1084.

[86] Sangjarusvichai, H., Dungchai, W., Siangproh, W., and Chailapakul, O. Rapid separation and highly sensitive detection methodology for sulfonamides in shrimp using a monolithic column coupled with BDD amperometric detection. Talanta 79(4) (2009): 1036-1041.

[87] Yano, T., Tryk, D.A., Hashimoto, K., and Fujishima, A. Electrochemical behavior of highly conductive boron-doped diamond electrodes for oxygen reduction in alkaline solution. Journal of the Electrochemical Society 145(6) (1998): 1870-1876.

[88] Santos, M.C.G., Tarley, C.R.T., Dall'Antonia, L.H., and Sartori, E.R. Evaluation of boron-doped diamond electrode for simultaneous voltammetric determination of hydrochlorothiazide and losartan in pharmaceutical formulations. Sensors and Actuators B-Chemical 188 (2013): 263-270.

[89] Pereira, P.F., Marra, M.C., Lima, A.B., dos Santos, W.T.P., Munoz, R.A.A., and Richter, E.M. Fast and simultaneous determination of nimesulide and paracetamol by batch injection analysis with amperometric detection on bare boron-doped diamond electrode. Diamond and Related Materials 39 (2013): 41-46.

[90] Heli, H., Majdi, S., and Sattarahmady, N. Ultrasensitive sensing of N-acetyl-L-cysteine using an electrocatalytic transducer of nanoparticles of iron(III) oxide core-cobalt hexacyanoferrate shell. Sensors and Actuators B-Chemical 145(1) (2010): 185-193.

[91] Zare, H.R. and Chatraei, F. Preparation and electrochemical characteristics of electrodeposited acetaminophen on ruthenium oxide nanoparticles and its

role as a sensor for simultaneous determination of ascorbic acid, dopamine and N-acetyl-L-cysteine. Sensors and Actuators B-Chemical 160(1) (2011): 1450-1457.

[92] Report of the National Cholesterol Education Program Expert Panel on Detection, Evaluation, and Treatment of High Blood Cholesterol in Adults. The Expert Panel. Arch Intern Med 148(1) (1988): 36-69.

[93] Ahmadalinezhad, A. and Chen, A. High-performance electrochemical biosensor for the detection of total cholesterol. Biosensors and Bioelectronics 26(11) (2011): 4508-4513.

[94] Qureshi, R.N., Kok, W.T., and Schoenmakers, P.J. Fractionation of human serum lipoproteins and simultaneous enzymatic determination of cholesterol and triglycerides. Analytica Chimica Acta 654(1) (2009): 85-91.

[95] Pires, C.K., Reis, B.F., Galhardo, C.X., and Martelli, P.B. A Multicommuted Flow Procedure for the Determination of Cholesterol in Animal Blood Serum by Chemiluminescence. Analytical Letters 36(14) (2003): 3011-3024.

[96] Cañabate-Díaz, B., et al. Separation and determination of sterols in olive oil by HPLC-MS. Food Chemistry 102(3) (2007): 593-598.

[97] Cao, S., Zhang, L., Chai, Y., and Yuan, R. Electrochemistry of cholesterol biosensor based on a novel Pt–Pd bimetallic nanoparticle decorated graphene catalyst. Talanta 109(0) (2013): 167-172.

[98] Solanki, P.R., Arya, S.K., Singh, S.P., Pandey, M.K., and Malhotra, B.D. Application of electrochemically prepared poly-N-methylpyrrole-p-toluene sulphonate films to cholesterol biosensor. Sensors and Actuators B: Chemical 123(2) (2007): 829-839.

[99] Ji, R., Wang, L., Wang, G., and Zhang, X. Synthesize Thickness Copper (I) Sulfide nanoplates on Copper Rod and It's Application as Nonenzymatic Cholesterol Sensor. Electrochimica Acta 130 (2014): 239-244.

[100] Burgoa Calvo, M.E., Domínguez Renedo, O., and Arcos Martínez, M.J. Determination of lamotrigine by adsorptive stripping voltammetry using silver nanoparticle-modified carbon screen-printed electrodes. Talanta 74(1) (2007): 59-64.

[101] Welch, C.M., Banks, C.E., Simm, A.O., and Compton, R.G. Silver nanoparticle assemblies supported on glassy-carbon electrodes for the electro-analytical detection of hydrogen peroxide. Analytical and Bioanalytical Chemistry 382(1) (2005): 12-21.

[102] Dhand, C., Singh, S.P., Arya, S.K., Datta, M., and Malhotra, B.D. Cholesterol biosensor based on electrophoretically deposited conducting polymer film derived from nano-structured polyaniline colloidal suspension. Analytica Chimica Acta 602(2) (2007): 244-251.

[103] Saxena, U., Chakraborty, M., and Goswami, P. Covalent immobilization of cholesterol oxidase on self-assembled gold nanoparticles for highly sensitive amperometric detection of cholesterol in real samples. Biosensors and Bioelectronics 26(6) (2011): 3037-3043.

[104] Singh, J., Srivastava, M., Kalita, P., and Malhotra, B.D. A novel ternary NiFe2O4/CuO/FeO-chitosan nanocomposite as a cholesterol biosensor. Process Biochemistry 47(12) (2012): 2189-2198.

[105] Liu, X., Nan, Z., Qiu, Y., Zheng, L., and Lu, X. Hydrophobic ionic liquid immoblizing cholesterol oxidase on the electrodeposited Prussian blue on glassy carbon electrode for detection of cholesterol. Electrochimica Acta 90(0) (2013): 203-209.

[106] Cai, X., Gao, X., Wang, L., Wu, Q., and Lin, X. A layer-by-layer assembled and carbon nanotubes/gold nanoparticles-based bienzyme biosensor for cholesterol detection. Sensors and Actuators B: Chemical 181 (2013): 575-583.

[107] Umar, A., Ahmad, R., Hwang, S.W., Kim, S.H., Al-Hajry, A., and Hahn, Y.B. Development of Highly Sensitive and Selective Cholesterol Biosensor Based on Cholesterol Oxidase Co-Immobilized with **α**-Fe2O3 Micro-Pine Shaped Hierarchical Structures. Electrochimica Acta 135 (2014): 396-403.

[108] Park, S., Boo, H., and Chung, T.D. Electrochemical non-enzymatic glucose sensors. Analytica Chimica Acta 556(1) (2006): 46-57.

[109] Wang, C.-H., Yang, C.-H., and Chang, J.-K. High-selectivity electrochemical non-enzymatic sensors based on graphene/Pd nanocomposites functionalized

with designated ionic liquids. Biosensors and Bioelectronics 89, Part 1 (2017): 483-488.

[110] Lin, Y., Lu, F., Tu, Y., and Ren, Z. Glucose Biosensors Based on Carbon Nanotube Nanoelectrode Ensembles. Nano Letters 4(2) (2004): 191-195.

[111] Hrapovic, S., Liu, Y., Male, K.B., and Luong, J.H.T. Electrochemical Biosensing Platforms Using Platinum Nanoparticles and Carbon Nanotubes. Analytical Chemistry 76(4) (2004): 1083-1088.

[112] Wang, J., Thomas, D.F., and Chen, A. Nonenzymatic electrochemical glucose sensor based on nanoporous PtPb networks. Analytical Chemistry 80(4) (2008): 997-1004.

[113] Jiang, L.C. and Zhang, W.D. A highly sensitive nonenzymatic glucose sensor based on CuO nanoparticles-modified carbon nanotube electrode. Biosensors & Bioelectronics 25(6) (2010): 1402-1407.

[114] Meng, L., Jin, J., Yang, G., Lu, T., Zhang, H., and Cai, C. Nonenzymatic Electrochemical Detection of Glucose Based on Palladium–Single-Walled Carbon Nanotube Hybrid Nanostructures. Analytical Chemistry 81(17) (2009): 7271-7280.

[115] Gao, H., Xiao, F., Ching, C.B., and Duan, H. One-Step Electrochemical Synthesis of PtNi Nanoparticle-Graphene Nanocomposites for Nonenzymatic Amperometric Glucose Detection. ACS Applied Materials & Interfaces 3(8) (2011): 3049-3057.

[116] Karra, S., Wooten, M., Griffith, W., and Gorski, W. Morphology of Gold Nanoparticles and Electrocatalysis of Glucose Oxidation. Electrochimica Acta 218 (2016): 8-14.

[117] Park, S., Chung, T.D., and Kim, H.C. Nonenzymatic Glucose Detection Using Mesoporous Platinum. Analytical Chemistry 75(13) (2003): 3046-3049.

[118] Song, Y.-Y., Zhang, D., Gao, W., and Xia, X.-H. Nonenzymatic Glucose Detection by Using a Three-Dimensionally Ordered, Macroporous Platinum Template. Chemistry – A European Journal 11(7) (2005): 2177-2182.

[119] Yuan, J.H., Wang, K., and Xia, X.H. Highly Ordered Platinum-Nanotubule Arrays for Amperometric Glucose Sensing. Advanced Functional Materials 15(5) (2005): 803-809.

[120] Ghanem, M.A., et al. Microwave activation of the electro-oxidation of glucose in alkaline media. Physical Chemistry Chemical Physics 7(20) (2005): 3552-3559.

[121] Niu, X., Lan, M., Zhao, H., and Chen, C. Highly Sensitive and Selective Nonenzymatic Detection of Glucose Using Three-Dimensional Porous Nickel Nanostructures. Analytical Chemistry 85(7) (2013): 3561-3569.

[122] Huang, T.-K., et al. Glucose sensing by electrochemically grown copper nanobelt electrode. Journal of Electroanalytical Chemistry 636(1–2) (2009): 123-127.

[123] Kang, X., Mai, Z., Zou, X., Cai, P., and Mo, J. A sensitive nonenzymatic glucose sensor in alkaline media with a copper nanocluster/multiwall carbon nanotube-modified glassy carbon electrode. Analytical Biochemistry 363(1) (2007): 143-150.

[124] Balamurugan, J., Thanh, T.D., Karthikeyan, G., Kim, N.H., and Lee, J.H. A novel hierarchical 3D N-Co-CNT@NG nanocomposite electrode for non-enzymatic glucose and hydrogen peroxide sensing applications. Biosensors and Bioelectronics 89, Part 2 (2017): 970-977.

[125] Veeramani, V., Madhu, R., Chen, S.-M., Veerakumar, P., Hung, C.-T., and Liu, S.-B. Heteroatom-enriched porous carbon/nickel oxide nanocomposites as enzyme-free highly sensitive sensors for detection of glucose. Sensors and Actuators B: Chemical 221 (2015): 1384-1390.

[126] Prasad, R. and Bhat, B.R. Multi-wall carbon nanotube–NiO nanoparticle composite as enzyme-free electrochemical glucose sensor. Sensors and Actuators B: Chemical 220 (2015): 81-90.

[127] Zhan, B., et al. Free-standing electrochemical electrode based on Ni(OH)2/3D graphene foam for nonenzymatic glucose detection. Nanoscale 6(13) (2014): 7424-7429.

[128] Sun, S., Zhang, X., Sun, Y., Yang, S., Song, X., and Yang, Z. Facile Water-Assisted Synthesis of Cupric Oxide Nanourchins and Their Application as Nonenzymatic Glucose Biosensor. ACS Applied Materials & Interfaces 5(10) (2013): 4429-4437.

[129] Madhu, R., Veeramani, V., Chen, S.-M., Manikandan, A., Lo, A.-Y., and Chueh, Y.-L. Honeycomb-like Porous Carbon–Cobalt Oxide Nanocomposite for High-Performance Enzymeless Glucose Sensor and Supercapacitor Applications. ACS Applied Materials & Interfaces 7(29) (2015): 15812-15820.

[130] Dong, X.-C., et al. 3D Graphene–Cobalt Oxide Electrode for High-Performance Supercapacitor and Enzymeless Glucose Detection. ACS Nano 6(4) (2012): 3206-3213.

[131] Stephens, I.E.L., Bondarenko, A.S., Gronbjerg, U., Rossmeisl, J., and Chorkendorff, I. Understanding the electrocatalysis of oxygen reduction on platinum and its alloys. Energy & Environmental Science 5(5) (2012): 6744-6762.

[132] Sheng, Q., Mei, H., Wu, H., Zhang, X., and Wang, S. PtxNi/C nanostructured composites fabricated by chemical reduction and their application in non-enzymatic glucose sensors. Sensors and Actuators B: Chemical 203 (2014): 588-595.

[133] Sun, Y., Buck, H., and Mallouk, T.E. Combinatorial Discovery of Alloy Electrocatalysts for Amperometric Glucose Sensors. Analytical Chemistry 73(7) (2001): 1599-1604.

[134] Li, M., Bo, X., Mu, Z., Zhang, Y., and Guo, L. Electrodeposition of nickel oxide and platinum nanoparticles on electrochemically reduced graphene oxide film as a nonenzymatic glucose sensor. Sensors and Actuators B: Chemical 192 (2014): 261-268.

[135] Zhang, J., Sasaki, K., Sutter, E., and Adzic, R.R. Stabilization of Platinum Oxygen-Reduction Electrocatalysts Using Gold Clusters. Science 315(5809) (2007): 220-222.

[136] Xu, J., Zhao, T., Liang, Z., and Zhu, L. Facile Preparation of AuPt Alloy Nanoparticles from Organometallic Complex Precursor. Chemistry of Materials 20(5) (2008): 1688-1690.

[137] Luo, J., et al. Phase Properties of Carbon-Supported Gold–Platinum Nanoparticles with Different Bimetallic Compositions. Chemistry of Materials 17(12) (2005): 3086-3091.

[138] Chang, G., et al. Synthesis of highly dispersed Pt nanoclusters anchored graphene composites and their application for non-enzymatic glucose sensing. Electrochimica Acta 157 (2015): 149-157.

[139] Li, M., Bo, X., Zhang, Y., Han, C., and Guo, L. One-pot ionic liquid-assisted synthesis of highly dispersed PtPd nanoparticles/reduced graphene oxide composites for nonenzymatic glucose detection. Biosensors and Bioelectronics 56 (2014): 223-230.

[140] Hu, Y., Zhang, H., Wu, P., Zhang, H., Zhou, B., and Cai, C. Bimetallic Pt-Au nanocatalysts electrochemically deposited on graphene and their electrocatalytic characteristics towards oxygen reduction and methanol oxidation. Physical Chemistry Chemical Physics 13(9) (2011): 4083-4094.

[141] Vassilyev, Y.B., Khazova, O.A., and Nikolaeva, N.N. Kinetics and mechanism of glucose electrooxidation on different electrode-catalysts. Journal of Electroanalytical Chemistry and Interfacial Electrochemistry 196(1) (1985): 105-125.

[142] Raj, V., Johnson, T., and Joseph, K. Cholesterol aided etching of tomatine gold nanoparticles: A non-enzymatic blood cholesterol monitor. Biosensors and Bioelectronics 60 (2014): 191-194.

[143] Zhang, J., Wang, W., Chen, S., Ruo, Y., Zhong, X., and Wu, X. Bi-pseudoenzyme synergetic catalysis to generate a coreactant of peroxydisulfate for an ultrasensitive electrochemiluminescence-based cholesterol biosensor. Biosensors and Bioelectronics 57 (2014): 71-76.

[144] Gholivand, M.B. and Khodadadian, M. Amperometric cholesterol biosensor based on the direct electrochemistry of cholesterol oxidase and catalase on a

graphene/ionic liquid-modified glassy carbon electrode. Biosensors and Bioelectronics 53 (2014): 472-478.

[145] Ahmad, R., Tripathy, N., Kim, S.H., Umar, A., Al-Hajry, A., and Hahn, Y.-B. High performance cholesterol sensor based on ZnO nanotubes grown on Si/Ag electrodes. Electrochemistry Communications 38 (2014): 4-7.

[146] Zhang, M., et al. A biosensor for cholesterol based on gold nanoparticles-catalyzed luminol electrogenerated chemiluminescence. Biosensors and Bioelectronics 32(1) (2012): 288-292.

[147] Li, J., Peng, T., and Peng, Y. A Cholesterol Biosensor Based on Entrapment of Cholesterol Oxidase in a Silicic Sol-Gel Matrix at a Prussian Blue Modified Electrode. Electroanalysis 15(12) (2003): 1031-1037.

[148] Singh, S., Solanki, P.R., Pandey, M.K., and Malhotra, B.D. Covalent immobilization of cholesterol esterase and cholesterol oxidase on polyaniline films for application to cholesterol biosensor. Analytica Chimica Acta 568(1–2) (2006): 126-132.

[149] Soylemez, S., Kanik, F.E., Nurioglu, A.G., Akpinar, H., and Toppare, L. A novel conducting copolymer: Investigation of its matrix properties for cholesterol biosensor applications. Sensors and Actuators B: Chemical 182 (2013): 322-329.

[150] Shin, Y.J. and Kameoka, J. Amperometric cholesterol biosensor using layer-by-layer adsorption technique onto electrospun polyaniline nanofibers. Journal of Industrial and Engineering Chemistry 18(1) (2012): 193-197.

[151] Santhiago, M., Henry, C.S., and Kubota, L.T. Low cost, simple three dimensional electrochemical paper-based analytical device for determination of p-nitrophenol. Electrochimica Acta 130 (2014): 771-777.

[152] Sun, G., Wang, P., Ge, S., Ge, L., Yu, J., and Yan, M. Photoelectrochemical sensor for pentachlorophenol on microfluidic paper-based analytical device based on the molecular imprinting technique. Biosensors and Bioelectronics 56 (2014): 97-103.

[153] Bhakta, S.A., Borba, R., Taba Jr, M., Garcia, C.D., and Carrilho, E. Determination of nitrite in saliva using microfluidic paper-based analytical devices. Analytica Chimica Acta 809 (2014): 117-122.

[154] Rattanarat, P., Dungchai, W., Cate, D., Volckens, J., Chailapakul, O., and Henry, C.S. Multilayer Paper-Based Device for Colorimetric and Electrochemical Quantification of Metals. Analytical Chemistry 86(7) (2014): 3555-3562.

[155] Tan, S.N., Ge, L., Tan, H.Y., Loke, W.K., Gao, J., and Wang, W. Paper-Based Enzyme Immobilization for Flow Injection Electrochemical Biosensor Integrated with Reagent-Loaded Cartridge toward Portable Modular Device. Analytical Chemistry 84(22) (2012): 10071-10076.

[156] Lankelma, J., Nie, Z., Carrilho, E., and Whitesides, G.M. Paper-Based Analytical Device for Electrochemical Flow-Injection Analysis of Glucose in Urine. Analytical Chemistry 84(9) (2012): 4147-4152.

[157] Yu, J., Wang, S., Ge, L., and Ge, S. A novel chemiluminescence paper microfluidic biosensor based on enzymatic reaction for uric acid determination. Biosensors and Bioelectronics 26(7) (2011): 3284-3289.

[158] Kuek Lawrence, C.S., Tan, S.N., and Floresca, C.Z. A "green" cellulose paper based glucose amperometric biosensor. Sensors and Actuators B: Chemical 193 (2014): 536-541.

[159] Nurak, T., Praphairaksit, N., and Chailapakul, O. Fabrication of paper-based devices by lacquer spraying method for the determination of nickel (II) ion in waste water. Talanta 114 (2013): 291-296.

[160] Majid, E., Male, K.B., and Luong, J.H.T. Boron Doped Diamond Biosensor for Detection of Escherichia coli. Journal of Agricultural and Food Chemistry 56(17) (2008): 7691-7695.

[161] Sochr, J., Švorc, Ľ., Rievaj, M., and Bustin, D. Electrochemical determination of adrenaline in human urine using a boron-doped diamond film electrode. Diamond and Related Materials 43 (2014): 5-11.

[162] Švorc, Ľ., Sochr, J., Rievaj, M., Tomčík, P., and Bustin, D. Voltammetric determination of penicillin V in pharmaceutical formulations and human urine

using a boron-doped diamond electrode. Bioelectrochemistry 88 (2012): 36-41.

[163] Rahman, M.M., Li, X.-b., Kim, J., Lim, B.O., Ahammad, A.J.S., and Lee, J.-J. A cholesterol biosensor based on a bi-enzyme immobilized on conducting poly(thionine) film. Sensors and Actuators B: Chemical 202 (2014): 536-542.

[164] Wang, C., et al. Highly-sensitive cholesterol biosensor based on platinum–gold hybrid functionalized ZnO nanorods. Talanta 94 (2012): 263-270.

[165] Safavi, A. and Farjami, F. Electrodeposition of gold–platinum alloy nanoparticles on ionic liquid–chitosan composite film and its application in fabricating an amperometric cholesterol biosensor. Biosensors and Bioelectronics 26(5) (2011): 2547-2552.

[166] Zhao, C., Wan, L., Jiang, L., Wang, Q., and Jiao, K. Highly sensitive and selective cholesterol biosensor based on direct electron transfer of hemoglobin. Analytical Biochemistry 383(1) (2008): 25-30.

[167] Martinez, A.W., Phillips, S.T., Butte, M.J., and Whitesides, G.M. Patterned Paper as a Platform for Inexpensive, Low-Volume, Portable Bioassays. Angewandte Chemie International Edition 46(8) (2007): 1318-1320.

[168] Cate, D.M., Noblitt, S.D., Volckens, J., and Henry, C.S. Multiplexed paper analytical device for quantification of metals using distance-based detection. Lab on a Chip 15(13) (2015): 2808-2818.

[169] Santhiago, M., Wydallis, J.B., Kubota, L.T., and Henry, C.S. Construction and Electrochemical Characterization of Microelectrodes for Improved Sensitivity in Paper-Based Analytical Devices. Analytical Chemistry 85(10) (2013): 5233-5239.

[170] Wang, Y., et al. A disposable electrochemical sensor for simultaneous determination of norepinephrine and serotonin in rat cerebrospinal fluid based on MWNTs-ZnO/chitosan composites modified screen-printed electrode. Biosensors and Bioelectronics 65 (2015): 31-38.

[171] Liu, W., Guo, Y., Li, H., Zhao, M., Lai, Z., and Li, B. A paper-based chemiluminescence device for the determination of ofloxacin. Spectrochimica Acta Part A: Molecular and Biomolecular Spectroscopy 137 (2015): 1298-1303.

[172] Thom, N.K., Lewis, G.G., Yeung, K., and Phillips, S.T. Quantitative Fluorescence Assays Using a Self-Powered Paper-Based Microfluidic Device and a Camera-Equipped Cellular Phone. RSC advances 4(3) (2014): 1334-1340.

[173] Santhiago, M. and Kubota, L.T. A new approach for paper-based analytical devices with electrochemical detection based on graphite pencil electrodes. Sensors and Actuators B: Chemical 177 (2013): 224-230.

[174] Dossi, N., Toniolo, R., Terzi, F., Impellizzieri, F., and Bontempelli, G. Pencil leads doped with electrochemically deposited Ag and AgCl for drawing reference electrodes on paper-based electrochemical devices. Electrochimica Acta 146 (2014): 518-524.

[175] Adkins, J.A. and Henry, C.S. Electrochemical detection in paper-based analytical devices using microwire electrodes. Analytica Chimica Acta 891 (2015): 247-254.

[176] Fosdick, S.E., Anderson, M.J., Renault, C., DeGregory, P.R., Loussaert, J.A., and Crooks, R.M. Wire, Mesh, and Fiber Electrodes for Paper-Based Electroanalytical Devices. Analytical Chemistry 86(7) (2014): 3659-3666.

[177] Määttänen, A., Ihalainen, P., Pulkkinen, P., Wang, S., Tenhu, H., and Peltonen, J. Inkjet-Printed Gold Electrodes on Paper: Characterization and Functionalization. ACS Applied Materials & Interfaces 4(2) (2012): 955-964.

[178] Kit-Anan, W., et al. Disposable paper-based electrochemical sensor utilizing inkjet-printed Polyaniline modified screen-printed carbon electrode for Ascorbic acid detection. Journal of Electroanalytical Chemistry 685 (2012): 72-78.

[179] Pereira, S.V., et al. A microfluidic device based on a screen-printed carbon electrode with electrodeposited gold nanoparticles for the detection of IgG anti-Trypanosoma cruziantibodies. Analyst 136(22) (2011): 4745-4751.

[180] Mettakoonpitak, J., et al. Electrochemistry on Paper-Based Analytical Devices: A Review. Electroanalysis (2016): n/a-n/a.

[181] Swamy, B.E.K. and Venton, B.J. Carbon nanotube-modified microelectrodes for simultaneous detection of dopamine and serotoninin vivo. Analyst 132(9) (2007): 876-884.

[182] Luong, J.H.T., Male, K.B., and Glennon, J.D. Boron-doped diamond electrode: synthesis, characterization, functionalization and analytical applications. Analyst 134(10) (2009): 1965-1979.

[183] Balmer, R.S., et al. Chemical vapour deposition synthetic diamond: materials, technology and applications. Journal of Physics: Condensed Matter 21(36) (2009): 364221.

[184] Compton, R.G., Foord, J.S., and Marken, F. Electroanalysis at Diamond-Like and Doped-Diamond Electrodes. Electroanalysis 15(17) (2003): 1349-1363.

[185] Hutton, L.A., Iacobini, J.G., Bitziou, E., Channon, R.B., Newton, M.E., and Macpherson, J.V. Examination of the Factors Affecting the Electrochemical Performance of Oxygen-Terminated Polycrystalline Boron-Doped Diamond Electrodes. Analytical Chemistry 85(15) (2013): 7230-7240.

[186] Kondo, T., et al. Direct Determination of Chemical Oxygen Demand by Anodic Decomposition of Organic Compounds at a Diamond Electrode. Analytical Chemistry 86(16) (2014): 8066-8072.

[187] Granger, M.C., et al. Standard electrochemical behavior of high-quality, boron-doped polycrystalline diamond thin-film electrodes. Anal Chem 72(16) (2000): 3793-804.

[188] Granger, M.C., Xu, J., Strojek, J.W., and Swain, G.M. Polycrystalline diamond electrodes: basic properties and applications as amperometric detectors in flow injection analysis and liquid chromatography. Analytica Chimica Acta 397(1–3) (1999): 145-161.

[189] Jolley, S., Koppang, M., Jackson, T., and Swain, G.M. Flow Injection Analysis with Diamond Thin-Film Detectors. Analytical Chemistry 69(20) (1997): 4099-4107.

[190] van den Brink, F.T.G., et al. Electrochemical Protein Cleavage in a Microfluidic Cell with Integrated Boron Doped Diamond Electrodes. Analytical Chemistry 88(18) (2016): 9190-9198.

[191] Stanković, D.M. and Kalcher, K. Amperometric quantification of the pesticide ziram at boron doped diamond electrodes using flow injection analysis. Sensors and Actuators B: Chemical 233 (2016): 144-147.

[192] Fischer, A.E. and Swain, G.M. Preparation and characterization of boron-doped diamond powder - A possible dimensionally stable electrocatalyst support material. Journal of the Electrochemical Society 152(9) (2005): B369-B375.

[193] Takeshi, K., et al. Screen-printed Modified Diamond Electrode for Glucose Detection. Chemistry Letters 42(4) (2013): 352-354.

[194] Graeff, F.G., Guimarães, F.S., De Andrade, T.G.C.S., and Deakin, J.F.W. Role of 5-HT in stress, anxiety, and depression. Pharmacology Biochemistry and Behavior 54(1) (1996): 129-141.

[195] Patel, A.N., Unwin, P.R., and Macpherson, J.V. Investigation of film formation properties during electrochemical oxidation of serotonin (5-HT) at polycrystalline boron doped diamond. Phys Chem Chem Phys 15(41) (2013): 18085-92.

[196] Sarada, B.V., Rao, T.N., Tryk, D.A., and Fujishima, A. Electrochemical Oxidation of Histamine and Serotonin at Highly Boron-Doped Diamond Electrodes. Analytical Chemistry 72(7) (2000): 1632-1638.

[197] Wang, J., Chen, G., Chatrathi, M.P., Fujishima, A., Tryk, D.A., and Shin, D. Microchip Capillary Electrophoresis Coupled with a Boron-Doped Diamond Electrode-Based Electrochemical Detector. Analytical Chemistry 75(4) (2003): 935-939.

[198] Ponchon, J.L., Cespuglio, R., Gonon, F., Jouvet, M., and Pujol, J.F. Normal pulse polarography with carbon fiber electrodes for in vitro and in vivo determination of catecholamines. Analytical Chemistry 51(9) (1979): 1483-1486.

[199] Kemper, T. and Sommer, S. Estimate of Heavy Metal Contamination in Soils after a Mining Accident Using Reflectance Spectroscopy. Environmental Science & Technology 36(12) (2002): 2742-2747.

[200] Chaiyo, S., Mehmeti, E., Žagar, K., Siangproh, W., Chailapakul, O., and Kalcher, K. Electrochemical sensors for the simultaneous determination of zinc, cadmium and lead using a Nafion/ionic liquid/graphene composite modified screen-printed carbon electrode. Analytica Chimica Acta 918 (2016): 26-34.

[201] Osswald, S., Yushin, G., Mochalin, V., Kucheyev, S.O., and Gogotsi, Y. Control of sp2/sp3 Carbon Ratio and Surface Chemistry of Nanodiamond Powders by Selective Oxidation in Air. Journal of the American Chemical Society 128(35) (2006): 11635-11642.

[202] Huang, J.T., Guo, W.H., Hwang, J., and Chang, H. Reliability of Hall effect measurements on chemical vapor deposited polycrystalline B-doped diamond films. Applied Physics Letters 68(26) (1996): 3784-3786.

[203] Lagrange, J.P., Deneuville, A., and Gheeraert, E. Activation energy in low compensated homoepitaxial boron-doped diamond films1. Diamond and Related Materials 7(9) (1998): 1390-1393.

[204] Guell, A.G., Meadows, K.E., Unwin, P.R., and Macpherson, J.V. Trace voltammetric detection of serotonin at carbon electrodes: comparison of glassy carbon, boron doped diamond and carbon nanotube network electrodes. Phys Chem Chem Phys 12(34) (2010): 10108-14.

[205] Nantaphol, S., Chailapakul, O., and Siangproh, W. Ultrasensitive and Simple Method for Determination of N-Acetyl-L-Cysteine in Drug Formulations Using a Diamond Sensor. Electroanalysis 26(5) (2014): 1024-1030.

[206] Bai, L., Yuan, R., Chai, Y., Yuan, Y., Wang, Y., and Xie, S. Direct electrochemistry and electrocatalysis of a glucose oxidase-functionalized bioconjugate as a trace label for ultrasensitive detection of thrombin. Chemical Communications 48(89) (2012): 10972-10974.

[207] Konopka, S.J. and McDuffie, B. Diffusion coefficients of ferri- and ferrocyanide ions in aqueous media, using twin-electrode thin-layer electrochemistry. Analytical Chemistry 42(14) (1970): 1741-1746.

[208] Chaiyo, S., Apiluk, A., Siangproh, W., and Chailapakul, O. High sensitivity and specificity simultaneous determination of lead, cadmium and copper using μPAD with dual electrochemical and colorimetric detection. Sensors and Actuators B: Chemical 233 (2016): 540-549.

[209] Ramaley, L. and Krause, M.S. Theory of square wave voltammetry. Analytical Chemistry 41(11) (1969): 1362-1365.

[210] Wang, J., Lu, J., Hocevar, S.B., Farias, P.A.M., and Ogorevc, B. Bismuth-Coated Carbon Electrodes for Anodic Stripping Voltammetry. Analytical Chemistry 72(14) (2000): 3218-3222.

[211] Nie, Z., et al. Electrochemical sensing in paper-based microfluidic devices. Lab on a Chip 10(4) (2010): 477-483.

[212] Xiao, L., et al. Simultaneous detection of Cd(II) and Pb(II) by differential pulse anodic stripping voltammetry at a nitrogen-doped microporous carbon/Nafion/bismuth-film electrode. Electrochimica Acta 143 (2014): 143-151.

[213] Zhao, D., Guo, X., Wang, T., Alvarez, N., Shanov, V.N., and Heineman, W.R. Simultaneous Detection of Heavy Metals by Anodic Stripping Voltammetry Using Carbon Nanotube Thread. Electroanalysis 26(3) (2014): 488-496.

[214] Wu, Y., Li, N.B., and Luo, H.Q. Simultaneous measurement of Pb, Cd and Zn using differential pulse anodic stripping voltammetry at a bismuth/poly(p-aminobenzene sulfonic acid) film electrode. Sensors and Actuators B: Chemical 133(2) (2008): 677-681.

APPENDIX

VITA

Miss Siriwan Nantaphol was born on December 11th, 1989 in Nongkhai, Thailand. She graduated with high school degree from Chumpholphonphisai School, Nongkhai in 2008. She received her Bachelor's degree of Science (Chemistry) from Srinakharinwirot University in 2012. Then, she became a Ph.D. student in Analytical Chemistry as a member of Electrochemistry and Optical Spectroscopy Research Unit under the director of Professor Dr. Orawon Chailapakul. She received the grant from the Thailand Research Fund through the Royal Jubilee Ph.D program. She had an opportunity to do research in Henry Group, Colorado State University, USA, under Proferssor Dr. Charles S. Henry for 11 months. And then, She also had an opportunity to do research in Einaga group, Keio University, Japan, under Professor Dr. Yasuaki Einaga for 3 months. After she came back, she continually did her research and then graduated with a Ph.D. Degree in Chemistry of academic year 2016 from Chulalongkorn University.